



# Photocatalytic Degradation of a Series of Direct Azo Dyes Using Immobilized $\text{TiO}_2$

A Major Qualifying Project Submitted to Faculty of  
Worcester Polytechnic Institute  
In Partial Fulfillment of the Requirements for the Degree of Bachelor of Science

Submitted by:  
Rebecca Byberg  
Jesse Cobb

Submitted to:  
Project Advisor:  
Professor Terri Camesano  
Professor Robert Thompson  
Site Advisor:  
Dr. Marie Noëlle Pons

March 3, 2012

This report represents the work of an undergraduate student at WPI submitted to the faculty as evidence of completion of a degree requirement. WPI routinely publishes these reports on its web site without editorial or peer review.

## Abstract

Azo dyes present in textile wastewater require removal due to their negative environmental and health effects. Although there are several ways to treat such wastewater, this study focused on photocatalytic degradation on a titanium dioxide (TiO<sub>2</sub>) paper substrate. The dyes studied were Direct Red 23, 80, and 81, Direct Yellow 27 and 50, and Direct Violet 51. Solutions of each dye were prepared at a concentration of 25 mg/L in water and run through a photocatalytic reactor. Color removal in the solution was monitored using UV-Vis spectroscopy. At the end of the experiment the final solution was tested for toxicity, total organic carbon, and the presence of ammonia and nitrate ions.

Complete color removal was observed for each dye. The results were modeled based on a pseudo-first order reaction. It was found the degradation rate of the azo dyes was related to the structural features. This rate increased with the presence of sulfate groups and decreased with molecules containing more than one azo groups and additional aromatic rings. Complete oxidation of the dye molecules was not achieved which resulted in many by-products formed. Nitrogen atoms in the structure of all tested dyes were converted to ammonia and nitrate. However, the results show that much of the nitrogen was converted to N<sub>2</sub> gas. Most solutions had a reduced total organic content of at least 80% with the minimum reduction being 60%. The majority of dye solutions increased in toxicity after exposure to the reactor due to the presence of aromatic amines. To decrease toxicity, a biological secondary treatment would be necessary as it would further degrade the toxic aromatic amines.

## **Acknowledgments**

We would like to send our deepest gratitude to Professor Terri Camesano for her hard work and allowing us the opportunity to travel to France and have this unique experience. We would like to thank Professor Robert Thompson for his help and guidance in the research. Thank you to Researcher Marie-Noëlle Pons, who supported us in Nancy, France. In addition, we would like to thank Steve Pontvianne and Aziz Assaad for their assistance in our research.

## Table of Contents

Abstract .....	2
Acknowledgments .....	3
List of Figures .....	5
List of Tables .....	5
List of Equations .....	5
Introduction .....	6
Background .....	7
Azo Dyes .....	7
Structure .....	7
Direct Dyes .....	7
Toxicity .....	8
Textile Wastewater .....	8
Current Treatment Methods .....	9
Treatment Issues .....	11
Regulations .....	11
Titanium Dioxide .....	12
History .....	12
Oxidation .....	12
Kinetics .....	13
Toxicity .....	14
Reactor .....	15
Design .....	15
Analytical Techniques .....	16
UV-Visible Spectroscopy .....	16
Total Organic Carbon .....	17
Ammonia .....	17
Ion Chromatography .....	18
Materials .....	19
Dyes .....	19
Titanium Dioxide Paper .....	19
Methods .....	20
Reactor .....	20
Method Development .....	20
Kinetics Experiments .....	20
UV-Visible Spectroscopy .....	20
Total Organic Carbon .....	21
Nessler Method .....	21
Ion Chromatography .....	21
Toxicity .....	22
Results and Discussions .....	23
Method Development .....	23
Kinetics .....	25
Total Organic Carbon .....	28
Ammonia and Nitrates .....	28
Toxicity .....	30

Conclusions.....	34
References.....	35
Appendices.....	38
Appendix A: UV Spectroscopy.....	38
Appendix B: Lettuce Test .....	63
Appendix C: Dye Information.....	64
Appendix D: Sample Calculations .....	66
Sample calculation for ammonia and nitrate .....	66

## List of Figures

Figure 1: Azo dye general structure.....	7
Figure 2: Image taken from Hashimoto 2005 showing the reversible reaction occurring in the surface of TiO <sub>2</sub> when exposed to UV-light.(Kazuhito Hashimoto 2005) .....	12
Figure 3: Photo and sketch of reactor used at ENSIC. ....	15
Figure 4: Color wheel showing the colors in the visible spectrum and their wavelengths.(Michigan State University).....	16
Figure 5: Absorbance spectrum of Direct Red 81 .....	23
Figure 6: Graph showing decrease in concentration of Direct Red 81 over time in the six trials. 24	
Figure 7: kapp of Direct Red 81 for method development .....	24
Figure 8: Example of UV-Vis spec. results for azo dyes. The absorbance decreases as time increases. The wavelength where absorbance was greatest, was used for determining concentration. ....	26
Figure 9: Results of kinetics study. kapp used to compare reaction rates between dyes.....	26
Figure 10: Presence of ammonia comparison.....	29
Figure 11: Lettuce Test Samples.....	30
Figure 12: Relative Toxicity Comparison of Dyes .....	31
Figure 13: Toxicity Removal Comparison of Dyes.....	32

## List of Tables

Table 1: Current Treatment Methods (Anjaneyulu, Sreedhara Chary et al. 2005).....	10
Table 2: Studied azo dyes .....	19
Table 3: Dye kapp and structural features .....	27
Table 4: Total Organic Carbon Tests.....	28

## List of Equations

Equation 1: Rate Law.....	13
Equation 2: Integrated Rate Law .....	13
Equation 3: Simplified Integrated Rate Law .....	<b>Error! Bookmark not defined.</b>
Equation 4: Relative Toxicity .....	22
Equation 5: Change in Toxicity .....	23

## Introduction

Concerns of textile dyes in the wastewaters from factories have been a growing concern for many years. Estimates state that as much as 15% of dye used in the staining process is released in the wastewater effluents.(Lachheb, Puzenat et al. 2002) Dye pollutants can have dramatic effects on the environment.(Baptista 2007) Textile dyes in wastewater are a concern not only because they are displeasing aesthetically but are linked to health hazards as well.(Sweeny, Chipman et al. 1994) It is therefore crucial to investigate techniques to remove these harmful pollutants safely.

Current methods in the removal of azo dyes either require the adsorption of the dye onto a material or chemical reactions.(Anjaneyulu, Sreedhara Chary et al. 2005) Adsorption onto sludge or activated carbon can be successful; however, the process generates secondary pollution that requires costly disposal. Chemical reactions with chlorine or coagulation techniques introduce harmful chemicals that are released into the environment. Developments in photocatalysis have led researchers to design reactors that oxidize azo dyes using photoactivated titanium dioxide ( $\text{TiO}_2$ ). (Kazuhito Hashimoto 2005) Exposing  $\text{TiO}_2$  in water to near UV-light produces hydroxyl radicals on the surface of the catalyst, these reactive radicals can completely oxidize organic compounds found in the water. The photocatalytic reactors are successful in the removal and purification of waters containing azo dyes and hold many promising benefits. The azo dyes themselves are oxidized into carbon dioxide and water leaving behind zero pollutants. The success of this advanced oxidation process has led research to pursue further investigations into the photocatalysis of organic compounds using irradiated  $\text{TiO}_2$ .

The oxidation of azo dyes over photoactivated  $\text{TiO}_2$  has been studied extensively,(Aguedach, Brosillon et al. 2005; Thiruvengkatachari, Vigneswaran et al. 2008) as well as investigations into the operational parameters that control the rate of oxidation.(Daneshvar, Salari et al. 2003) However, many of these experiments were only carried out with a single dye. It was the purpose of this research to study the kinetics of the oxidation of several azo dyes and investigate the importance of dye structure on their degradation. The dyes were tested in a batch reactor system using  $\text{TiO}_2$  powder supported on a non-woven synthetic paper that was irradiated by UV lamps. The reaction rate and kinetics were monitored throughout the experiment using UV-Vis spectroscopy. Total organic carbon tests and ion detection through the Nessler method and

chromatography were conducted on the final solutions as well as a simple toxicity test using plant seeds.

## Background

### Azo Dyes

Azo dyes are a common classification of dyes, accounting for between 60-70% of all dyes. This class of dyes gives off bold colors in a variety of hues. Although most commercially available azo dyes are reds, oranges, and yellows, it is theoretically possible for the entire spectrum to be produced. As research continues, more colors of azo dyes will be produced. This section will discuss azo dyes in to the context of their chemical structure, direct dye class, and toxicity.

### Structure

One of the practical ways to classify dyes is by their chemical structure. The shared feature in each group of dyes is the common structural groups. The structural similarity that characterizes azo dyes is the presence of at least one  $-N=N-$  group,(Kurbiel 1978; Price 2002) as shown in Figure 1: Azo dye general structure.



Figure 1: Azo dye general structure

The R and R' components of the azo functional group can be either aryl or alkyl groups.

### Direct Dyes

The "direct dye" classification in the Color Index system “refers to various planar, highly conjugated molecular structures that also contain one or more anionic sulfonate group.” Most direct dyes are azo dyes. They are water-soluble, anionic compounds (Types of Dyes). Their flat shape and their length enable them to lie along-side cellulose fibers and maximize the Van-der-Waals, dipole and hydrogen bonds .

Direct dyes are commonly used in the textile industry. They are advantageous since they are available in powdered form, making them much easier to handle and measure. In addition, they can be applied directly to textiles without needing a separate adhesion mechanism. A

disadvantage to direct dyes, however, is that it is common for a textile dyed with a direct dye to 'bleed.' To counter this disadvantage, there are some treatments that can be used to help keep the direct dyed textiles from losing their color.

### **Toxicity**

One concern about using azo dyes is their toxicity. There are three known ways by which azo dyes can be toxic.(Brown and De Vito 1993) First, azo dyes themselves may be carcinogenic, a characteristic determined by the structure. For example, the different isomers of hydrophobic azo dyes containing amino groups, para-isomers are carcinogenic and ortho-isomers are not carcinogenic.(Cancer 2010) Second, reduced azo dyes and cleavage of the azo linkage produces toxic aromatic amines, which have one or more aromatic rings in their molecular structure. Some of these compounds have negative environmental or health-related effects. Dyes are one of the major sources of aromatic amines found in the environment.(Pinheiro, Touraud et al. 2004) Third, azo dyes can be activated via direct oxidation of the azo linkage to highly reactive electrophilic diazonium salts.

### **Textile Wastewater**

Natural dyes had been used for centuries as the only method of dyeing textiles. These dyes were rare and costly, so textile dyeing was limited. Synthesized dyes transformed the textile industry since they were cheaper and readily available. This transformation sparked great exploration of synthetic dyes and helped create a commercial market that continues to grow, even today.(Dorner 2002)

However, the wastewaters generated by the textile industry's dyeing process contain significant amounts of dissolved dye, mostly azo dyes. It is believed that up to 15% of dyes used for production are released in the dyeing process effluent stream.(Lachheb, Puzenat et al. 2002)

Few published studies demonstrated the presence of dyes in the aquatic environment. Azo disperse dyes are hydrophobic and are not expected to be found in the water column but adsorbed on the sediment. However, since the dyes are combined with dispersing agents, the hydrophilic properties of the products are much higher than the dyes alone, allowing for an increased presence of dyes in waters that receive effluents from textile processing plants.(de Aragão Umbuzeiro, Freeman et al. 2005)



There are several reasons why the colors of dyes cause problems in textile waste water. Acute and/or chronic effects can occur from direct exposure. Even small amounts of released colorant cause aesthetic changes due to the coloration of surface waters. The absorption and reflection of sunlight entering the water is changed by the presence of dyes. This change interferes with growth of bacteria and can significantly change the level of biological impurities in the water.(Slokar and Majcen Le Marechal 1998) In addition, international environmental standards are heightening, creating the need for more technology to remove the azo dye pollution.(Lachheb, Puzenat et al. 2002)

### **Current Treatment Methods**

There are several methods that are available for waste water treatment. The methods discussed in Table 1: Current Treatment Methods are specified to the textile industry and include physical, chemical, biological, and emerging technologies.

Treatment Methodology	Treatment	Advantages	Limitations
<b>Physical Methods</b>			
1. Adsorption			
a. Activated carbon	Pre/post	Economically attractive. Good removal efficiency	Cost intensive regeneration process
b. Peat	Pre	Effective adsorbant due to cellular structure. No activation required.	Surface area is lower than activated carbon.
c. Wood chips	Pre	Good sorption for specific colorant.	Larger contact times and huge quantities are required.
2. Ion-exchange	Main	Regeneration with low loss of adsorbents.	Specific application
<b>Chemical Methods</b>			
1. Oxidation		Effective for both soluble and insoluble colorants.	Problem with sludge disposal.
a. Fenton's reagent	Pre/main	Capable of decolorizing wide variety of wastes. No alternation in volume.	Prohibitively expensive
b. Ozonation	Main	Effective for azo dye removal	Not suitable for dispersed dyes. Released aromatic amines.
2. Coagulation and precipitation	Pre/main	Short detention time and low capital costs. Good removal efficiencies	High cost of chemicals for pH adjustment. Dewatering and sludge handling problems.
<b>Biological methods</b>			
1. Aerobic process	Main	Color removal is facilitated along with COD removal.	Longer detention times and substrate specific removal. Less resistant to recalcitrant.
2. Single cell (Fungal, Algal, and Bacterial)	Post	Good removal efficiency for low volumes and concentrations. Very effective for specific colorant removal.	Culture maintenance is cost intensive. Cannot cope up with large volumes of colored effluents.
<b>Emerging Technologies</b>			
1. Advanced oxidation processes	Main	Complete mineralization ensured. Growing number of commercial application. Effective pretreatment methodology in integrated systems enhances biodegradability	Cost intensive process
2. Photocatalysis	Post	Process carried out at ambient conditions. Inputs are atoxic and inexpensive. Complete mineralization with short detention times.	Effective for small amount of colorants. Expensive process.
3. Sonication	Pre	Simplicity in use. Very effective in integrated systems	Relatively new method and awaiting full scale application.
4. Engineering Wetland Systems	Pre/post	Cost effective technology and can be operated with huge volumes of wastewater	High initial installation cost. Requires expertise and managing during monsoon becomes difficult.

Table 1: Current Treatment Methods (Anjaneyulu, Sreedhara Chary et al. 2005)

### **Treatment Issues**

Wastewater from textile dyeing is usually treated in an activated sludge plant and the liquid effluent is released. However, studies have shown the ineffectiveness of this method. Regarding the degradation of C.I. Disperse Blue 79: after processing using a conventionally operated activated sludge, 85% of the dye remained in the systems, of which 3% was retained in the primary sludge, 62% by the activated sludge, and 20% was found in the final liquid effluent released into the environment. The use of biological treatment improved the effectiveness of sludge systems, but exhibited increased levels of mutagenic activity.(de Aragão Umbuzeiro, Freeman et al. 2005)

In the Cristais River, for example, the concentration of the discharged effluent was around 3%. Due to the particular dyes (Disperse blue 373, Disperse Orange 37, Disperse Violet 93) used in the upstream facility, there were high levels of mutagenicity in the *Salmonella*/microsome assay. The intestinal microflora may play an important role in the activation of these compounds because of the involvement of nitro reduction and azo reduction in the activation of these dyes. Therefore, if these dyes were ingested, one of the first organs to suffer would be the intestines.(Alves de Lima, Bazo et al. 2007)

### **Regulations**

Due to the toxicity of textile wastewater, many countries have passed regulations to control these effluent outputs. One country that has enacted such regulations is the United States. In 1972, the U.S Environmental Protection Agency (EPA) created the Clean Water Act to restore and maintain the chemical, physical, and biological integrity of the nation's waters. As a result of this act, all toxic pollutants were to be identified and arrangements were to be created for the removal and appropriate disposal of materials.(EPA 1972)

From 1972 to 1975, research into wastewater treatment was performed at the Cracow Water Protection Section at the Water Economy Research Institute (IGW) in Warsaw, Poland as part of an agreement with the EPA. The focus of the research was to analyze the various techniques, summarized in Table 1: Current Treatment Methods (Anjaneyulu, Sreedhara Chary et al. 2005), to treat wastewater (removal of color, detergents, other refractory pollutants) and determine the most effective and economic solution. Initially, the following technologies were analyzed: rapid filtration on single and multi-media beds, adsorption on granular activated carbon, ion exchange

on anionic and cationic resins, coagulation with the use of typical coagulants and with the application of auxiliary chemicals, oxidation with ozone and chloride, and reverse osmosis results were used to create regulations.(Kurbiel 1978)

## Titanium Dioxide

### History

Titanium dioxide has seen many applications for its unique photocatalytic properties. Sunlight and near-UV light photoactivates the  $\text{TiO}_2$ . In the presence of water, the catalyst produces hydroxyl radicals that are capable of oxidizing organic compounds to carbon dioxide and water. Because of this important quality,  $\text{TiO}_2$  has seen many uses in water treatment and purification.(Tang and Huren 1995; Pizarro, Guillard et al. 2005)  $\text{TiO}_2$  is a great material to work with because of its stability, low cost, and is nontoxic. There are two common forms of titanium dioxide, anatase and rutile, with anatase being the stronger oxidizer. However, most  $\text{TiO}_2$  powders contain both types since performance is enhanced with the presence of rutile.(Thiruvengkatachari, Vigneswaran et al. 2008) The fascination with titanium dioxide has continued to grow and products incorporating the material have reached market.(Staff 2009) Because of the knowledge, familiarity and wide acceptance in the scientific community,  $\text{TiO}_2$  is an ideal material to use in studies. Moreover, it is one of the most efficient photocatalysts. (Reutergårdh and Iangphasuk 1997) Extensive studies have been carried out using  $\text{TiO}_2$  for the degradation of organic compounds in attempts to understand the oxidation process.(Tang and Huren 1995; Pizarro, Guillard et al. 2005; Liu, Hsieh et al. 2006)

### Oxidation

Titanium dioxide exposed to sunlight becomes photoactive, the surface of the catalysts generates free electrons, and valance band holes form. (Thiruvengkatachari, Vigneswaran et al. 2008) Water encounters the valance holes and the water oxidizes to form hydroxyl radicals. Hydroxyl radicals are non-selective, strong oxidizers and very

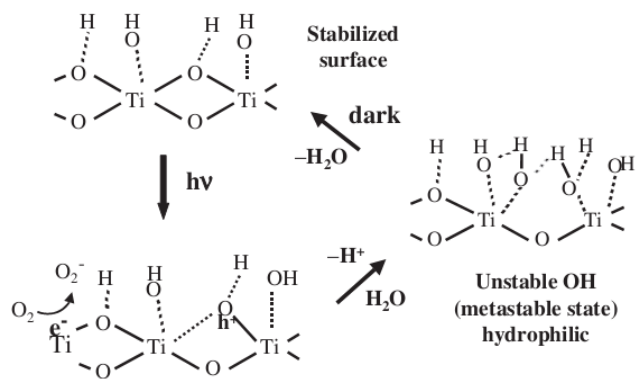


Figure 2: Image taken from Hashimoto 2005 showing the reversible reaction occurring in the surface of  $\text{TiO}_2$  when exposed to UV-light.(Kazuhito Hashimoto 2005)

reactive. The free radicals are able to oxidize organic compounds in solution and almost completely degrade contaminants.(Konstantinou and Albanis 2004) Oxygen from the air and dissolved in the water can accept the free electrons on the surface of photoactivated TiO<sub>2</sub> generating the radical anion, O<sub>2</sub><sup>-</sup>. The anions can further oxidize the organic compounds. The electrons and valance band gaps can also react directly with organics for further degradation. (Thiruvengkatachari, Vigneswaran et al. 2008) Many of the reactions occurring on the surface of titanium dioxide lead to the breakdown of the dyes making it an efficient photocatalyst. There are many parameters that control the extent of oxidation including pH, concentration of the organic compounds and TiO<sub>2</sub>, and the presence of reagents.(Daneshvar, Salari et al. 2003)

### Kinetics

The kinetics of the photodegradation of azo dyes has been well published.(Konstantinou and Albanis 2004; Aguedach, Brosillon et al. 2005) Most results have been found to fit the Langmuir-Hinshelwood (L-H) model, where a monolayer of adsorption is occurring on the surface.(Langmuir 1918) The L-H model is widely used in analyzing heterogenous reactions occurring on the surface of catalysts, where two molecules are required to absorb on the surface for the reaction to occur.(Fogler 2005) Therefore, the reaction is dependent on the concentrations of both species. The rate law derived from the model is defined by Equation 1: Rate Law.

#### Equation 1: Rate Law

$$r = \frac{dC}{dt} = \frac{-kKC}{1 + KC}$$

Where  $r$  is the rate if the reaction,  $C$  is the dye concentration in solution,  $t$  is time,  $k$  is the reaction constant and  $K$  is the adsorption equilibrium factor for the reactant on a surface. Testing was done using this model for the kinetics of the oxidation of azo dyes. If we assume the term  $K*C$  is negligible, that term in the denominator is eliminated. Integrating the simplified rate law equation yields the following equation used to model the data.

#### Equation 2: Integrated Rate Law

$$\ln \frac{C}{C_0} = -k_{app}t$$

Where  $C_0$  is the initial concentration and  $k_{app}$  is the apparent reaction constant.

## Toxicity

Recent studies have shown that titanium dioxide as nanoparticles are toxic. The toxicity has to do with the nano-size of the  $\text{TiO}_2$  rather than the compound itself, because in nano-form the particles can be absorbed through the skin and penetrate cells.(M.N 2006) A study on algae and daphnids showed that titanium dioxide did inhibit growth of both tested organisms proving biological toxicity.(Hund-Rinke and Simon 2006) Tests with nano sized  $\text{TiO}_2$  on human lung cells also show carcinogenic properties.(Falck, Lindberg et al. 2009) It has become a growing concern that investigations into the health and environment effects have been ignored while the list of applications for nanoparticles grows.(Som, Wick et al. 2011) Nanoparticles have the potential for being great alternatives to harmful chemicals currently used in processes, however if they prove toxic themselves this obviously hinders the technology. It is also uncertain which properties of the nanoparticles influence toxicity such as size, shape, density, or coatings. Effects of long-term accumulation of nanoparticles in bodies are currently unknown and difficult to study, but the findings in the acute effects of  $\text{TiO}_2$  are enough to cause concern.

Most studies on the oxidation of textile dyes with  $\text{TiO}_2$  have been done in slurry reactors with the nanoparticles suspended in the solution.(Tang and Huren 1995) Nanoparticles have proven to be difficult to separate from systems due to their size so more steps to remove the nanoparticles are required to produce safe wastewater. Researchers are now exploring alternatives to slurry reactors with  $\text{TiO}_2$  supported onto surfaces.

Methods for supporting  $\text{TiO}_2$  are currently being used in studies. Embedding the titanium dioxide onto glass slides have resulted in successful experiments.(Khataee, Pons et al. 2009; Lu, Chien et al. 2010) The  $\text{TiO}_2$  remains on the surface of the glass while the solution cascades down as a thin film over the slide. The supported  $\text{TiO}_2$  retains its photocatalytic properties and the UV light is able to penetrate the thin film of solution leading to the oxidation of the organic compounds. An easier to use synthetic paper product can be purchased from suppliers that contain the  $\text{TiO}_2$  nanoparticles on the fibers. The paper can be cut to size and manipulated easily to fit different applications. The  $\text{TiO}_2$  paper has been successful in promoting the breakdown of organic compounds in water.(Aguedach, Brosillon et al. 2005; Pelton, Geng et al. 2006) As research continues, it is important for innovators to develop safe technologies with nanoparticles to ensure a healthy and sustainable future.

## Reactor

### Design

Researchers at ENSIC University in Nancy, France have designed and constructed a batch reactor for the oxidation of azo dyes. It has already been used in research by M.N. Pons.(Khataee, Pons et al. 2009) The reactor consists of a reservoir containing dye and a peristaltic pump that pumps the dye to the top of a sloped surface. The dye distributes over the reactor in a thin-film cascading down the slope. The dye passes over a paper embedded with photocatalytic titanium dioxide nanoparticles. A cover with UV lamps sits over the reactor in order to photoactivate the TiO<sub>2</sub> and oxidation to occur. The effluent dye returns to the reservoir where it is recycled through the system.

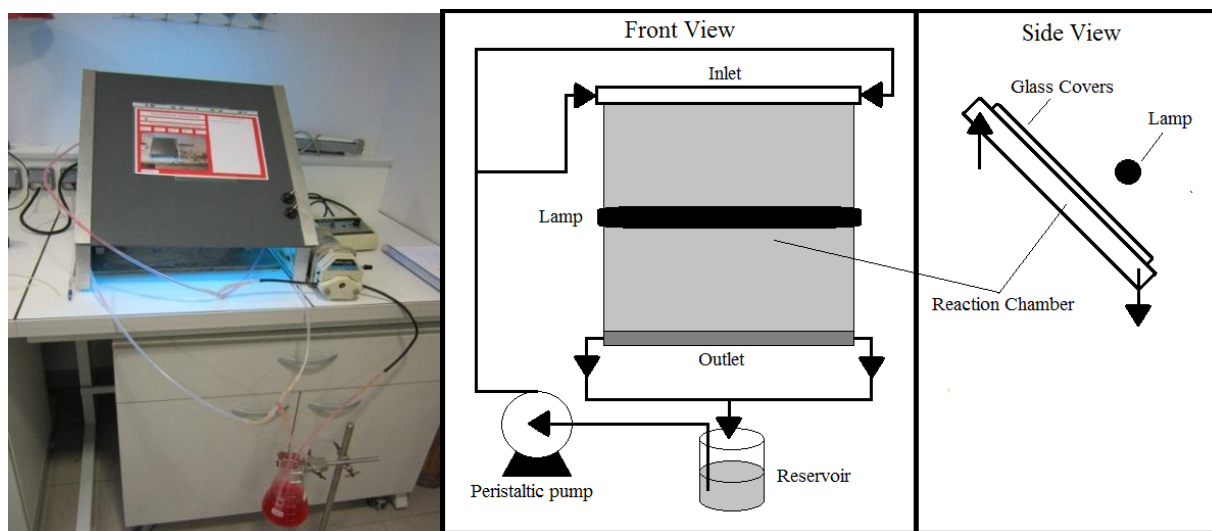


Figure 3: Photo and sketch of reactor used at ENSIC.

## Analytical Techniques

### UV-Visible Spectroscopy

UV-Visible spectroscopy is a useful analytic technique in determining the color and concentration of a compound. Molecules containing non-binding valence electrons, such as pi-bonds, have unique properties that emit color when excited by light. (Michigan State University) These light absorbing groups are called chromophores. The energy difference between the higher and lower-occupied orbital is directly related to a wavelength of light ( $\lambda = h \cdot c / \Delta E$ ). The wavelength that excites the electrons into a higher orbital is absorbed and gives the molecule its color. (Thermo

Scientific) Most dyes and pigments contain many chromophores conjugated together in order for the molecule to absorb light in the visible spectrum. Auxochromes are functional groups attached to chromophores that modify the wavelength absorbance of the chromophores but auxochromes do not produce any colors themselves. Often auxochromes are charged altering the electron cloud of the chromophores. Azo dyes contain many delocalized electrons and differing structures of the azo dyes yield unique colors. Colors seen by the eye are actually the wavelengths not absorbed and reflect back from the compound. So the color seen is the complimentary color of the color absorbed, see Figure 4. (Michigan State University) The detector uses UV light as well as visible light because not all absorbance occurs in the visible spectrum.

A spectrophotometer uses these mentioned properties to determine the color and concentration of compounds in a solution. For the spectrophotometer, a sample is prepared by placing a small amount of the solution in a cuvette. The cuvette has clear walls that allow the light from the spectrophotometer to pass through the sample. The spectrophotometer then shines a range of wavelengths on the sample measuring the amount of light absorbed once it has passed through the sample. The amount of absorbance to the wavelength of light produces a plot with large peaks at wavelengths where the electrons raise to their excited state. That peak wavelength can be used to identify compounds. If the concentration of the sample is known in the solution, the absorbance can be corrected to the molar absorbance.

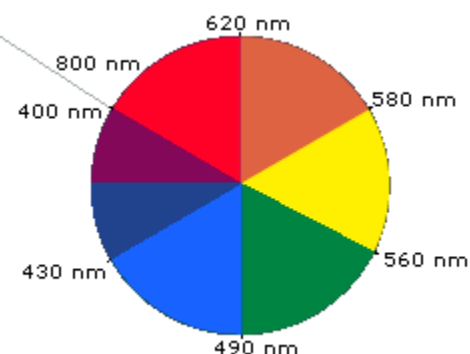


Figure 4: Color wheel showing the colors in the visible spectrum and their wavelengths. (Michigan State University)



### **Total Organic Carbon**

Total organic carbon has been a concern in water supplies since the passing of the Safe Water Drinking Act in 1976. Several sources can exist for organic compounds in water and once there, the molecules can be harmful to the environment and require expensive treatment processes to remove.(Schumacher 2002) Therefore, it is important to remove as much of the organics at the source of wastewaters before they are released into the environment to improve overall water quality. Removal of organics are required for safe drinking and if left in the environment, the organics can participate in reactions creating harmful products.(Volk, Wood et al. 2002) Organic carbon plays an important role in the ecosystem as well and it is crucial not to disturb this delicate balance.(Fisher and Likens 1973)

Total organic carbon is measured by the amount of carbon dioxide produced after the combustion of the compounds.(Shimadzu) Compounds in the sample are vaporized, carried to a reactor and oxidized completely to carbon dioxide. The carrier gas is analytical air that contains the same molar ratio of air (21% oxygen, 79% nitrogen) so oxygen is present for the reaction, but it has no carbon dioxide present so all carbon dioxide in the system is from the combustion of the sample. The generated carbon dioxide passes a non-dispersive infrared detector (NDIR) for measurement.

There are several methods in TOC measurements. The analysis method used in this study for TOC was Non-Purgeable Organic Carbon (NPOC). NPOC is different from typical TOC measurements because the measured total inorganic carbon is not subtracted from the total carbon to get the TOC. Instead, the sample is acidified with hydrogen peroxide to remove all carbonates leaving only organic carbon behind in the solution. This method assumes there are no purgeable organic carbon compounds that would be removed from the sample by sparging with the analytical gas. In most water samples, there are very little purgeable organic compounds so NPOC was considered accurate for TOC analysis.

### **Ammonia**

Ammonia has been detected in the final solutions of azo dye degradation.(Augugliaro, Baiocchi et al. 2002) This is an environmental concern because ammonia decrease water quality.(EPA2011) Excess ammonia in wastewater can enhance growth in aquatic life causing problems such as toxic algae blooms.(Vitousek, Aber et al. 1997) Therefore, it is important to

monitor ammonia concentrations in the oxidation of azo dyes and the most widely used method for nitrate detection is the Nessler method.

Nessler method is a common method for the detection of ammonia in a solution. The method was first published in 1868 by Julius Nessler who discovered when potassium tetraiodomercurate,  $K_2[HgI_4]$ , is added to a solution containing ammonia the solution changes to a yellow-brown color.(Nessler 1868) Nessler reagent refers to  $K_2[HgI_4]$  and Nesslerization is still a common analytical technique. Current use of the Nessler method is a modified version from the original 1898 version for a more accurate and quantitative analysis. The Nessler reagent is added to the distillate product causing a color change upon reaction with the ammonia. Samples were observed using a UV-Vis Spectrophotometer and concentrations determined from a linear calibration curve.

### **Ion Chromatography**

Ion chromatography has become one of the most important techniques in modern analytical chemistry. By exploiting the pKa values of compounds in a sample it is possible to separate the components and measure their concentrations.(Jackson 2000) The molecules in the sample absorb onto a solid phase in the chromatography column through ionic bonding. A wash is applied the system and the pH is increased incrementally and the different compounds desorb one at a time separating the molecules. The eluent competes with the solute ions for the functional group on the solid phase matrix. The ions with the weaker charges are knocked off first.(Haddad and Jackson 1990) The compounds are detected by either a UV spectrophotometer or a mass spectrophotometer. A chromatogram is produced showing peaks representing different compounds with the area related to the concentration. Ion chromatography is an accurate and robust analytical technique.

Ion chromatography is very practical in environmental analyses. By-products of the oxidation of azo dyes are nitrates and other anions, which can be harmful. Nitrates in the water supply are very harmful and can cause Methemoglobinemia which can be fatal in infants.(Self and Waskorn 2008) In the design of an oxidation reactor for azo dyes it is important that compounds produced are safer than the starting dyes. Ion chromatography was vital in the design of the system since alternatives for detecting anions are lacking.

## Materials

### Dyes

Table 2: Studied azo dyes

The azo dyes tested in this report were purchased from Sigma-Aldrich (US-MO) and are summarized in Table 2: Studied azo dyes. More complete information on the dyes can be found in Appendix C: Dye Information. Stock solutions of the dyes were dissolved in ultrapure water and used to prepare solutions for experiments.

Studied Azo Dyes	$M_w$ (g/mol)	$\lambda_{max}$ (nm)
Direct Red 23	813.71	502
Direct Red 80	1371.07	529
Direct Red 81	675.60	510
Direct Yellow 27	662.62	398
Direct Yellow 50	956.82	395
Direct Violet 17	719.1	546

### Titanium Dioxide Paper

Titanium dioxide supported on non-woven paper (Ahlstrom Research & Services, Pont-Eveque, France) was used as the photocatalyst for all experiments. The deposited  $TiO_2$  powder on the paper was PC-500 and bound with  $SiO_2$ . SEM images show the photocatalytic paper before and after experiments.

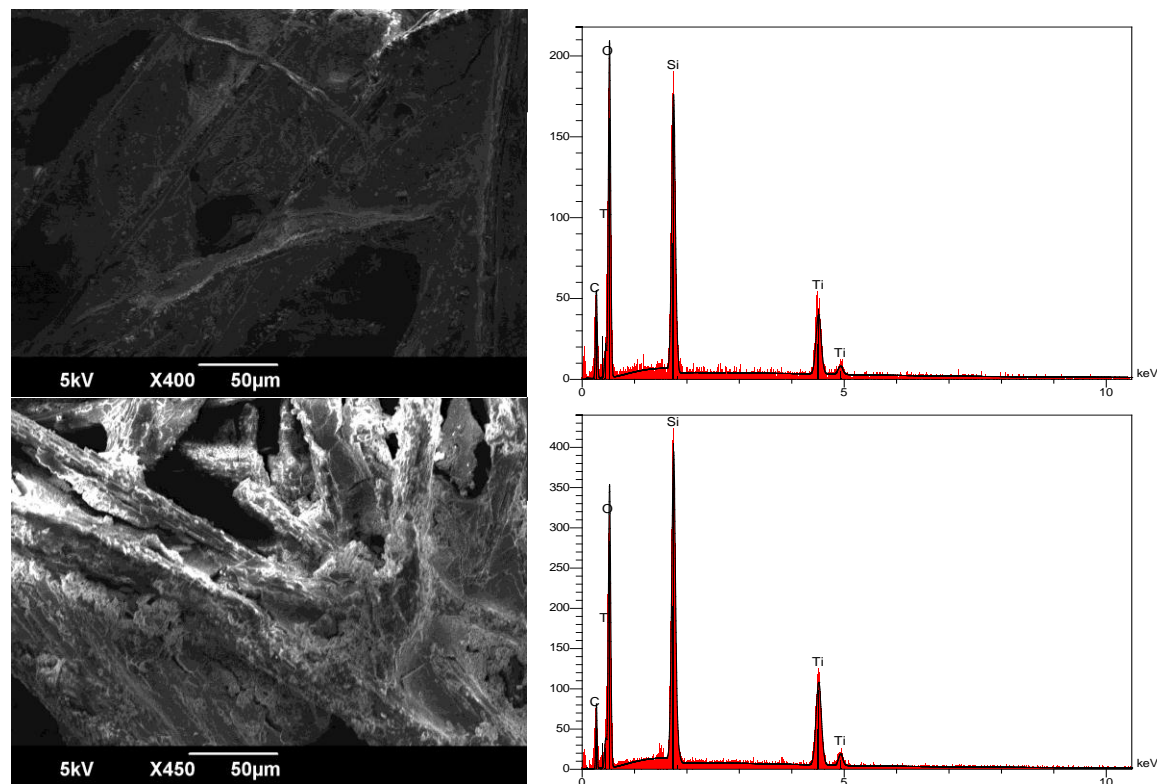


Figure 5: SEM Images: Above, paper before experiments. Below, paper after experiments.

## Methods

### Reactor

The photocatalytic reactor built at ENSIC (Nancy, France) using photocatalytic paper was used for the oxidation of the tested azo dyes. Dye solutions were pumped at 108 mL/min using a peristaltic pump to the top of the reactor where the solution was distributed in a thin film over the photocatalytic paper. The circulation rates used for each experiment were the same. At the bottom of the reactor, tubes returned the dye back to the reservoir.

### Method Development

Before testing the different azo dyes, it was important to establish a routine for the reactor that would yield consistent results for the dyes. The first four trials using Direct Red 81 at a concentration of 25 mg/L were conducted. At the start of each experiment, the reactor was equalized with the dye for 30 minutes with the UV lamps off. After 30 minutes, a sample was collected and the lights were turned on and the reactor was left to run for roughly 24 hours. Samples were collected from the reservoir periodically for UV-Vis measurements through the duration of testing. Between each trial, the reactor was cleaned with a rinse of ultrapure water and around 35  $\mu$ M of hydrogen peroxide for the day with the UV lamps on. At the end of the day, the reactor was washed overnight with ultrapure water with the UV lamps off. After trials four and trial five, the reactor was cleaned only with ultrapure water with lamps remaining on. There was no 30-minute initial incubation for trials five and six.

### Kinetics Experiments

In order to test the significance of dye structure to the kinetics of oxidation, 25 mg/L samples of dye were prepared and run through the photocatalytic reactor for eight hours. The dye was pumped at 108 mL/min. The UV lamps were left on continuously, even between experiments. While the reactor was running around 10 mL of sample was collected from the reservoir for UV-Vis spectroscopy. At the end of the experiment around 40 mL of sample from the reservoir was taken for TOC, ammonia, chromatography and toxicity tests. The reactor was rinsed with ultrapure water between dyes.

### UV-Visible Spectroscopy

UV-Vis Spectroscopy (model Anthelic, SECOMAM) was performed on samples taken from the reservoir throughout the experiment. A one-centimeter quartz cuvette was used for all

measurements. A spectrum analysis was performed on each sample from 200 nm to 700 nm in wavelength. A blank cuvette filled with ultrapure water was used prior to each measurement. For sample measurements, the cuvette was rinsed with the sample, dumped, and more sample added before being measured. Linear calibration curves were generated separately comparing concentration of the dye to the intensity of the absorption at the highest peak, these curves were used to determine the concentration and the percent of color removed from the solution over the course of the experiment.

### **Total Organic Carbon**

Samples from the beginning and the end of the experiment were taken to perform total organic carbon (TOC) measurements. Measurements were performed using combustion catalytic oxidation with a non-dispersive infrared detector (NDIR) (model TOC-VCSH, Shimadzu). In the instrument acid was added to the samples to remove all inorganic carbon following the non-purgeable organic carbon method. The acidified sample was then combusted and oxidized to carbon dioxide over a platinum catalyst. The amount of carbon dioxide generated was correlated to the TOC dissolved in the solution. The inorganic carbon was not detected, but since ultrapure water was used in the sample preparation it was assumed that little to no inorganic carbon was present and the TOC measurements following this method were accurate.

### **Nessler Method**

The concentration of ammonia in the final solutions was determined through Nesslerization. 10 mL of the final solutions were placed in test tubes. Two drops of polyvinyl alcohol, a dispersing agent, and two drops of a mixture of potassium sodium tartrate and sodium citrate, mineral stabilizers, were added to each sample. 400  $\mu$ L of Nessler reagent ( $K_2[HgI_4]$ ) was added to each sample. The absorbance at  $\lambda=425$ nm was measured by a DR/2400 portable Spectrophotometer (HACH, US-CO). The resulting absorbance was multiplied by a factor determined from a linear calibration curve that determined the concentration of ammonia in the sample.

### **Ion Chromatography**

Nitrates were measured by ion chromatography. 2 mL of sample was collected from the final solutions and filtered through a 0.45  $\mu$ m syringe filter.(VWR, US-PA) Samples were tested on Dionex chromatography system including a dual pump, eluent generator, and detector modules.

An IonPac AS18 column (Dionex, US-CA) was used for the separation of anions and the anions were detected through conductivity.

## Toxicity

The toxicity of the dyes was compared using a lettuce test. Two samples of each dye were used, one prior to the experiment and one following the experiment. A mineral water sample (Vittel) was used as a normal control and a salt water sample was used as a negative control.

Each sample was tested in its own container. A piece of absorbent paper was placed at the bottom of the container, 3 mL of the sample was added to the container, eight lettuce seeds were placed on the absorbent paper, the container was covered with aluminum foil, four small holes were made in the aluminum foil, and the container was placed in a heated cabinet at approximately 25°C for five days.

At the end of the five days, the containers were opened and analyzed. The number of germinated seeds was counted and the length of each germinated seed root was measured. If a seed did not germinate, the length of “0.0 cm” was not included in the average length calculation. The average length of seed roots in each dye sample was measured and compared to the controls. The greater the difference between the length of the dye sample roots and the normal control, the more likely that there were toxic chemicals in the water.

The two main goals of this experiment were to 1) identify and compare initial toxicities and 2) calculate and compare toxicity removal for each of the dyes. In order to make these comparisons, each sample was assigned a relative toxicity, RT, based on the lengths of the germinated seeds. The relative toxicity of any given solution is defined by Equation 3: Relative Toxicity.

### Equation 3: Relative Toxicity

$$RT = \frac{L_{Water} - L_{Solution}}{L_{Water} - L_{SaltWater}}$$

where ‘L’ is the average length of the germinated seeds for the particular sample. From this equation, the relative toxicity of pure water is zero and the relative toxicity of salt water is 100. Using the relative toxicity, the change in toxicity of the solutions was calculated using Equation 4: Change in Toxicity. If  $\Delta RT$  is positive, toxicity increased; if  $\Delta RT$  is negative, toxicity decreased.

#### Equation 4: Change in Toxicity

$$\Delta RT = RT_{Final} - RT_{Initial}$$

## Results and Discussions

### Method Development

The Direct Red 81 samples taken from the reservoir for the method development were tested in the UV-Vis spectrophotometer with a spectrum analysis from 200-700nm, the UV-Vis spectrum absorbance for direct red 81 is shown in Figure 6. The concentration in the reservoir was monitored using the absorbance at 510 nm since it was the highest peak for the Direct Red 81. Figure 7 shows the results for the dye concentration over time. Using the integrated rate law derived in the background, a linear trend line fitted the data well. In most cases, the  $R^2$  value was greater than 0.98 with the lowest value of 0.952. This indicated that the assumption of the equilibrium term  $K*C$  being negligible was correct due to the linearity of the data.  $k_{app}$  (1/min), the apparent first-order rate constant, was used to compare rates for each experiments and are summarized in Figure 8.

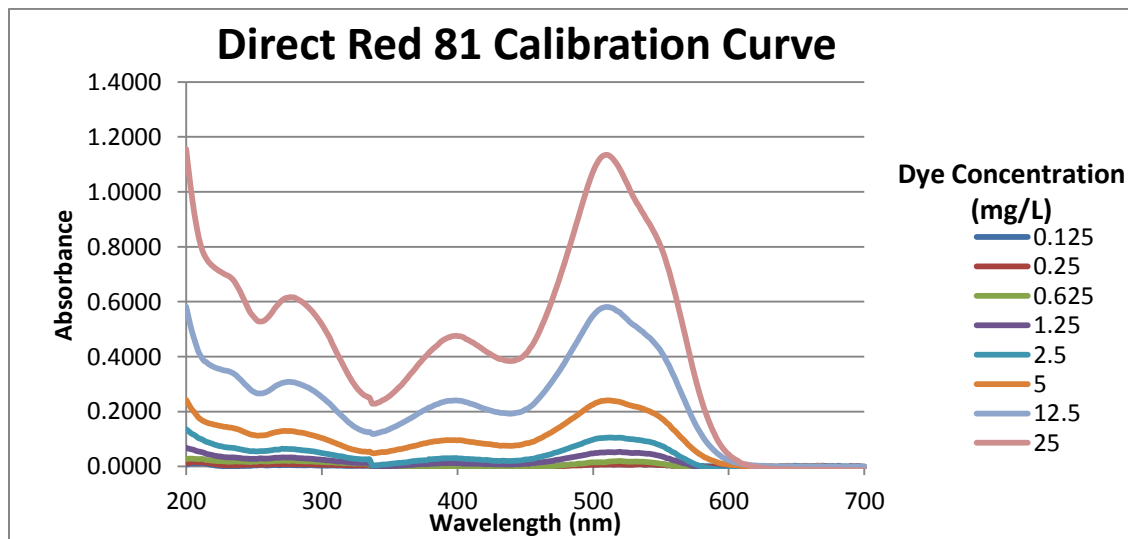


Figure 6: Absorbance spectrum of Direct Red 81

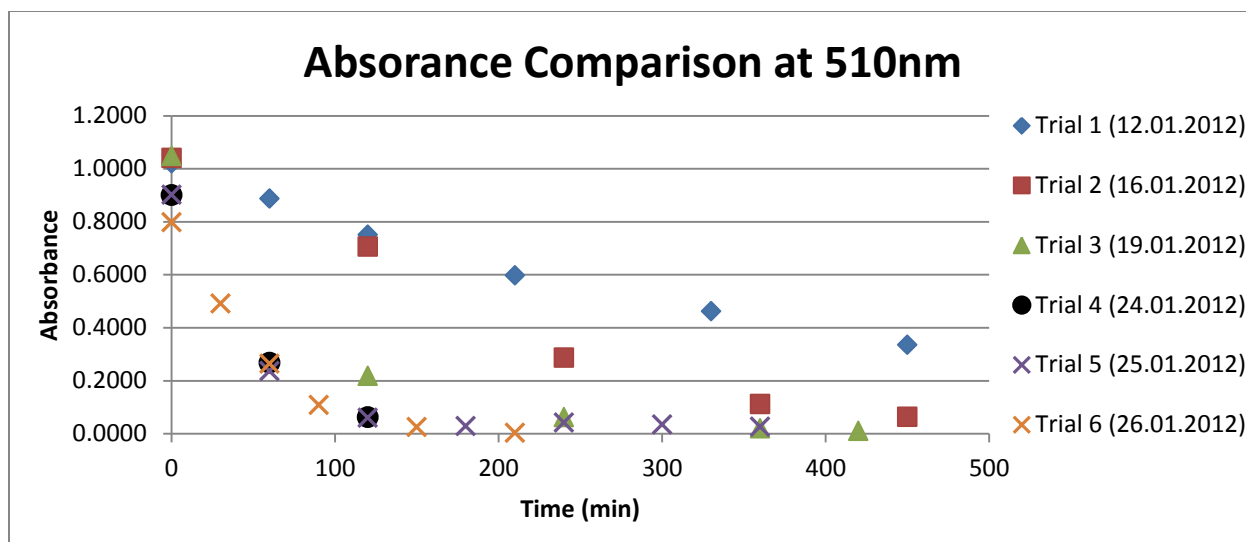


Figure 7: Graph showing decrease in concentration of Direct Red 81 over time in the six trials.

It was found that  $k_{app}$  increased for the first three trials. It was theorized that the down time between experiments with the UV lamps off could be influencing the reaction rate. It is understood that the irradiated  $TiO_2$  becomes hydrophilic and after two hours of exposure to UV light, the contact angle is reduced to zero. (Kazuhito Hashimoto 2005) Removing the source of UV light caused the photoactivated  $TiO_2$  to lose its hydrophilic properties but at a very slow rate. So depending on the duration of time the  $TiO_2$  was in the dark, the initial mass transfer and adsorption rates may be affected. The amount of time between trials one, two and three followed this pattern, as there was less down time between experiments as work progressed.

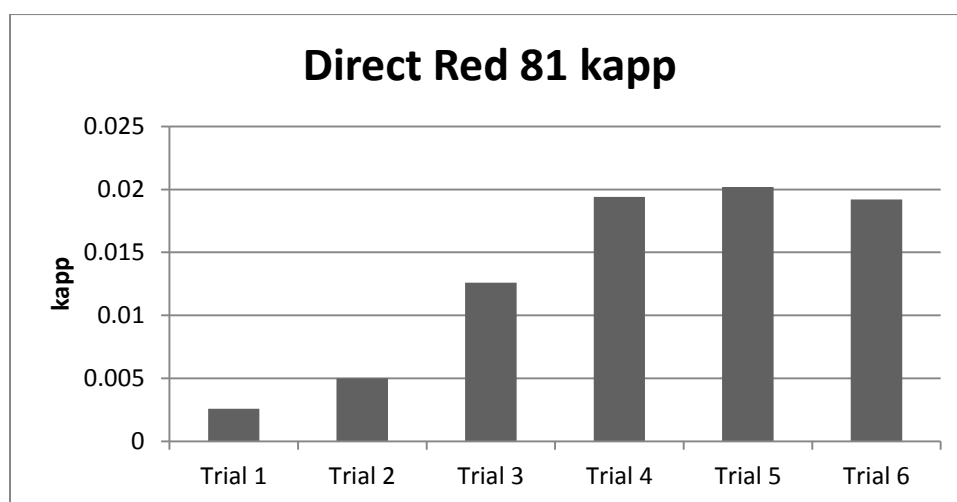


Figure 8:  $k_{app}$  of Direct Red 81 for method development



To test this theory trial four was started three days after the UV lamps had been turned off, this was longer than any down time between experiments. Therefore, it was expected that the reaction rate would decrease when compared to trial two and three. The  $k_{app}$  for trial four increased from trial three suggesting that rest periods may not be affecting the reaction rate as originally proposed so another explanation was tested.

Previous studies have used hydrogen peroxide to improve the photocatalytic rates for  $\text{TiO}_2$ . (Mahmoodi, Arami et al. 2005) Hydrogen peroxide was used in our cleaning method and some of the hydrogen peroxide might have been retained in the reactor despite the washing. Or the hydrogen peroxide might be reacting with  $\text{TiO}_2$  binding agent with the paper somehow. To test this theory two more trials were carried out without using hydrogen peroxide in the cleaning procedure. The reaction rate for trials four, five and six remained close to constant when compared to each other. Consistent results were finally achieved and a method could be established to compare the azo dyes to one another. These results supported the theory that the hydrogen peroxide used in the cleaning after experiments was affecting the reaction rate of the following experiment. It should be noted that the actual cause for the shift in reaction was not fully understood and the actual effect of hydrogen peroxide on the system was not investigated further. For the kinetics experiments, hydrogen peroxide was not used for cleaning and the UV lamps were left on between experiments to ensure that light exposure would not be a factor.

## Kinetics

All tested azo dyes achieved complete discoloration. The color of the solution was monitored with the UV-Vis spectrometer and Figure 9 is an example of the results from the UV-Vis spec. Each dye had a distinct peak in the visible light range where absorbance was greatest. These peaks were used to monitor the concentration of the dye in the solution over time. The longer the solution was in the reactor the more color reduction there was. This is seen in the reduction of the absorbance of the large peak. Eventually the UV-Vis spec would not be able to detect any absorbance at the peak and thus complete discoloration had occurred. Using the linear concentration curves developed for each dye, the concentration of dye in the solution was interpolated. Knowing the dye concentration over time allowed better analysis for the kinetics. All UV-Vis spec. graphs used in the analysis are included in the appendix.

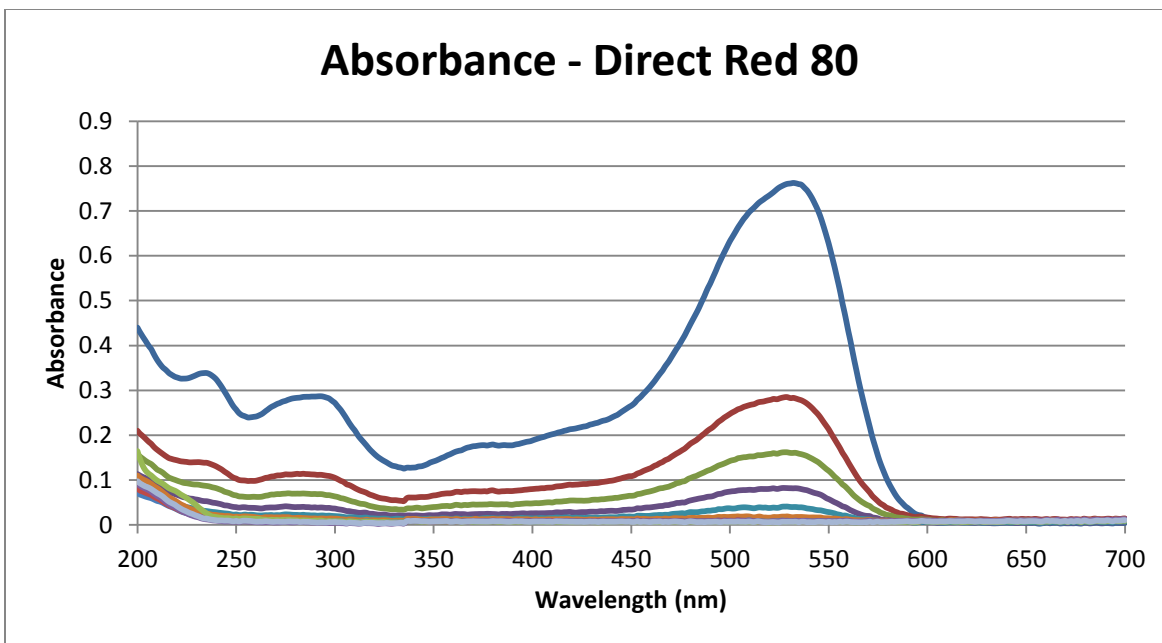


Figure 9: Example of UV-Vis spec. results for azo dyes. The absorbance decreases as time increases. The wavelength where absorbance was greatest, was used for determining concentration.

Figure 10 summarizes the results of the kinetics experiments. The pseudo-first order reaction constant was found from the semi-log plot of the natural log of the original concentration over the concentration versus time. The slope of the line was the reaction constant and the adsorption coefficient grouped together, called  $k_{app}$  for the purpose of this report. The larger the  $k_{app}$ , the faster the reaction occurred.  $k_{app}$  was important for ranking dyes based on their reaction rates. Once the dyes were organized, that was analyzed in order to establish a trend in the rate based on the dye structures.

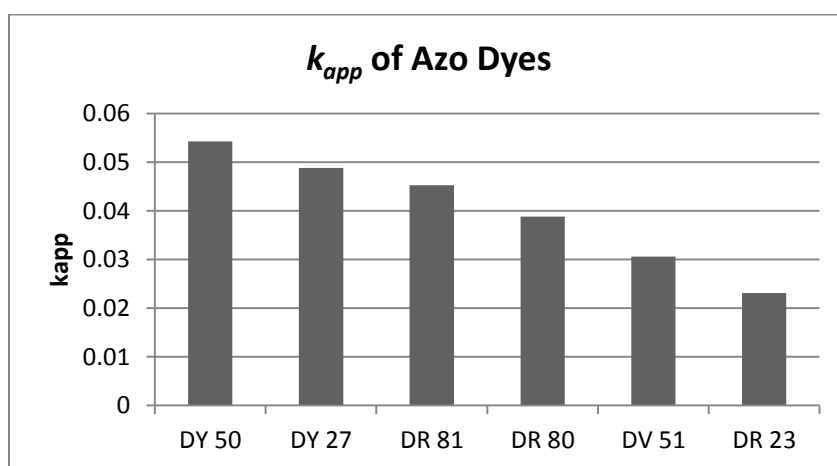


Figure 10: Results of kinetics study.  $k_{app}$  used to compare reaction rates between dyes.

Table 3 lists the dyes fastest to slowest as well as significant structural features of the dyes. At first it appeared that the rate of degradation for the dyes is random but upon closer observation a pattern emerged. It was clear from the data that one structural feature did not control the rate of color removal, rather it was a combination of features that determined the rate. One of these features was the negatively charged sulfate groups. A common group found in azo dyes the sulfate groups make the dye molecule more polar, which in turn increases the solubility of the organic molecule in the inorganic solvent water. These findings agreed with a previous study on acid azo dyes.(Muthukumar, Sargunamani et al. 2005) The increased solubility would improve the mass transfer between the dye and surface of the catalyst. This would explain why Direct Red 80, the largest dye molecule, was still faster in degradation than some of the smaller molecules, and why Direct Yellow 50 was the fastest in discoloration.

**Table 3: Dye kapp and structural features**

<b>Dye</b>	<b>kapp</b>	<b>Sulfates</b>	<b>Azo groups</b>	<b>Rings</b>
<b>DY 50</b>	0.0543	4	2	6
<b>DY 27</b>	0.0488	2	1	4
<b>DY 81</b>	0.0453	2	2	4
<b>DR 80</b>	0.0389	6	4	8
<b>DV 51</b>	0.0306	2	2	5
<b>DR 23</b>	0.0231	2	2	6

What is interesting in these findings, is the presence of anions has been shown to inhibit the rate of degradation,(Özkan, Özkan et al. 2004) but in these finding when the negatively charged groups are on the molecule they appear to increase the rate. A possible explanation for this phenomenon is the better-dissolved dye molecule has better mass transfer with the surface of the catalyst and the free hydroxyl radicals in the solution. When the sulfate groups do become free, there may be so many active sites on the catalyst that a few occupied sites by the sulfate groups do little to inhibit the reaction.

The number of azo groups also appeared to influence the degradation rate. Most of the azo dyes studied had at least two azo bonds except for Direct Yellow 27. The impact of the number of azo groups has been seen before in previous studies that concluded similar results, the more azo groups the longer the reaction.(Shu and Huang 1995; Tanaka, Padermpole et al. 2000)

The number of aromatic rings also seemed to be another factor. When comparing the dye molecules that have the same number of sulfates and azo groups the rates arranged themselves

fastest to slowest based on the number of rings. This makes sense logically since the greater number on bonds that need to be oxidized the longer it will take to degrade the molecule.

## Total Organic Carbon

Table 4: Total Organic Carbon Tests

Dye	Initial TOC (mg/L)	Final TOC (mg/L)	% removed	Content
Direct Red 23	2.194	0.8618	60.7 %	30 %
Direct Red 80	2.966	0.3911	86.8 %	25 %
Direct Red 81	4.674	0.8462	81.9 %	50 %
Direct Violet 51	4.089	0.7401	81.9 %	50 %
Direct Yellow 27	4.465	0.3728	91.7 %	40 %
Direct Yellow 50	2.768	0.5875	78.8 %	40 %

Table 4 summarizes the results of the total organic carbon tests. The solutions contained at least 60% less organic carbon after running through the photocatalytic reactor for eight hours. Most solutions were reduced by at least 80%. The results show the destructive power of the photocatalytic reactor. The azo dyes in the initial solutions were reduced to carbon dioxide and water. The carbon dioxide escapes the reactor and explains the removal of organic carbon from the system. The percentage of removed organic carbon appears to depend on the rate of reaction as well as the size of the molecule. The color from the samples had been removed for several hours before TOC samples were collected. These results suggested that the azo bond is the primary target of the hydroxyl radicals. The color was removed early in the reaction from the breaking of the azo bond but the byproducts remained in the system and continued to oxidize.

Initial organic carbon concentrations vary between dyes even though solutions were prepared at equal concentrations of 25 mg/L. The differences are related to the dye content of the dye powders from the suppliers. Also, the dye structures contain different amounts of carbon.

## Ammonia and Nitrate

Figure 11 summarizes the results for the presence of ammonia anions. Each tested sample was the final product after eight hours of testing in the reactor. DR 23F was a sample collected after the reactor was run overnight. The concentration of ammonia in the final solution was dependent on the number of nitrogen atoms in the dye structure as well as the rate of the reaction. The faster reactions tended to have lower concentrations of ammonia in the final solution than the slower reactions. The formed ammonia molecules continued to oxidize, eventually becoming nitrates ( $\text{NO}_3^-$ ). The reduction of ammonia and formation of nitrate from the sample collected after eight hours and the sample collected the following morning of Direct Red 23 supported this theory. It

appears though the oxidation of ammonia was a slow reaction, since a small decrease in the concentration of ammonia was observed.

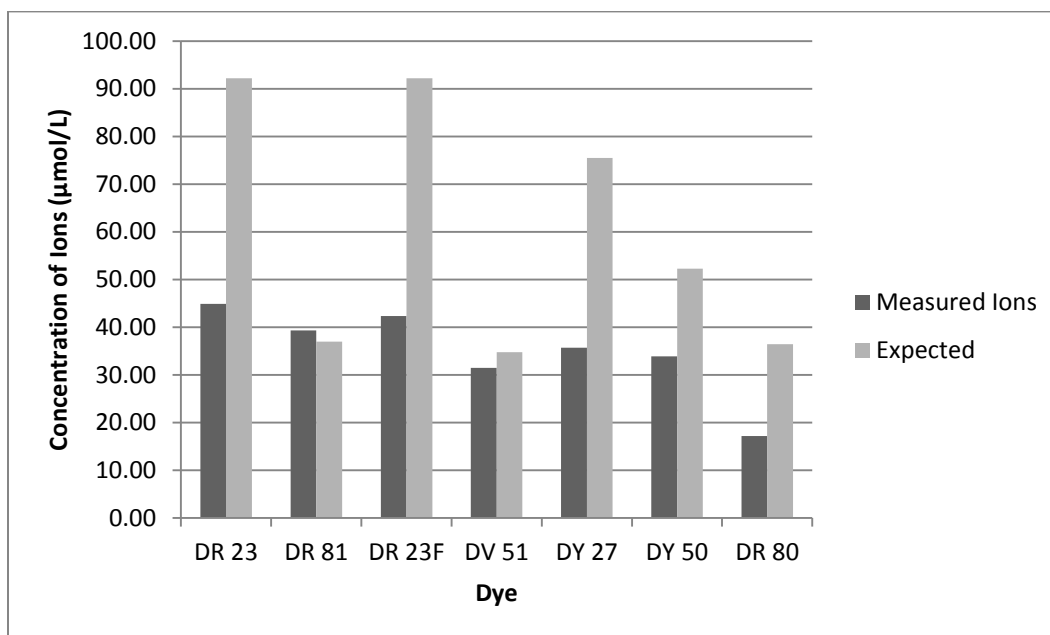
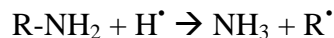
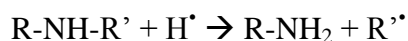


Figure 11: Presence of ions comparison

Previous research by Herrmann et al. went into significant detail on the evolution of ammonia and nitrates in the photocatalysis of azo dyes. (Lachheb, Puzenat et al. 2002) They showed strong evidence that the process favors the formation of nitrogen gas over ammonia and nitrate as the concentration of the ions was far below the expected value. Ammonia can be generated following protonation reactions of nitrogen bonds.



The ammonia can then be oxidized to nitrates by hydroxyl radicals. Assuming all the nitrogen molecules not in the azo bonds were converted to ammonia, the expected concentration of ammonia was predicted. Sample calculations can be found in Appendix E. For all cases except for Direct Red 81, the measured amount of ammonia and nitrates was below the potential maximum amount of ions. The difference between the measured ions and the expected were

typically large. Less ammonia and nitrates in the product effluent was beneficial since there would be less impact on aquatic life.

### SEM Analysis

SEM Analysis on the paper substrate before and after experiments should show a reduction in the amount of carbon present on the sample. A likely source of carbon would be a binding agent for the  $\text{SiO}_2$  and  $\text{TiO}_2$ . After continuous use of the paper, some of the binding agent might have washed away. This could explain why the reaction rates increased after uses, as more catalyst was exposed as the binder was removed. Some  $\text{SiO}_2$  and  $\text{TiO}_2$  might have washed away as well but in the end the SEM analysis showed that the weight ratios of  $\text{SiO}_2$  and  $\text{TiO}_2$  increased with  $\text{TiO}_2$  almost doubling in percentage from 6.42% to 10.29%.

### Toxicity

To test for toxicity, lettuce seed growth test was performed in pure water, salt water, and the initial and final solutions of the tested dyes. Figure 12: Lettuce Test Samples shows all 14 samples on Day Zero, prior to being placed in the heated cabinet (at  $25^\circ\text{C}$ ), and the initial and final Direct Violet 51 samples on Day 5.

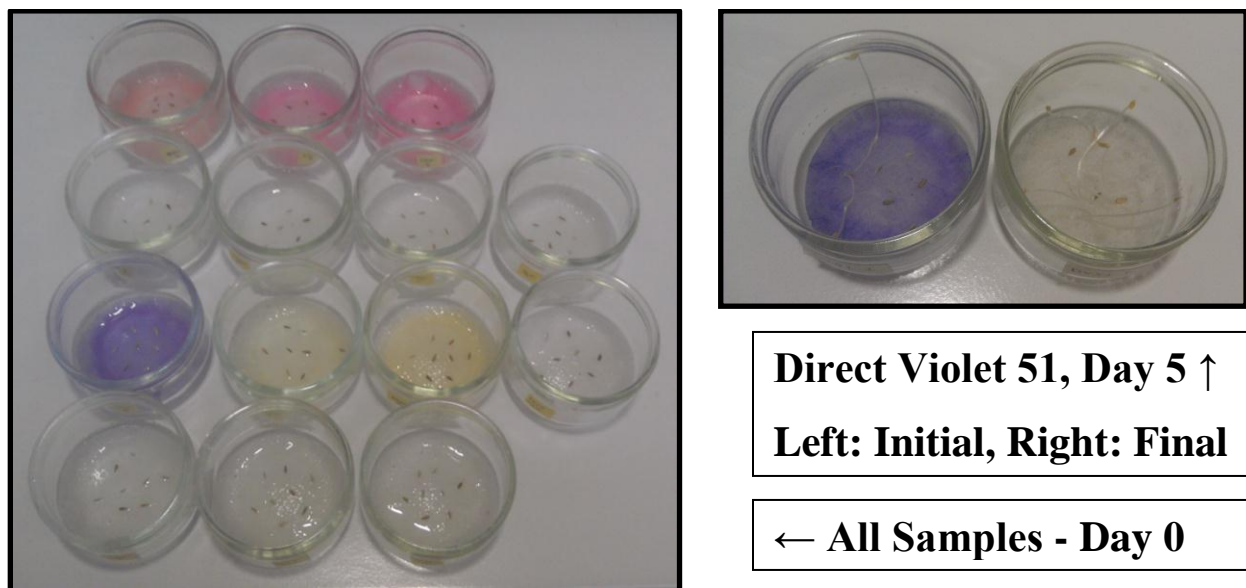


Figure 12: Lettuce Test Samples

When the samples were removed from the heated oven, the lengths of the germinated seeds were recorded. The data table for all of the seed lengths can be found in

Appendix B: Lettuce Test. Figure 13: Relative Toxicity Comparison of Initial Dye compares the initial relative toxicities of the dyes. The relative toxicities were calculated by Equation 3: Relative Toxicity. Since the length of the germinated seeds in water sample was lower than several other samples, indicating a higher toxicity, the actual length of the water sample was not used in the relative toxicity equation. Instead, 5.0 cm was used as the base length as it was greater than all the other average lengths. The seeds in the saltwater sample did not grow as expected and was used as the bottom baseline. Using this calculation, the dye with the highest initial relative toxicity was Direct Yellow 50 and the dye with the lowest relative toxicity was Direct Violet 51.

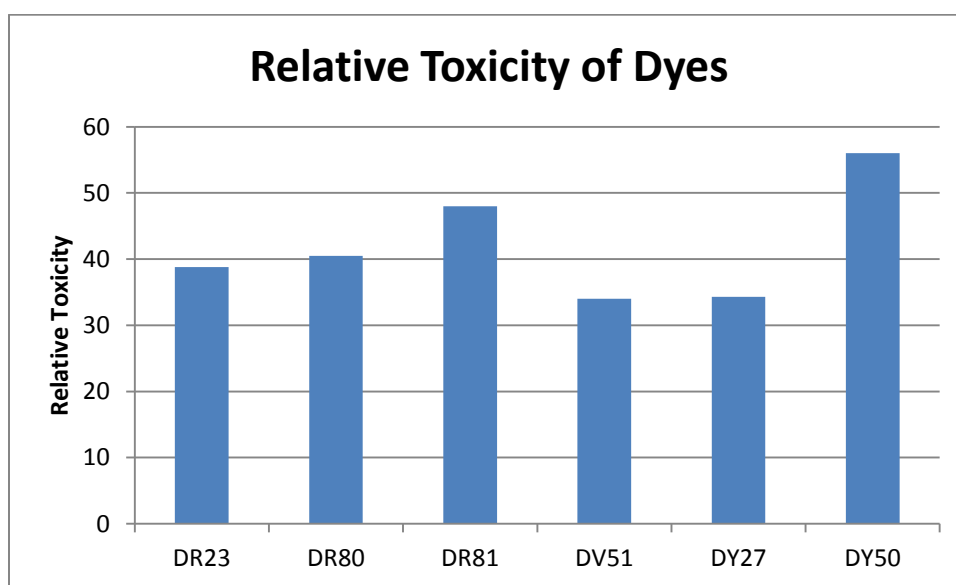


Figure 13: Relative Toxicity Comparison of Initial Dye Solutions

Two types of toxicity were considered for the lettuce test analysis: azo dye and aromatic amine products. For samples taken at the beginning of a trial, the toxicity was attributed to the azo dyes. During the trials, the azo dyes degraded and aromatic amines were produced. Since UV-Vis spectroscopy analysis showed that the dyes had completely degraded, the toxicity of the samples taken at the end of a trial was attributed to the aromatic amines. Therefore, the comparison of toxicity from beginning to end of a trial gave insight into what was more toxic, the azo dyes or aromatic amines produced during azo dye degradation.

The comparison of toxicity removal between the initial and final sample for each dye is shown in Figure 14: Toxicity Removal Comparison of Dyes. The change in toxicity used for the comparison was calculated by Equation 4: Change in Toxicity. The only two dyes that decreased

in toxicity were Direct Violet 51 and Direct Yellow 27 which had the greatest toxicity removal of all the dyes. Direct Red 23, 80, and 81 and Direct Yellow 50 all increased in toxicity. Direct Red 23 had the great increase in toxicity.

It is known that varying structure of dyes yield different toxicities.(Cancer 2010) However, in addition to the large source of error, the small sample of dyes included in the test—each with very different structures—did not allow for a detailed analysis of toxicity compared to structural features. At this point in the experimental series, the most important result was that not all dyes decreased in toxicity between initial and final exposure to the reactor.

It is challenging to compare toxicity of the dye solutions between studies due to the relative nature of studies. For example, in a study of toxicity reduction of textile wastewater using E. coli cultures, performed at Universidade Estadual de Campinas in Brazil, the maximum toxicity removal by photocatalysis was 50%,(Gomes de Moraes, Sanches Freire et al. 2000) very different results from those obtained during this study.

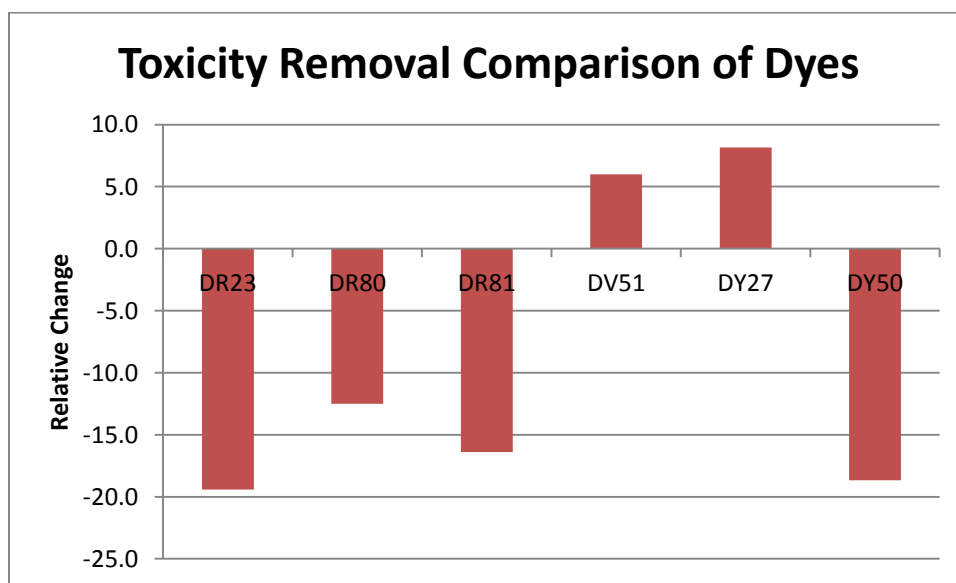


Figure 14: Toxicity Removal Comparison of Dyes

One of the reasons textile wastewater is treated is to remove any toxic components. If a treatment method results in a more toxic product, the treatment method may be considered ineffective. Since the photocatalytic treatment method does not consistently produce a solution with decreased toxicity, it would be necessary to incorporate a secondary treatment method. Biological treatment methods show promise; as the majority of the colorant would be removed



prior to this secondary treatment, the biological treatment disadvantage of being unable to process large volumes of colorant effluents would not be a concern.(Anjaneyulu, Sreedhara Chary et al. 2005)

In a study at the Université de Rennes 1 in Rennes, France, the treatment of azo dyes has been reported coupling photocatalysis and biological treatment. A commercial strain of *P. fluorescens* Migula 1895 was cultivated with glucose, yeast extract, and the considered azo dye. Samples were taken at regular time intervals and analyzed using UV-Vis spectroscopy to monitor dye degradation. The study confirmed the feasibility of integrating these two treatment methods.(Brosillon, Djelal et al. 2008)

## Conclusions

Six direct azo dyes were successfully degraded and the color completely removed from all solutions. However, the dye molecules were not completely degraded after eight hours of photocatalysis. TOC results showed that organic compounds remained in the solution, but the amount of organic carbon was reduced significantly suggesting the oxidation of the dye molecules to carbon dioxide gas. As expected, ammonia and nitrate ions were produced during the mineralization of the compounds. The concentration of the ions was far below the highest possible concentration that could be achieved from the degradation, suggesting the favored reaction was the conversion to nitrogen gas.

The kinetics of the reaction varied between dyes. All dyes followed a pseudo-first order reaction based on the linear relation of the  $\ln(C_0/C)$  versus time. It was theorized that the difference in reaction rates was based on the different structural features in each dye. Sulfate groups increased reaction rates possibly by increasing the solubility and thus the mass transfer between the dye and the hydroxyl radicals. Discoloration was achieved long before total degradation of the dye molecules suggesting that the azo bond is the primary target of the hydroxyl radicals. A higher number of azo bonds resulted in a longer reaction time. Molecules containing larger numbers of aromatic rings took longer to oxidize than the smaller molecules. These results suggested that the oxidation of aromatic rings was a much slower reaction than the oxidation of the azo bond, so larger molecules will take longer to completely mineralize. It was concluded that not one structural characteristic controlled the reaction rate entirely, but rather a combination of features influenced the kinetics.

Toxicity results showed that the majority of the dyes increased in toxicity meaning the degradation by-products, the aromatic amines produced during dye degradation, were more toxic than the dyes themselves. To better understand the varying results, further trials should be performed to study the effects of specific dye structural features on toxicity change. In order to decrease toxicity in the dye solutions, a biological secondary treatment was recommended.

## References

- Agency, E. P. (2011). "Water: Monitoring & Assessment." Retrieved Feb. 1st, 2012.
- Aguedach, A., S. Brosillon, et al. (2005). "Photocatalytic degradation of azo-dyes reactive black 5 and reactive yellow 145 in water over a newly deposited titanium dioxide." Applied Catalysis B: Environmental **57**(1): 55-62.
- Alves de Lima, R. O., A. P. Bazo, et al. (2007). "Mutagenic and carcinogenic potential of a textile azo dye processing plant effluent that impacts a drinking water source." Mutation Research/Genetic Toxicology and Environmental Mutagenesis **626**(1–2): 53-60.
- Anjaneyulu, Y., N. Sreedhara Chary, et al. (2005). "Decolourization of Industrial Effluents – Available Methods and Emerging Technologies – A Review." Reviews in Environmental Science and Biotechnology **4**(4): 245-273.
- Augugliaro, V., C. Baiocchi, et al. (2002). "Azo-dyes photocatalytic degradation in aqueous suspension of TiO<sub>2</sub> under solar irradiation." Chemosphere **49**(10): 1223-1230.
- Baptista, R. J. (2007). "Brooklyn, New York Dye Industry." Retrieved January 19, 2012, from <http://colorantshistory.org/BrooklynDyeIndustry.html>.
- Brosillon, S., H. Djelal, et al. (2008). "Innovative integrated process for the treatment of azo dyes: coupling of photocatalysis and biological treatment." Desalination **222**(1–3): 331-339.
- Brown, M. A. and S. C. De Vito (1993). "Predicting azo dye toxicity." Critical Reviews in Environmental Science and Technology **23**(3): 249-324.
- Cancer, W. H. O.-I. A. f. R. o. (2010). "General Introduction to the Chemistry of Dyes." IARC Monographs on the Evaluation of Carcinogenic Risks to Humans **99**: 55-67.
- Daneshvar, N., D. Salari, et al. (2003). "Photocatalytic degradation of azo dye acid red 14 in water: investigation of the effect of operational parameters." Journal of Photochemistry and Photobiology A: Chemistry **157**(1): 111-116.
- de Aragão Umbuzeiro, G., H. S. Freeman, et al. (2005). "The contribution of azo dyes to the mutagenic activity of the Cristais River." Chemosphere **60**(1): 55-64.
- "Direct Dyes." Retrieved 12 January, 2012, from <http://www.dyescolours.com/direct-dyes.html>.
- Dorner, M. (2002). "Early Dye History and the Introduction of Synthetic Dyes Before the 1870s." Silk Circa 1840 Retrieved 12 January, 2012, from <http://www.smith.edu/hsc/silk/papers/dorner.html>.
- EPA (1972). Federal Water Pollution Control Act. 33 U.S.C. 1251. U. S. E. P. Agency.
- Falck, G., H. Lindberg, et al. (2009). "Genotoxic effects of nanosized and fine TiO<sub>2</sub>." Hum Exp Toxicol **28**(339).
- Fisher, S. G. and G. E. Likens (1973). "Energy Flow in Bear Brook, New Hampshire: An Integrative Approach to Stream Ecosystem Metabolism." Ecological Monographs **43**(4): 421-439.
- Fogler, H. S. (2005). Elements of Chemical Reaction Engineering, Prentice Hall.
- Gomes de Moraes, S., R. Sanches Freire, et al. (2000). "Degradation and toxicity reduction of textile effluent by combined photocatalytic and ozonation processes." Chemosphere **40**(4): 369-373.
- Haddad, P. R. and P. E. Jackson (1990). Ion chromatography: principles and applications, Elsevier.
- Hund-Rinke, K. and M. Simon (2006). "Ecotoxic Effect of Photocatalytic Active Nanoparticles (TiO<sub>2</sub>) on Algae and Daphnids (8 pp)." Environmental Science and Pollution Research **13**(4): 225-232.
- Jackson, P. E. (2000). Ion Chromatography in Environmental Analysis. Encyclopedia of Analytical Chemistry. R. A. Meyers. Chichester, John Wiley & Sons Ltd.: 2779-2801.
- Kazuhito Hashimoto, H. I., Akira Fujishima (2005). "TiO<sub>2</sub> Photocatalysis: A Historical Overview and Future Prospects." Japanese Journal of Applied Physics **44**(12): 8269-8285.

- Khataee, A. R., M. N. Pons, et al. (2009). "Photocatalytic degradation of three azo dyes using immobilized TiO<sub>2</sub> nanoparticles on glass plates activated by UV light irradiation: Influence of dye molecular structure." Journal of Hazardous Materials **168**(1): 451-457.
- Konstantinou, I. K. and T. A. Albanis (2004). "TiO<sub>2</sub>-assisted photocatalytic degradation of azo dyes in aqueous solution: kinetic and mechanistic investigations: A review." Applied Catalysis B: Environmental **49**(1): 1-14.
- Kurbiel, J. (1978). Removal of Color, Detergents, and Other Refractory Substances from Textile Wastewater, Polish Institute of Meteorology and Water Management.
- Lachheb, H., E. Puzenat, et al. (2002). "Photocatalytic degradation of various types of dyes (Alizarin S, Crocein Orange G, Methyl Red, Congo Red, Methylene Blue) in water by UV-irradiated titania." Applied Catalysis B: Environmental **39**(1): 75-90.
- Langmuir, I. (1918). "THE ADSORPTION OF GASES ON PLANE SURFACES OF GLASS, MICA AND PLATINUM." Journal of the American Chemical Society **40**(9): 1361-1403.
- Liu, C.-C., Y.-H. Hsieh, et al. (2006). "Photodegradation treatment of azo dye wastewater by UV/TiO<sub>2</sub> process." Dyes and Pigments **68**(2-3): 191-195.
- Lu, P.-J., C.-W. Chien, et al. (2010). "Azo dye degradation kinetics in TiO<sub>2</sub> film-coated photoreactor." Chemical Engineering Journal **163**(1-2): 28-34.
- M.N, M. (2006). "Do nanoparticles present ecotoxicological risks for the health of the aquatic environment?" Environment International **32**(8): 967-976.
- Mahmoodi, N. M., M. Arami, et al. (2005). "Decolorization and aromatic ring degradation kinetics of Direct Red 80 by UV oxidation in the presence of hydrogen peroxide utilizing TiO<sub>2</sub> as a photocatalyst." Chemical Engineering Journal **112**(1-3): 191-196.
- Muthukumar, M., D. Sargunamani, et al. (2005). "Statistical analysis of the effect of aromatic, azo and sulphonic acid groups on decolouration of acid dye effluents using advanced oxidation processes." Dyes and Pigments **65**(2): 151-158.
- Nessler, J. (1868). "Ueber Bestimmung des Ammoniaks und der Salpetersäure in sehr verdünnten Lösungen." Fresenius' Journal of Analytical Chemistry **7**(1): 415-416.
- Pelton, R., X. Geng, et al. (2006). "Photocatalytic paper from colloidal TiO<sub>2</sub>—fact or fantasy." Advances in Colloid and Interface Science **127**(1): 43-53.
- Pinheiro, H. M., E. Touraud, et al. (2004). "Aromatic amines from azo dye reduction: status review with emphasis on direct UV spectrophotometric detection in textile industry wastewaters." Dyes and Pigments **61**(2): 121-139.
- Pizarro, P., C. Guillard, et al. (2005). "Photocatalytic degradation of imazapyr in water: Comparison of activities of different supported and unsupported TiO<sub>2</sub>-based catalysts." Catalysis Today **101**(3-4): 211-218.
- Price, H. (2002). "Dye Classification." The Chemistry of Dyes Retrieved 12 January, 2012, from <http://www.chm.bris.ac.uk/webprojects2002/price/classify.htm>.
- Reutergårdh, L. B. and M. Iangphasuk (1997). "Photocatalytic decolourization of reactive azo dye: A comparison between TiO<sub>2</sub> and us photocatalysis." Chemosphere **35**(3): 585-596.
- Schumacher, B. A. (2002). Methods for the Determination of Total Organic Carbon (TOC) in Soils and Sediments. U. S. E. P. Agency. Las Vegas, NV, Ecological Risk Assessment Support Center.
- Scientific, T. Basic UV-Vis Theory, Concepts and Applications.
- Self, J. R. and R. M. Waskorn (2008). Nitrates in Drinking Water. Colorado, United States, Colorado State University Extension. **Fact Sheet No. 0.517**.
- Shimadzu Total Organic Carbon Analyzer.
- Shu, H.-Y. and C.-R. Huang (1995). "Degradation of commercial azo dyes in water using ozonation and UV enhanced ozonation process." Chemosphere **31**(8): 3813-3825.

- Slokar, Y. M. and A. Majcen Le Marechal (1998). "Methods of decoloration of textile wastewaters." Dyes and Pigments **37**(4): 335-356.
- Som, C., P. Wick, et al. (2011). "Environmental and health effects of nanomaterials in nanotextiles and façade coatings." Environment International **37**(6): 1131-1142.
- Staff, N. (2009). "Titanium Dioxide (TiO<sub>2</sub>) Nanoparticles In Household Products Linked To Cancer In Mice." Retrieved January, 18, 2012, from [http://www.science20.com/news\\_articles/titanium\\_dioxide\\_tio2\\_nanoparticles\\_household\\_products\\_linked\\_cancer\\_mice](http://www.science20.com/news_articles/titanium_dioxide_tio2_nanoparticles_household_products_linked_cancer_mice).
- Sweeny, E. A., J. K. Chipman, et al. (1994). "Evidence for Direct-acting Oxidative Genotoxicity by Reduction Products of Azo Dyes." Environ Health Perspect **102**(6): 119-122.
- Tanaka, K., K. Padermpole, et al. (2000). "Photocatalytic degradation of commercial azo dyes." Water Research **34**(1): 327-333.
- Tang, W. Z. and A. Huren (1995). "UV/TiO<sub>2</sub> photocatalytic oxidation of commercial dyes in aqueous solutions." Chemosphere **31**(9): 4157-4170.
- Textile School (2010). "Types of Dyes." Textile School Retrieved 12 January, 2012.
- Thiruvengkatahari, R., S. Vigneswaran, et al. (2008). "A review on UV/TiO<sub>2</sub> photocatalytic oxidation process (Journal Review)." Korean Journal of Chemical Engineering **25**(1): 64-72.
- University, M. S. "UV-Visible Spectroscopy." Retrieved 1/12/2012, 2012, from <http://www2.chemistry.msu.edu/faculty/reusch/VirtTxtJml/Spectrpy/UV-Vis/spectrum.htm#uv1>.
- Vitousek, P. M., J. D. Aber, et al. (1997). "HUMAN ALTERATION OF THE GLOBAL NITROGEN CYCLE: SOURCES AND CONSEQUENCES." Ecological Applications **7**(3): 737-750.
- Volk, C., L. Wood, et al. (2002). "Monitoring dissolved organic carbon in surface and drinking waters." Journal of Environmental Monitoring **4**: 43-47.
- Özkan, A., M. H. Özkan, et al. (2004). "Photocatalytic degradation of a textile azo dye, Sirius Gelb GC on TiO<sub>2</sub> or Ag-TiO<sub>2</sub> particles in the absence and presence of UV irradiation: the effects of some inorganic anions on the photocatalysis." Journal of Photochemistry and Photobiology A: Chemistry **163**(1-2): 29-35.

## Appendices

### Appendix A: UV Spectroscopy

**Key:**

Series 1: Trials were used to develop experimental method and varied in set-up.

DR81\_T1 to DR81\_T6

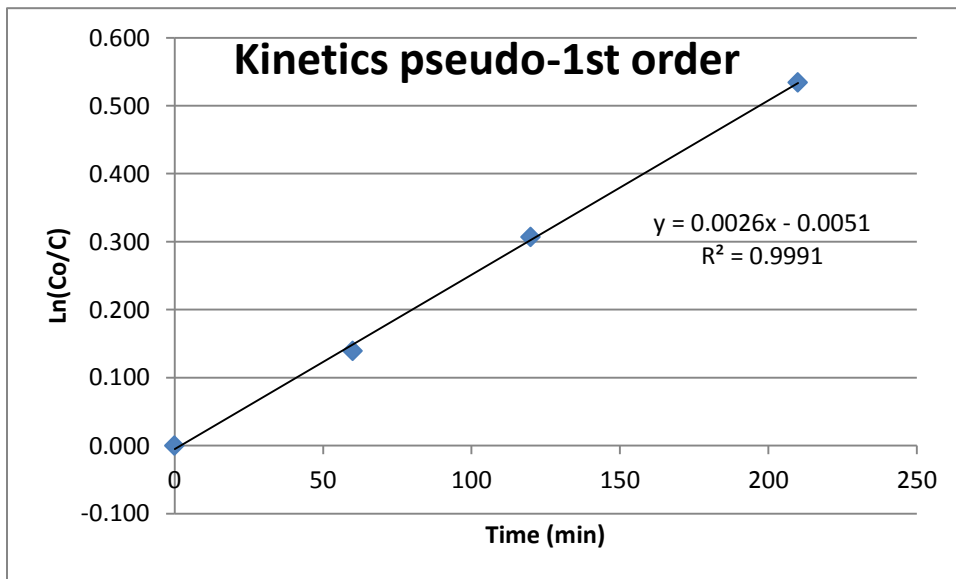
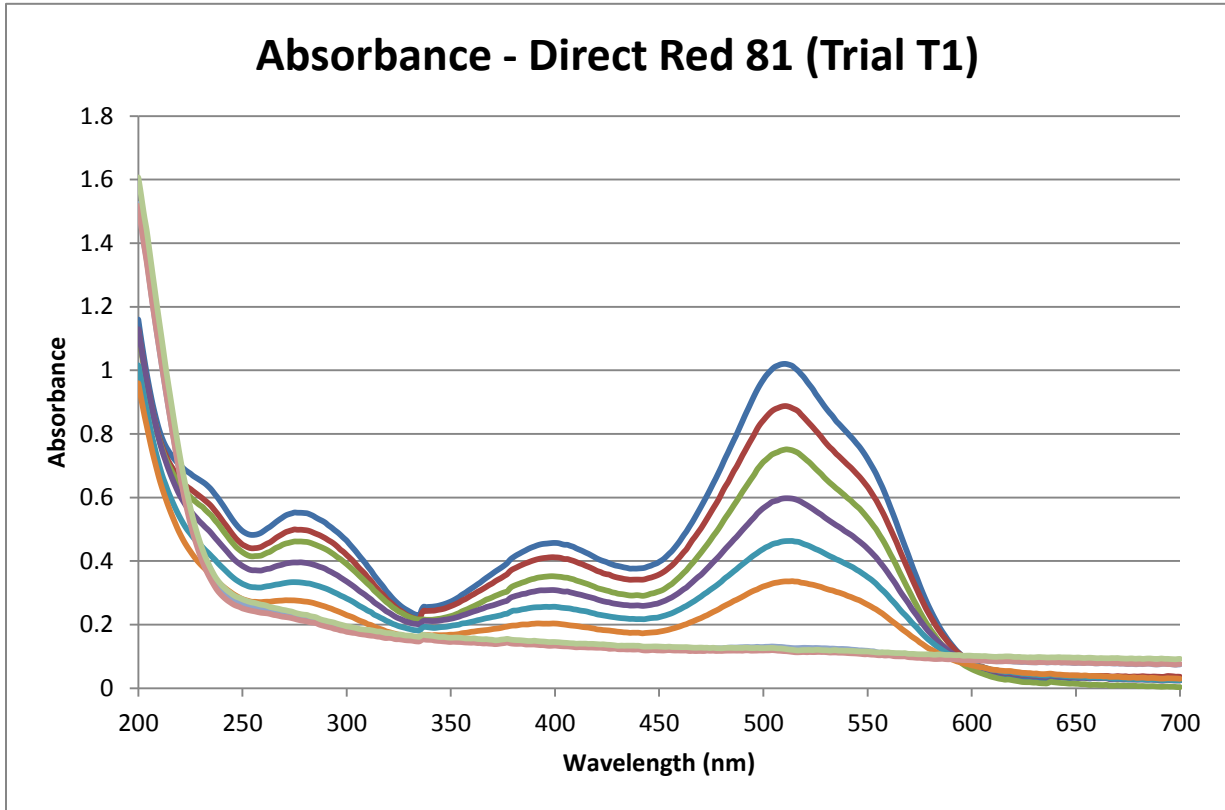
Series 2: Trials were run for up to 3 hours with samples taken every 15 minutes. UV light remained on for entire series and reactor was cleaned for at least an hour between trials.

DR23\_1, DR23\_2, DR80\_1, DR80\_2, DR81\_1, DR81\_2, DV51\_1, DV51\_2, DY27\_1, DY27\_2, DY50\_1, DY50\_2

Calibration Curves: Data was collected for all six dyes

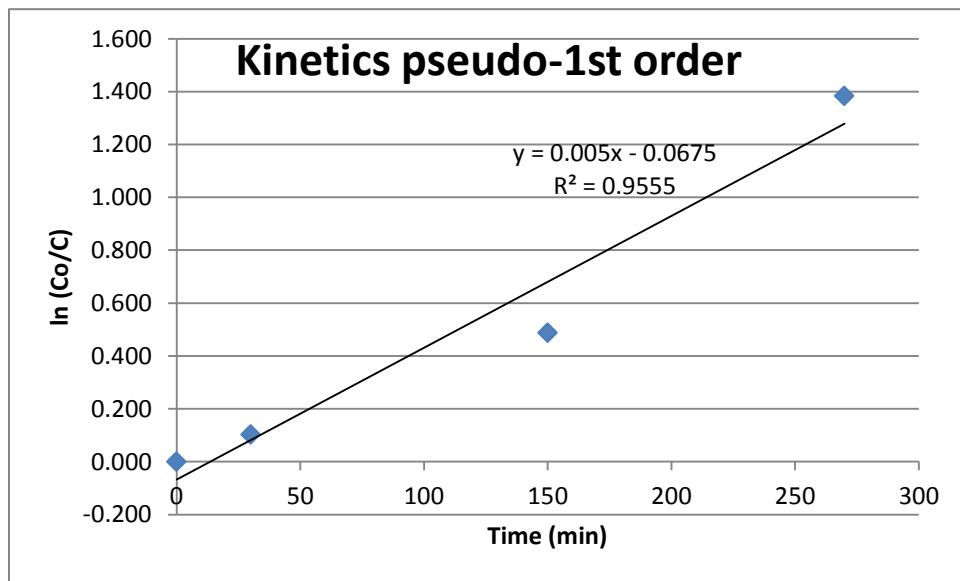
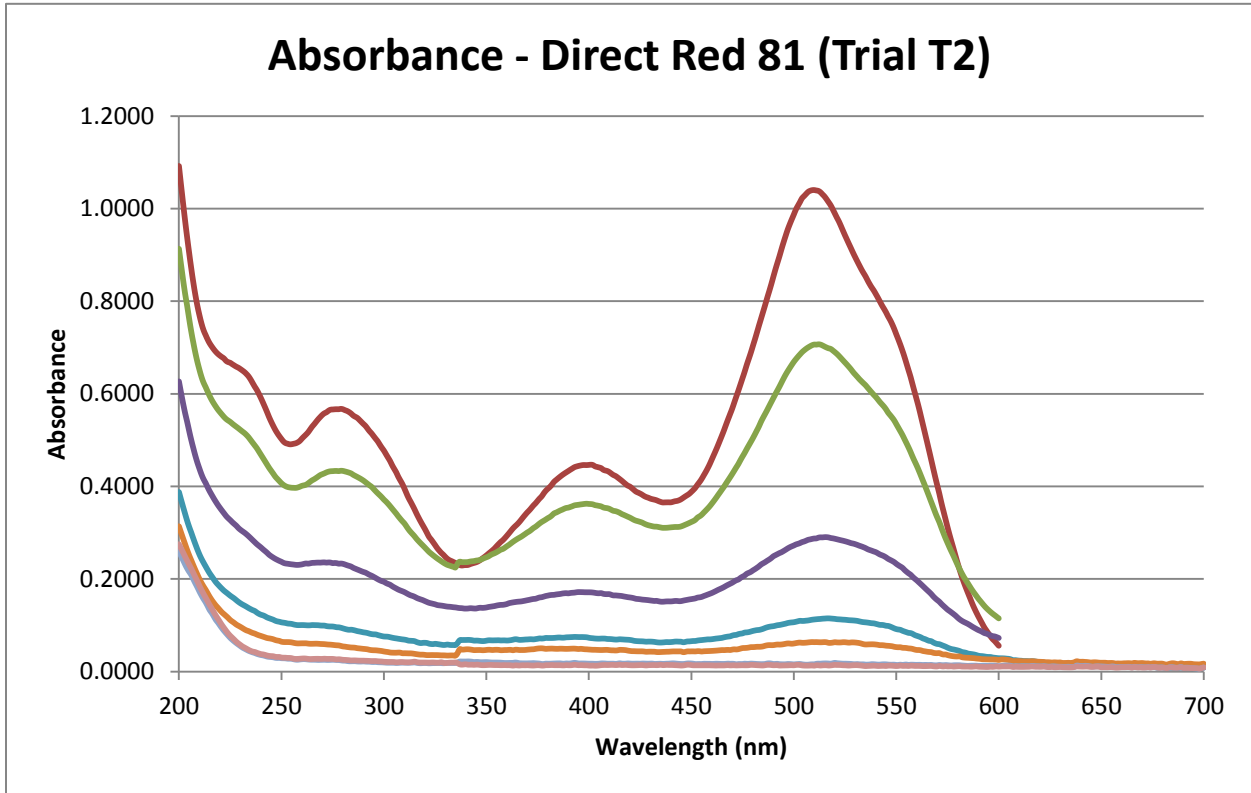
DR23\_C, DR80\_C, DR81\_C, DV51\_C, DY27\_C, DY50\_C

Sample	S1	S3	S5	S6	S7	S8	S9	S10	S11
Time	0	60	120	210	330	450	1365	1485	1665
Peak (at $\lambda_{max}$ )	1.020	0.887	0.750	0.597	0.462	0.336	0.129	0.117	0.124
Concentration	22.33	19.43	16.43	13.09	10.14	7.38	2.86	2.60	2.75
$\ln(C_0/C)$	0.000	0.139	0.307	0.534	0.789	1.107	2.054	2.152	2.093



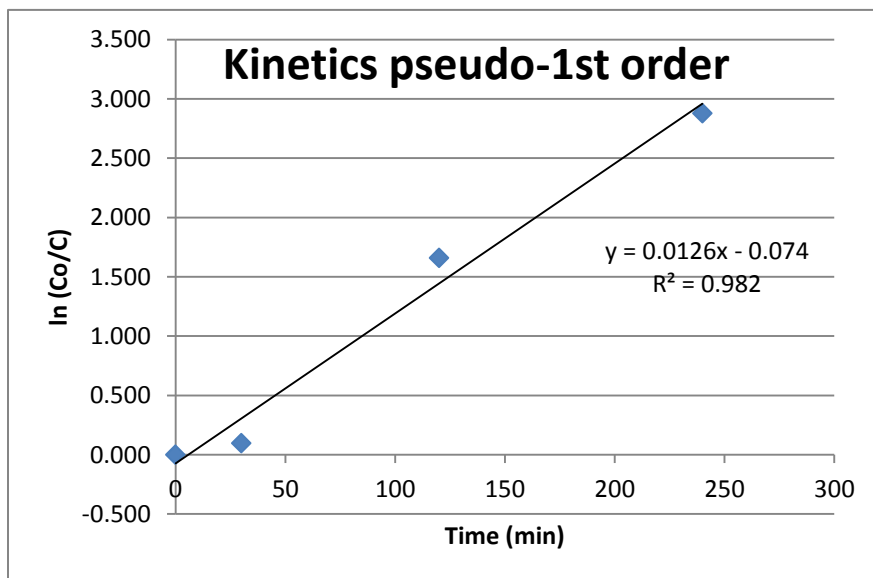
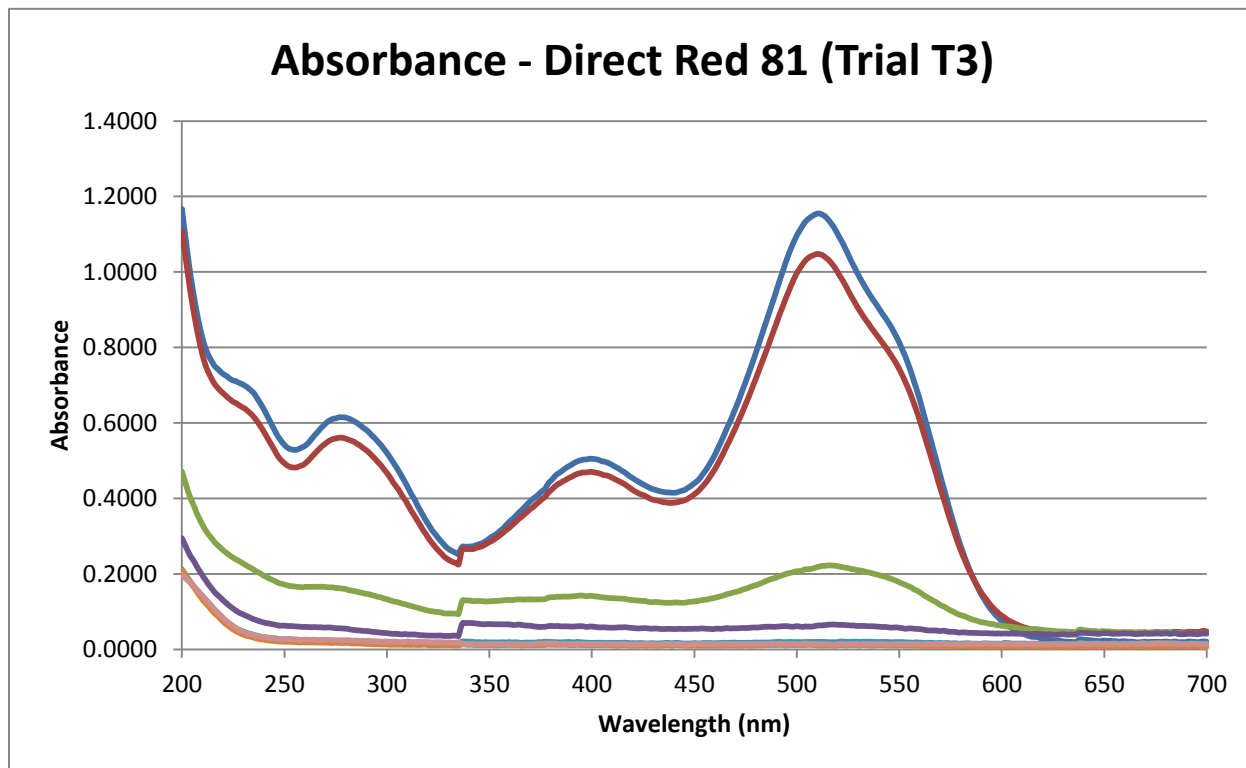
DR81\_T2

Sample	S1	S2	S3	S4	S5	S6	S7	S8
Time	0	30	150	270	390	480	1380	1500
Peak (at $\lambda_{max}$ )	1.152	1.040	0.706	0.287	0.112	0.064	0.016	0.013
Concentration	25.20	22.76	15.47	6.32	2.50	1.43	0.39	0.33
$\ln(C_0/C)$	0.000	0.102	0.488	1.383	2.309	2.866	4.166	4.350

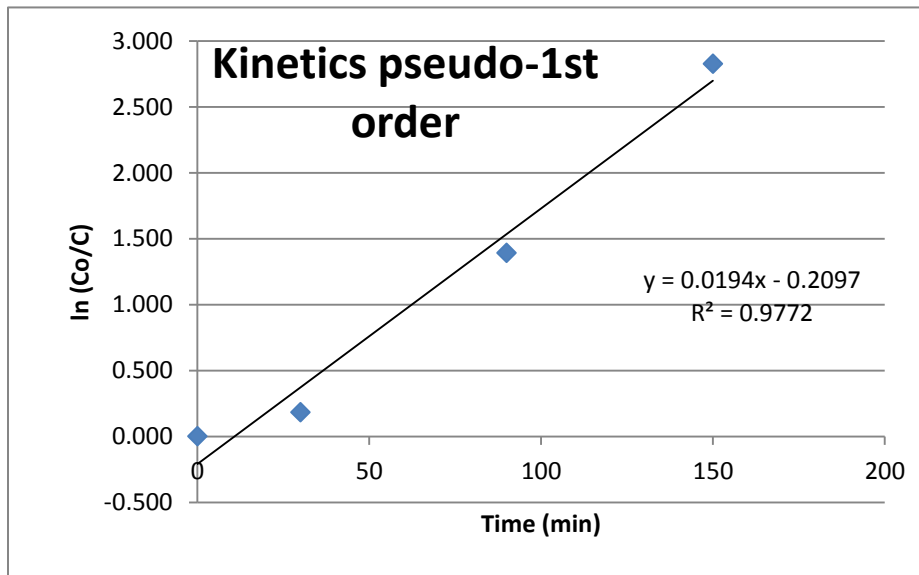
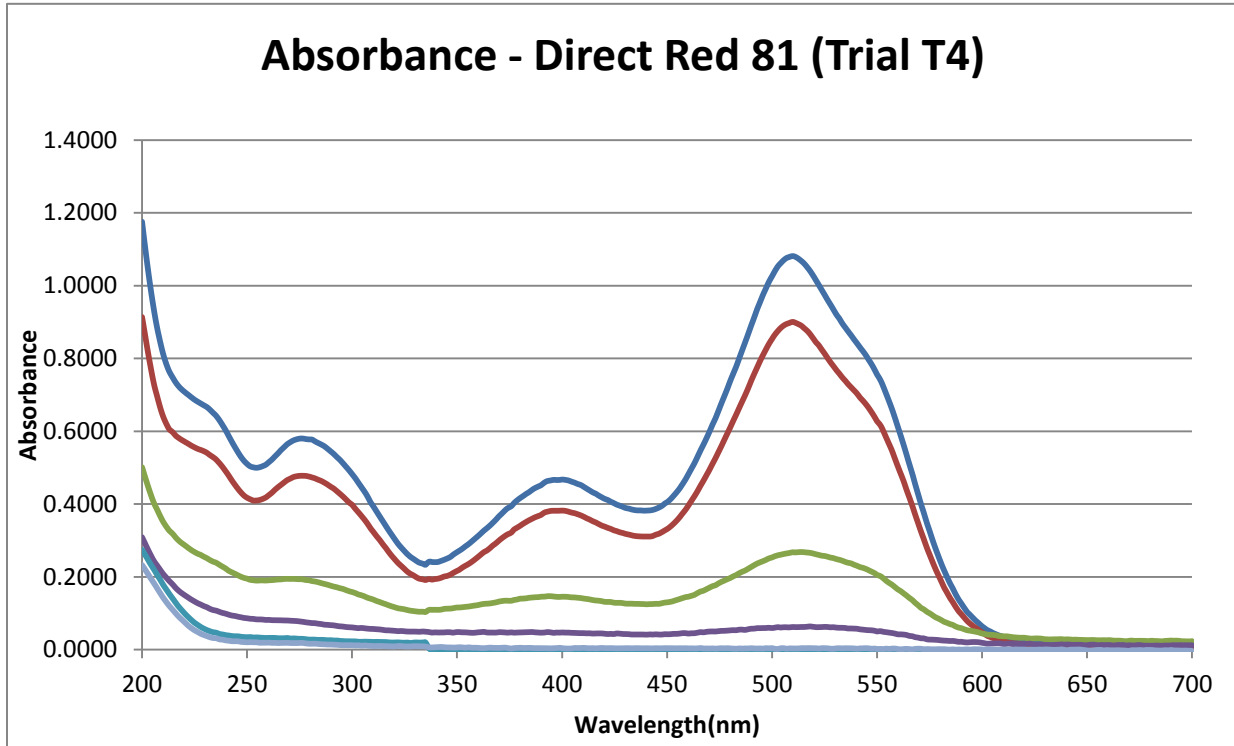




Sample	S1	S2	S3	S4	S5	S6	S7
Time	0	30	120	240	360	420	1360
Peak (at $\lambda_{max}$ )	1.155	1.048	0.218	0.063	0.020	0.010	0.014
Concentration	25.26	22.93	4.81	1.42	0.48	0.27	0.35
$\ln(C_0/C)$	0.000	0.097	1.658	2.876	3.962	4.528	4.275

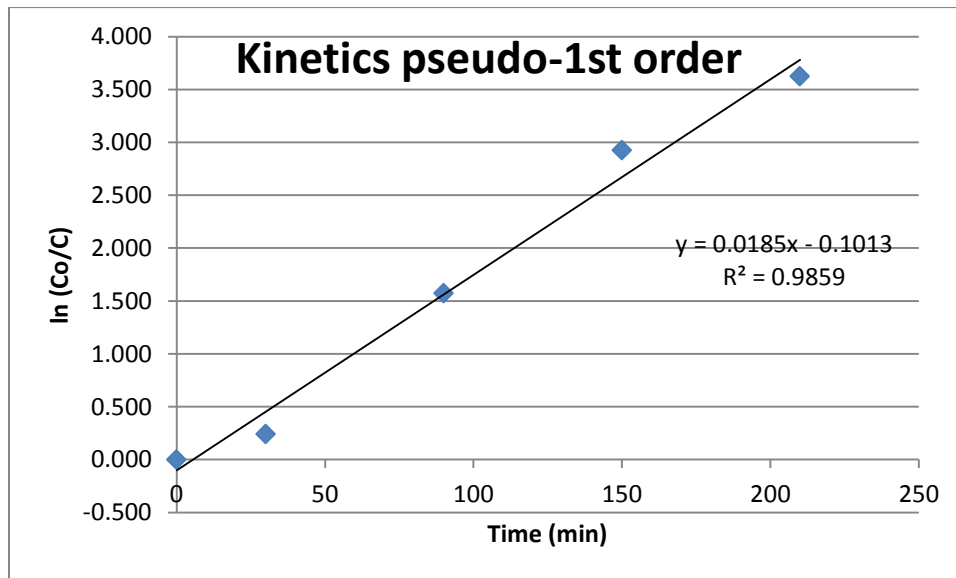
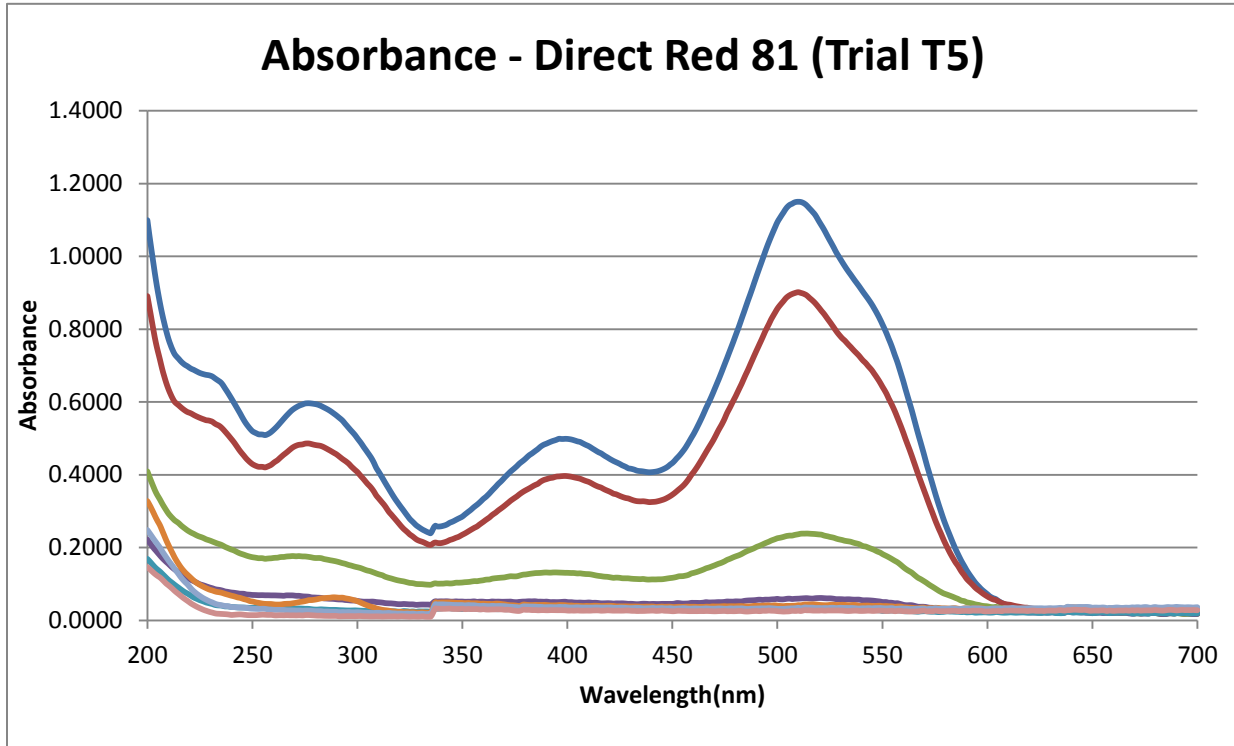


Sample	S1	S2	S3	S4	S5	S6
Time	0	30	120	240	360	420
Peak (at $\lambda_{max}$ )	0	30	90	150	270	350
Concentration	1.081	0.900	0.267	0.062	-0.004	0.003
$\ln(C_0/C)$	23.65	19.71	5.89	1.40	-0.03	0.12

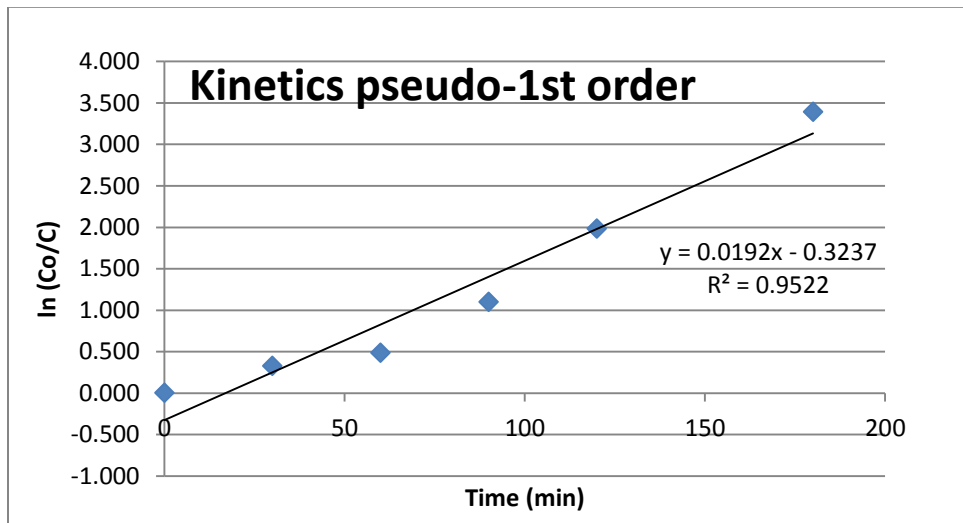
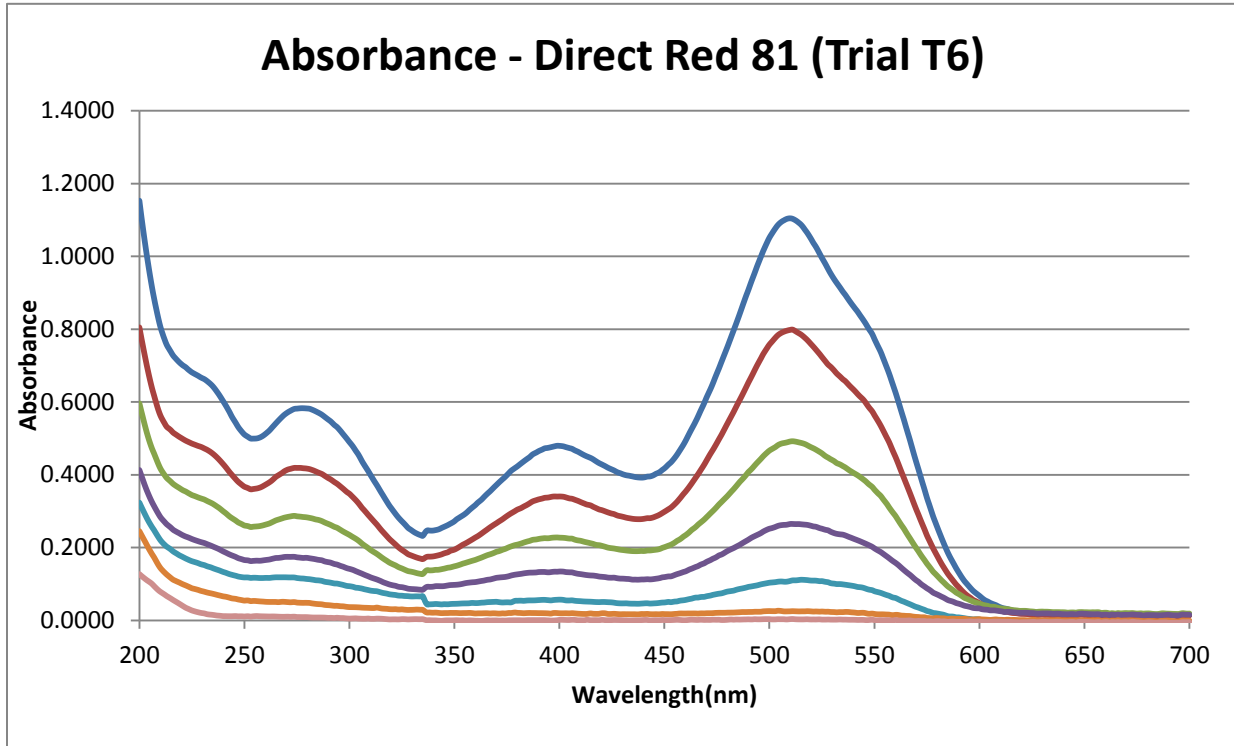


DR81\_T5

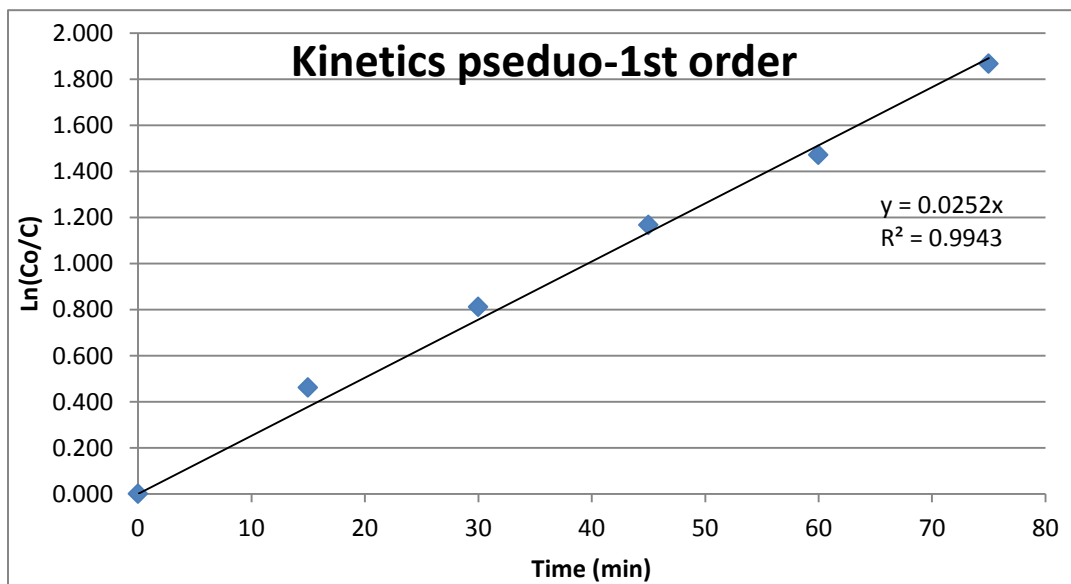
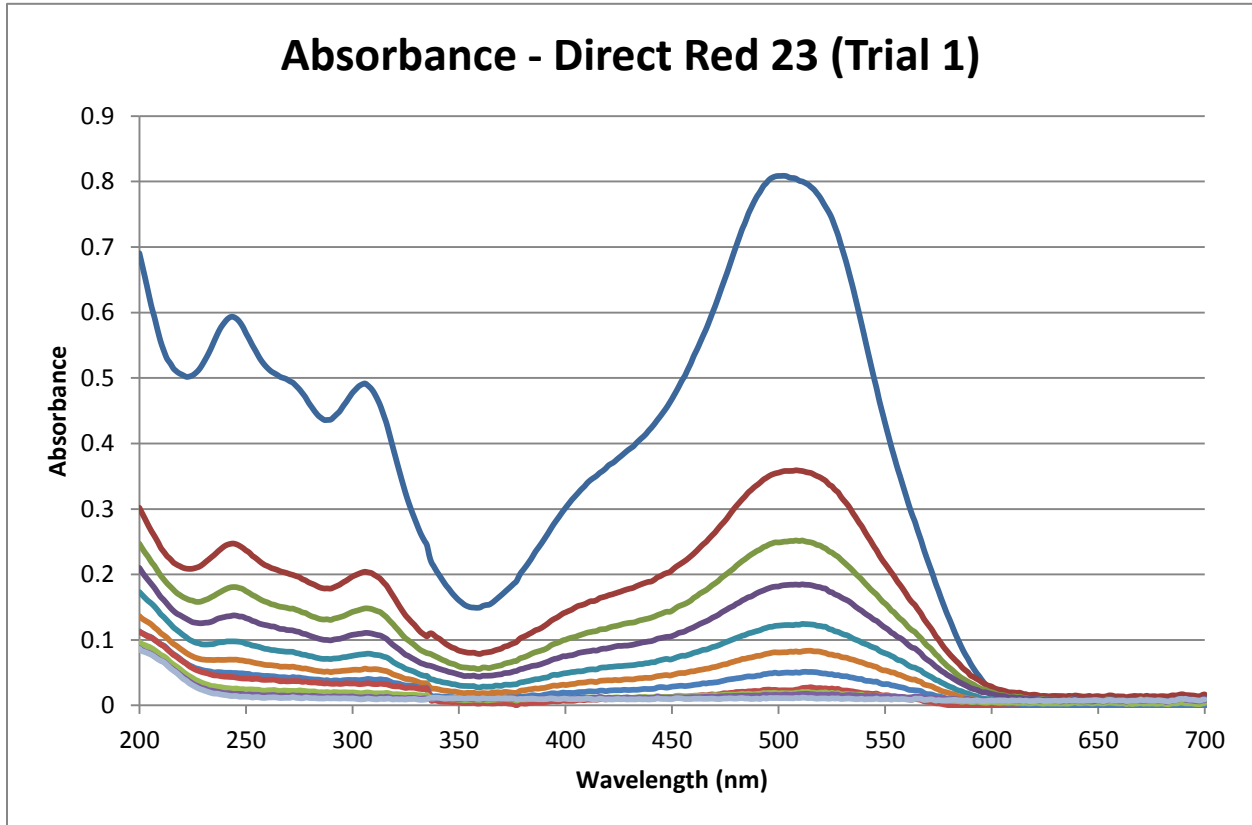
Sample	S1	S2	S3	S4	S5	S6	S7	S8
Time	0	30	90	150	210	270	300	360
Peak (at $\lambda_{max}$ )	1.150	0.901	0.236	0.059	0.029	0.042	0.034	0.026
Concentration	25.16	19.73	5.21	1.35	0.67	0.96	0.80	0.62
$\ln(C_0/C)$	0.000	0.243	1.574	2.927	3.625	3.270	3.449	3.696



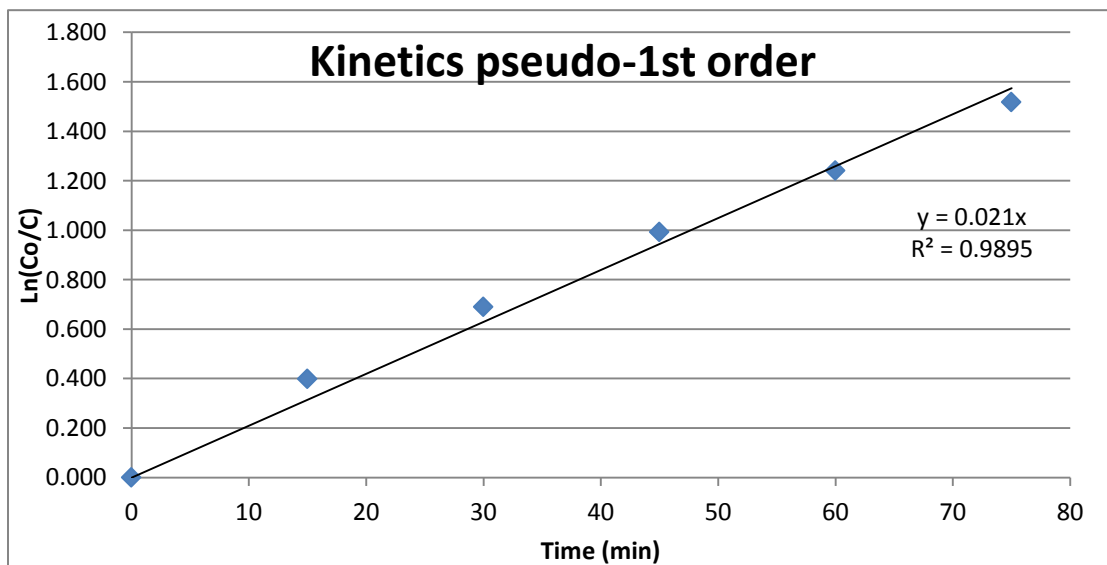
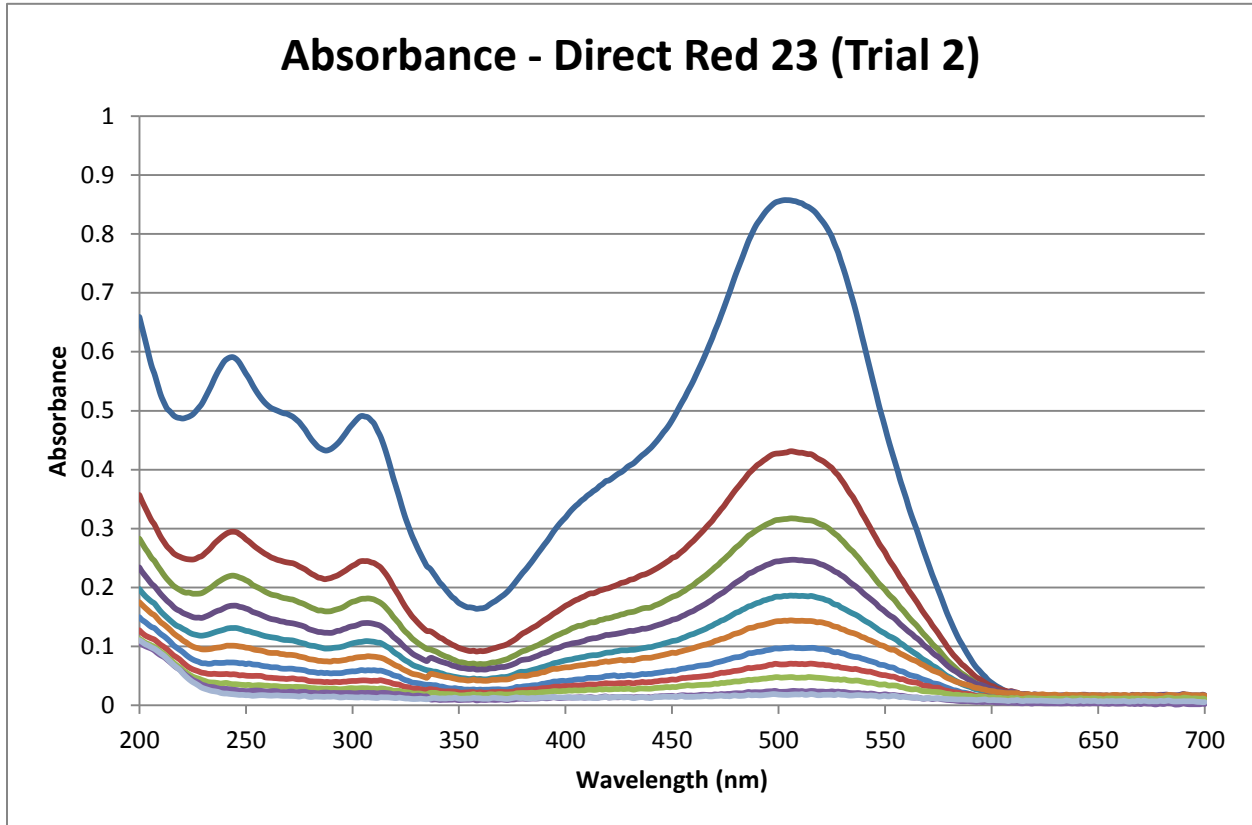
Sample	S1	S2	S3	S4	S5	S6	S7
Time	0	30	60	90	120	180	210
Peak (at $\lambda_{max}$ )	1.104	0.798	0.491	0.265	0.108	0.025	0.003
Concentration	24.16	17.47	10.78	5.83	2.41	0.59	0.12
$\ln(C_0/C)$	0.000	0.324	0.483	1.098	1.980	3.389	4.980



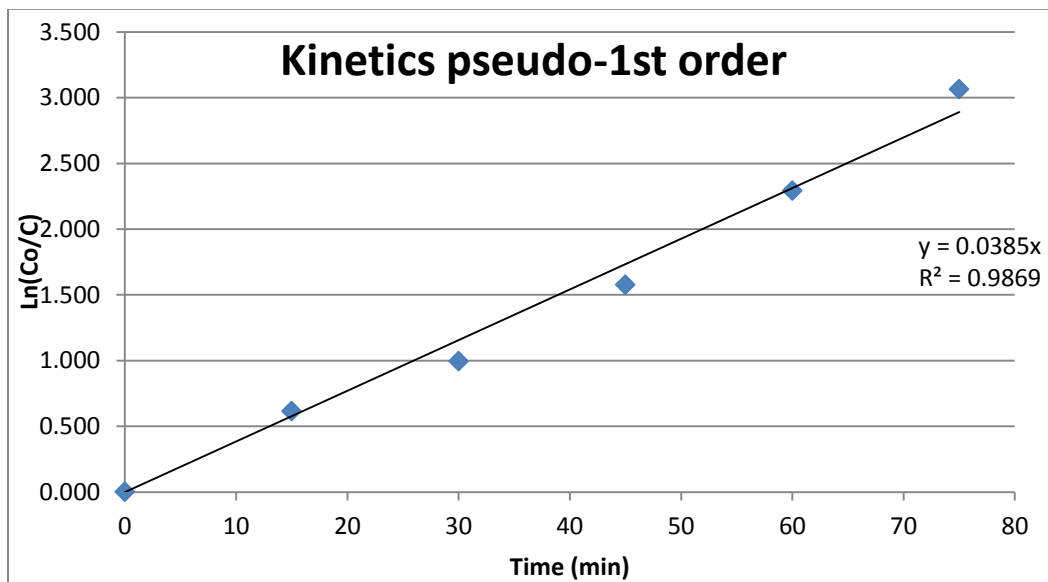
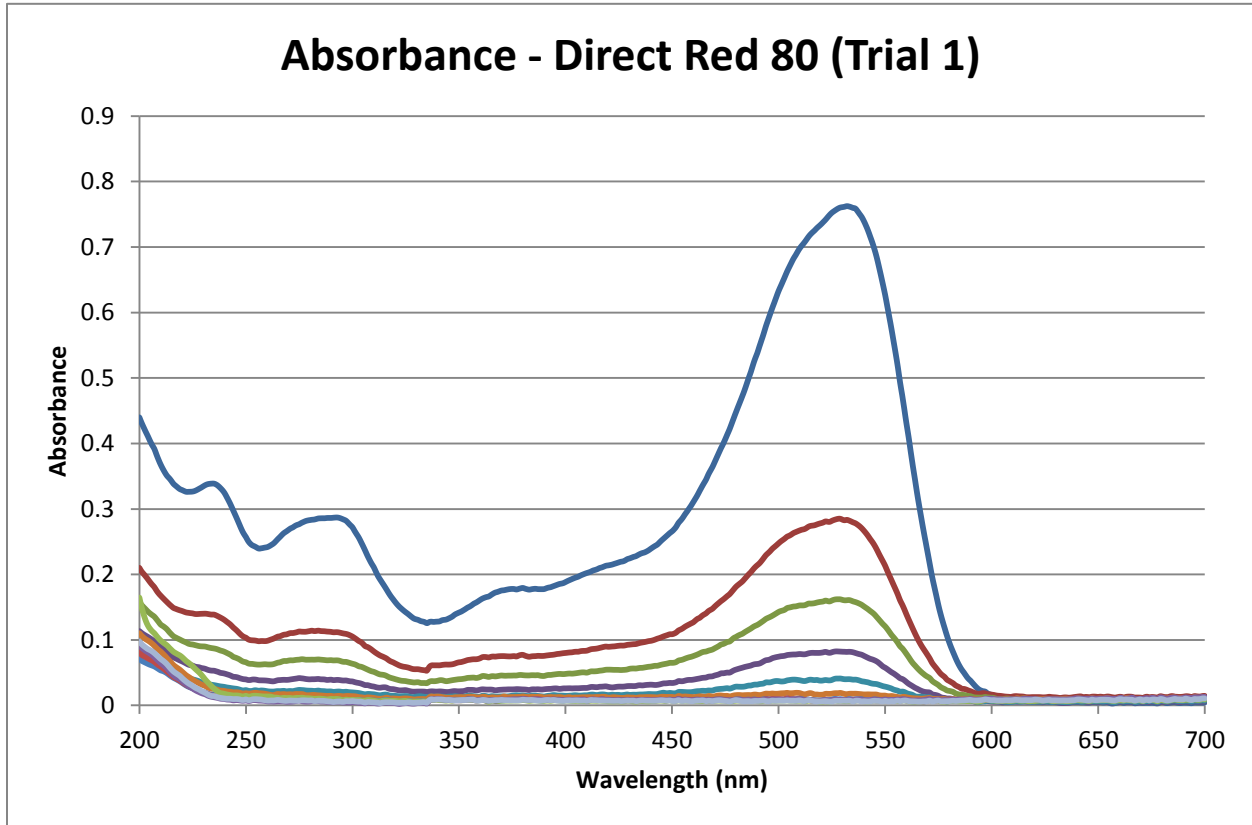
Sample	S1	S2	S3	S4	S5	S6	S7	S8	S9	S10	S11	S12
Time	0	15	30	45	60	75	90	105	120	135	150	165
Peak (at $\lambda_{max}$ )	0.809	0.509	0.357	0.250	0.183	0.122	0.081	0.050	0.023	0.019	0.016	0.011
Concentration	24.02	15.14	10.67	7.48	5.51	3.71	2.49	1.56	0.78	0.65	0.57	0.42
ln(Co/C)	0.000	0.462	0.812	1.167	1.471	1.867	2.266	2.733	3.433	3.613	3.744	4.046



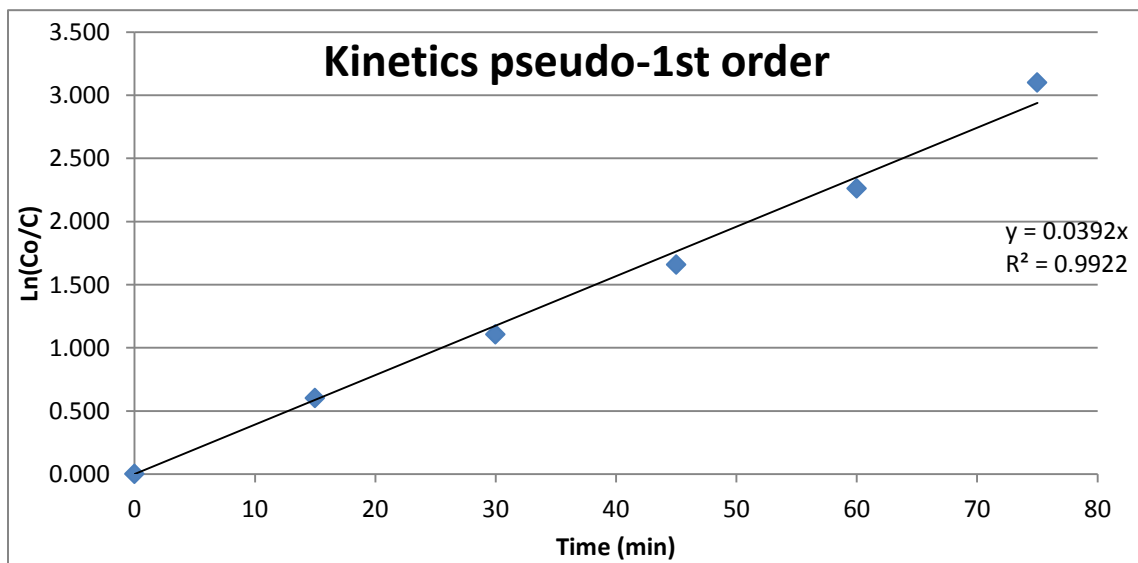
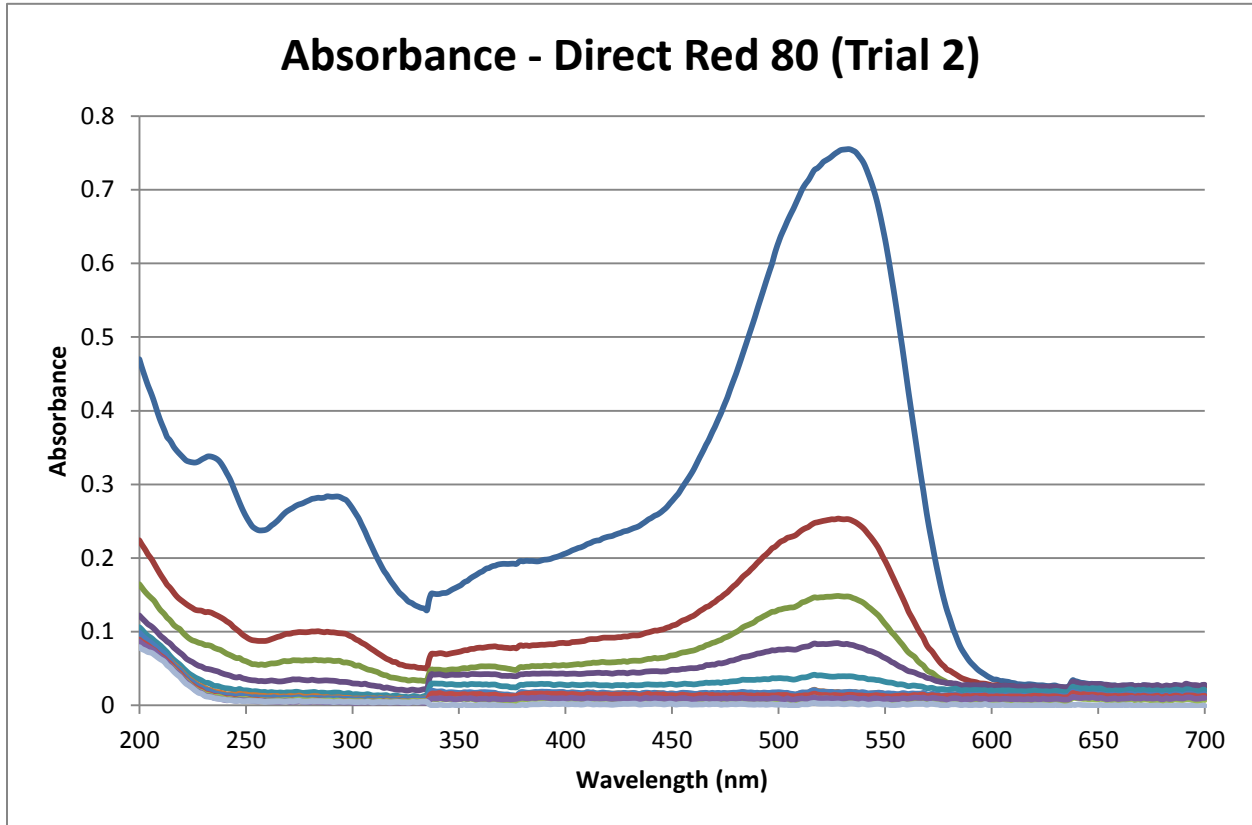
Sample	S1	S2	S3	S4	S5	S6	S7	S8	S9	S10	S11	S12
Time	0	15	30	45	60	75	90	105	120	135	150	165
Peak (at $\lambda_{max}$ )	0.857	0.574	0.428	0.316	0.246	0.185	0.144	0.097	0.069	0.047	0.023	0.018
Concentration	25.45	17.08	12.76	9.43	7.36	5.57	4.34	2.96	2.15	1.49	0.78	0.62
$\ln(C_0/C)$	0.000	0.399	0.690	0.992	1.240	1.518	1.769	2.150	2.472	2.839	3.491	3.708



Sample	S1	S2	S3	S4	S5	S6	S7	S8	S9	S10	S11	S12
Time	0	15	30	45	60	75	90	105	120	135	150	165
Peak (at $\lambda_{max}$ )	0.760	0.414	0.285	0.162	0.082	0.041	0.019	0.010	0.008	0.007	0.008	0.007
Concentration	24.66	13.33	9.12	5.10	2.50	1.15	0.43	0.12	0.07	0.04	0.09	0.04
$\ln(C_0/C)$	0.000	0.615	0.994	1.575	2.290	3.062	4.038	5.291	5.838	6.364	5.633	6.444

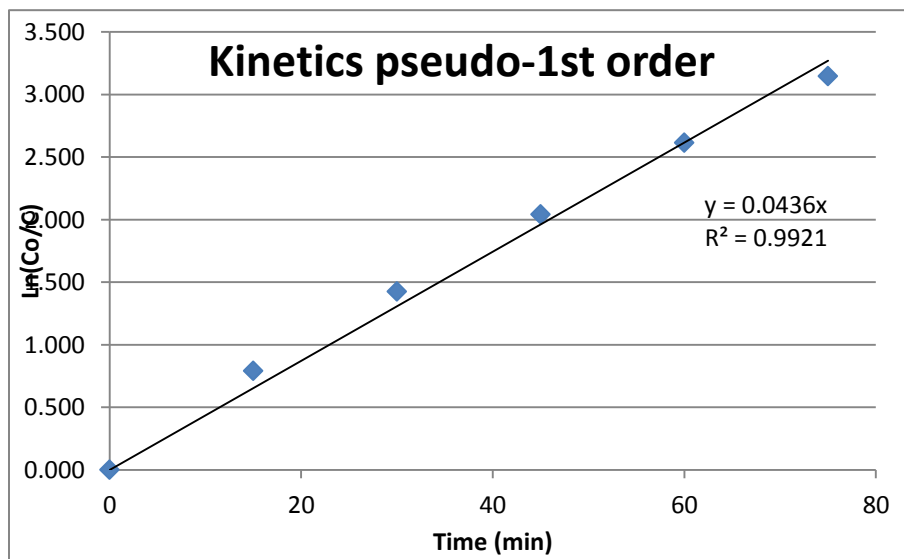
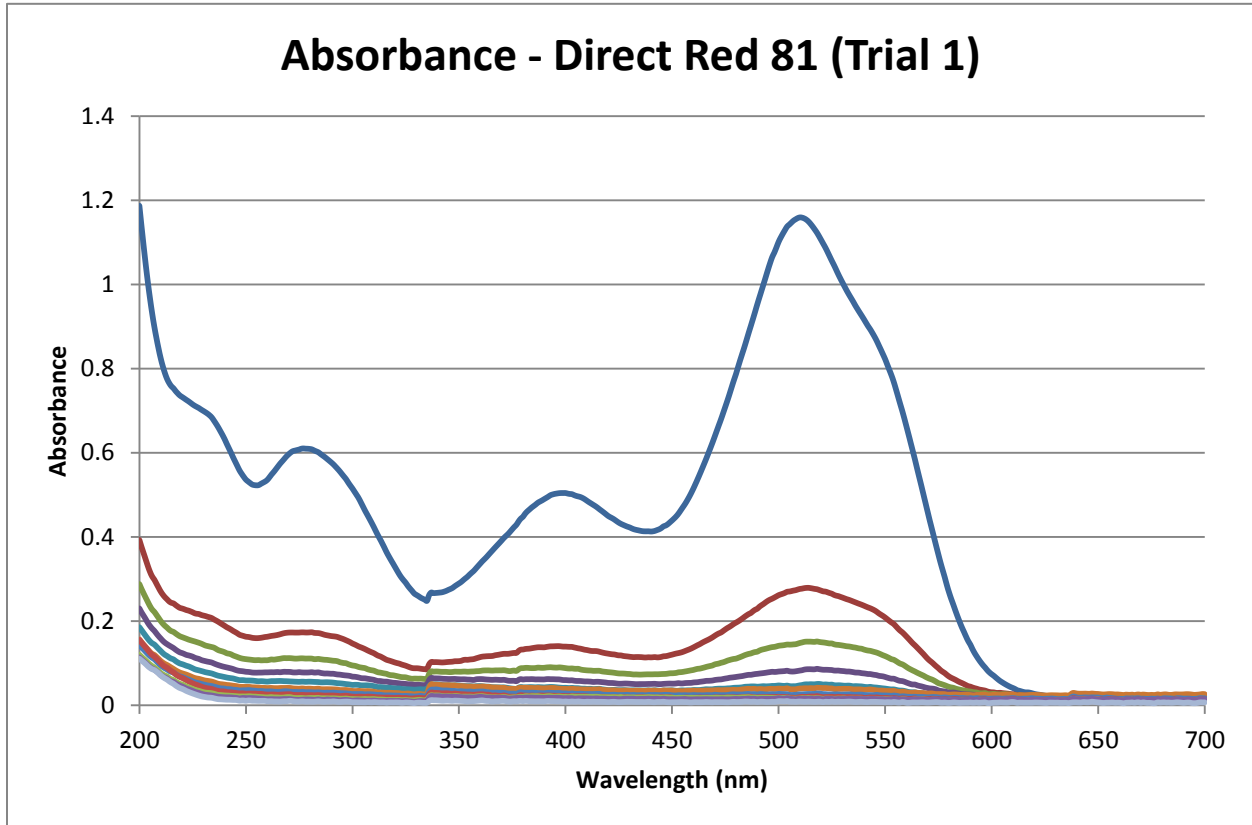


Sample	S1	S2	S3	S4	S5	S6	S7	S8	S9	S10	S11	S12
Time	0	15	30	45	60	75	90	105	120	135	150	165
Peak (at $\lambda_{max}$ )	0.754	0.416	0.253	0.148	0.084	0.039	0.017	0.018	0.013	0.008	0.009	0.002
Concentration	24.44	13.39	8.08	4.65	2.55	1.10	0.38	0.39	0.25	0.08	0.09	-0.12
ln(Co/C)	0.000	0.601	1.107	1.658	2.262	3.100	4.166	4.141	4.576	5.742	5.552	--

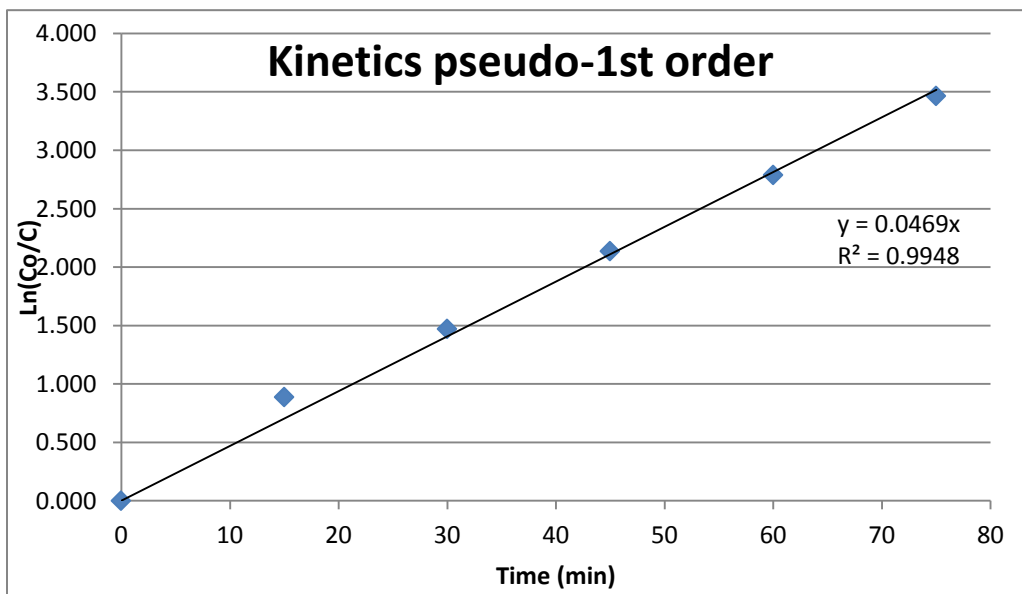
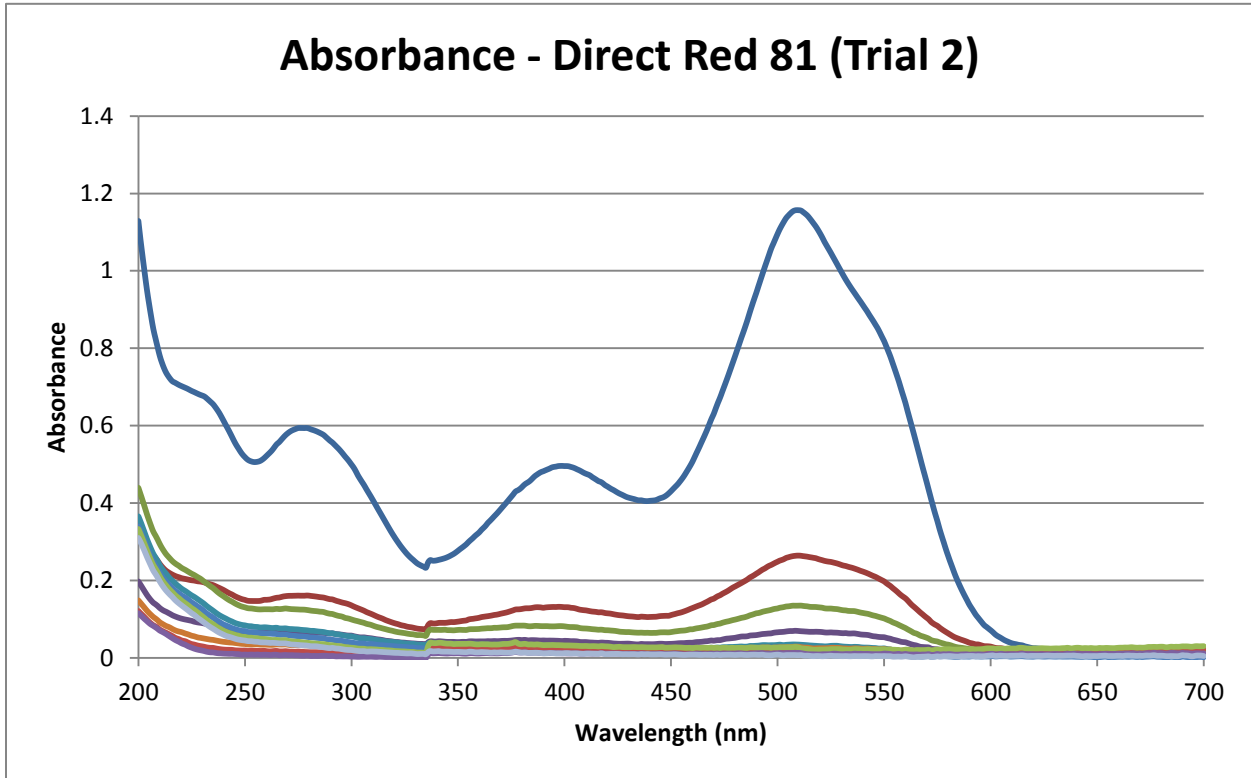




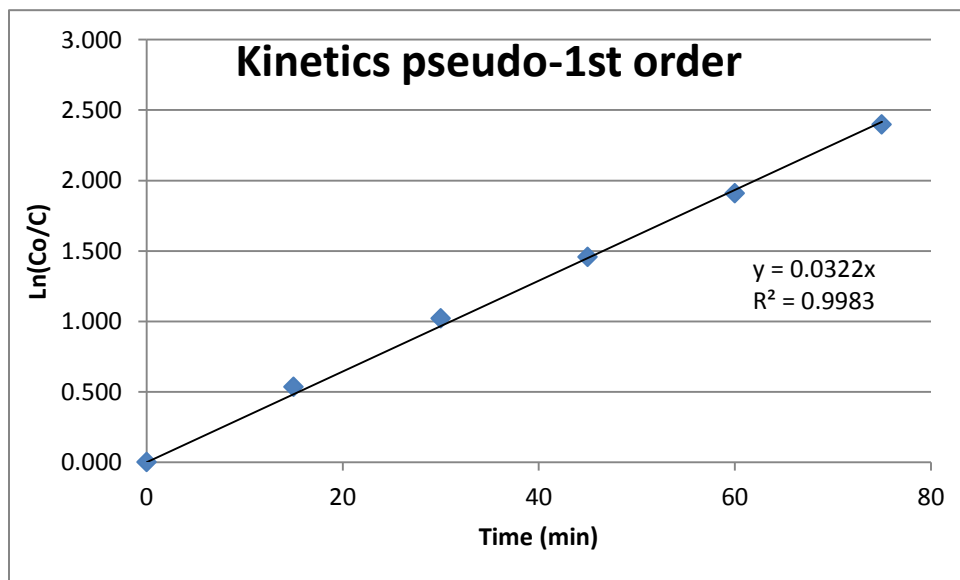
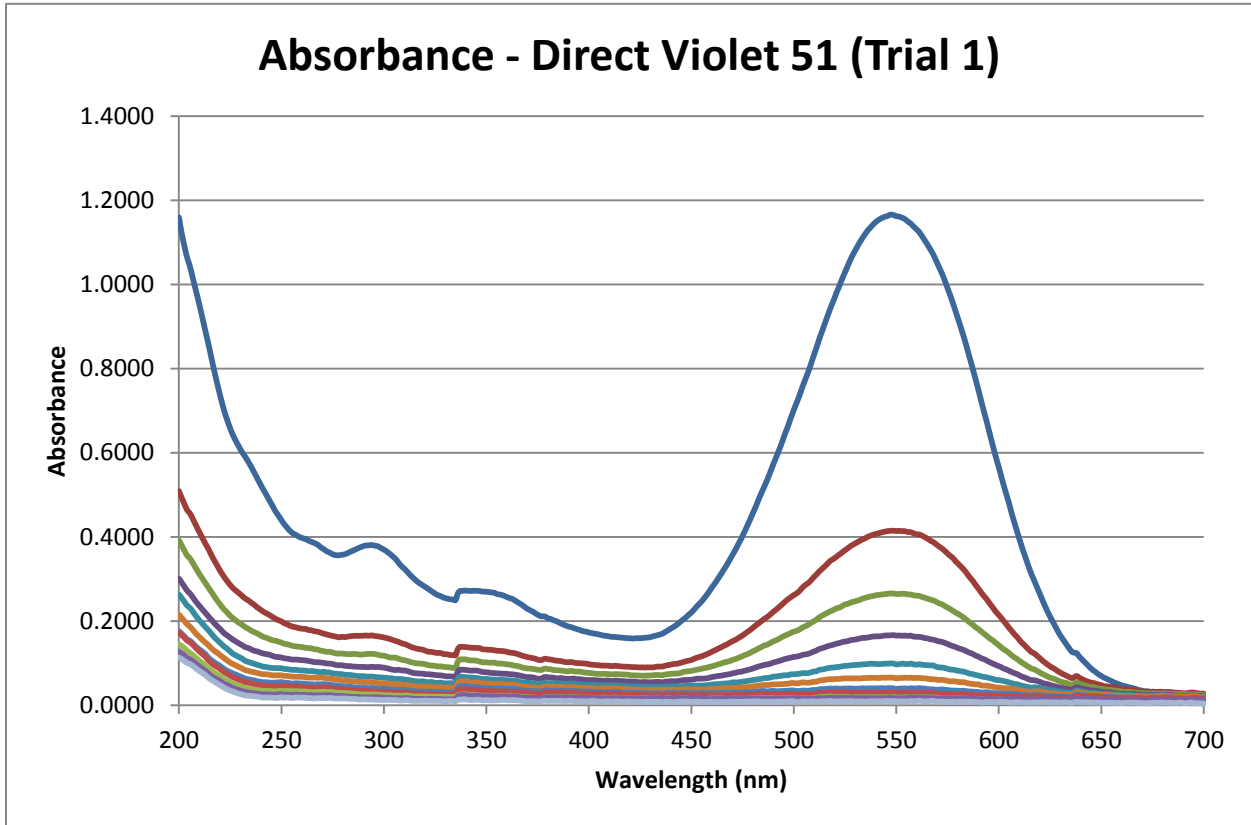
Sample	S1	S2	S3	S4	S5	S6	S7	S8	S9	S10	S11	S12
Time	0	15	30	45	60	75	90	105	120	135	150	165
Peak (at $\lambda_{max}$ )	1.159	0.525	0.277	0.148	0.083	0.048	0.040	0.026	0.020	0.017	0.016	0.009
Concentration	25.36	11.50	6.09	3.29	1.86	1.09	0.93	0.62	0.48	0.41	0.40	0.25
$\ln(C_0/C)$	0.000	0.791	1.427	2.043	2.615	3.147	3.310	3.704	3.971	4.124	4.156	4.615



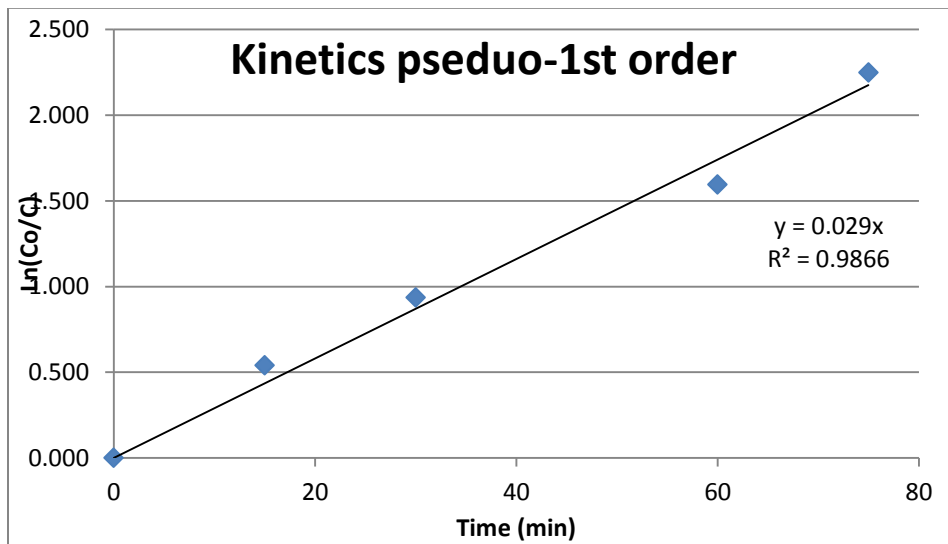
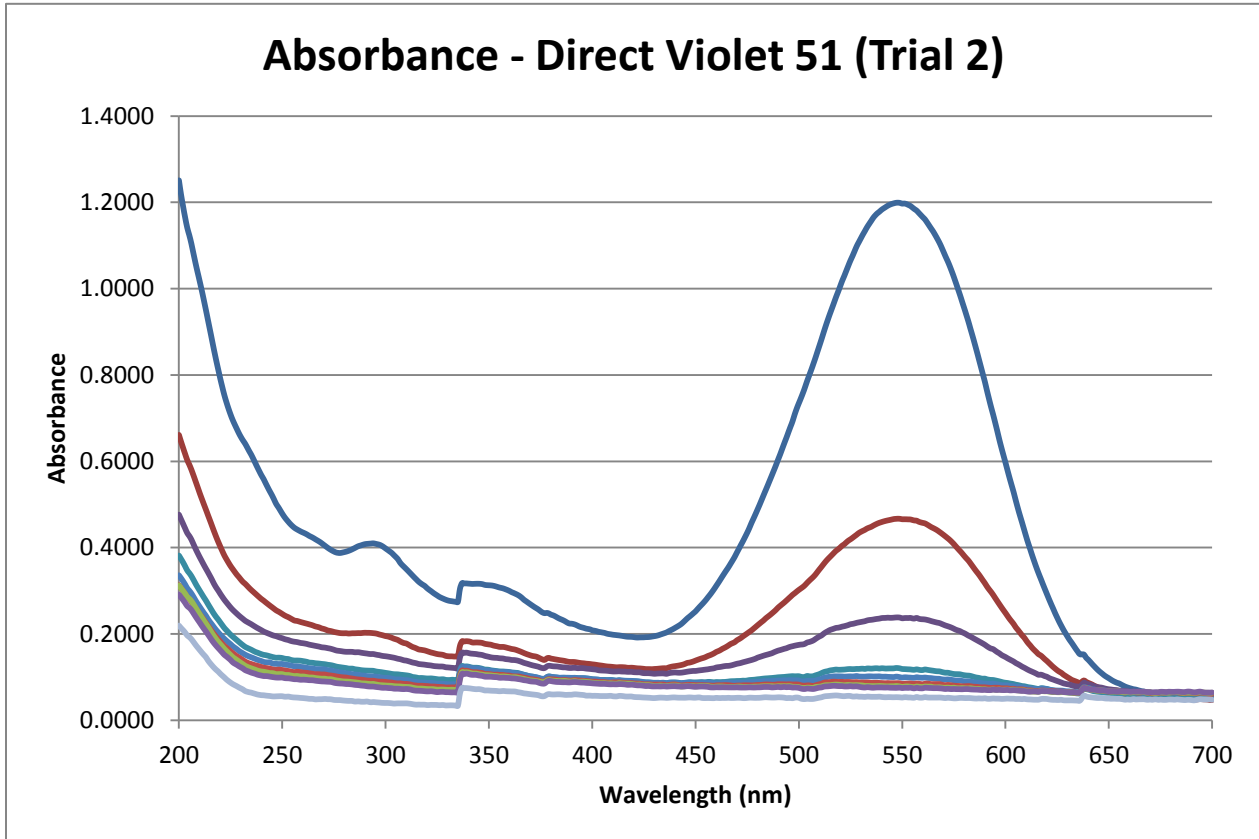
Sample	S1	S2	S3	S4	S5	S6	S7	S8	S9	S10	S11	S12
Time	0	15	30	45	60	75	90	105	120	135	150	165
Peak (at $\lambda_{max}$ )	1.157	0.475	0.264	0.135	0.069	0.034	0.028	0.014	0.025	0.027	0.013	0.007
Concentration	25.30	10.43	5.81	2.99	1.56	0.79	0.67	0.34	0.59	0.63	0.33	0.20
$\ln(C_0/C)$	0.000	0.886	1.471	2.135	2.787	3.463	3.634	4.295	3.763	3.691	4.354	4.847



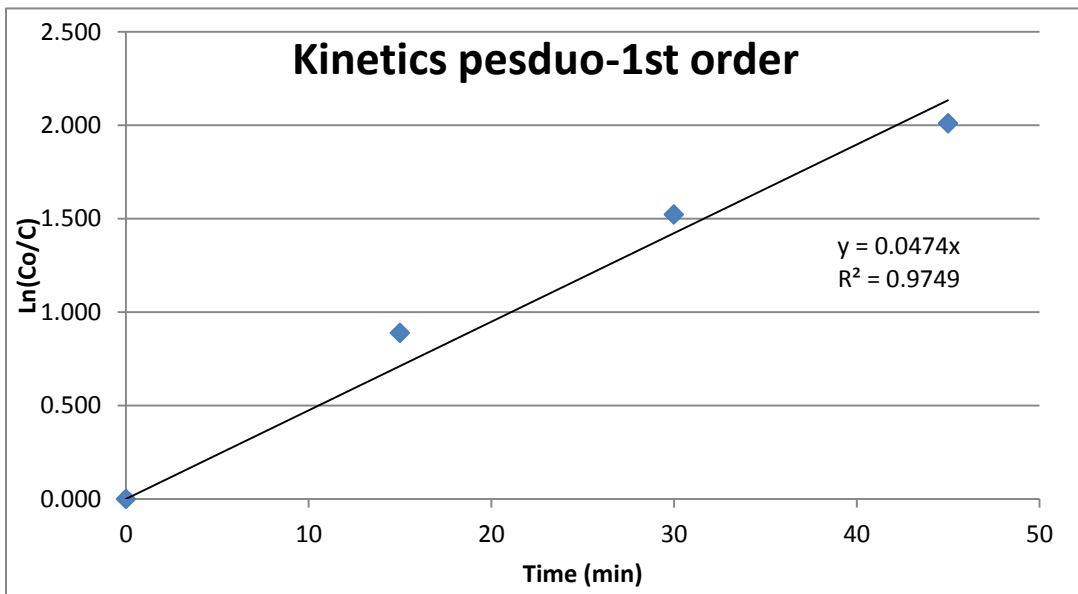
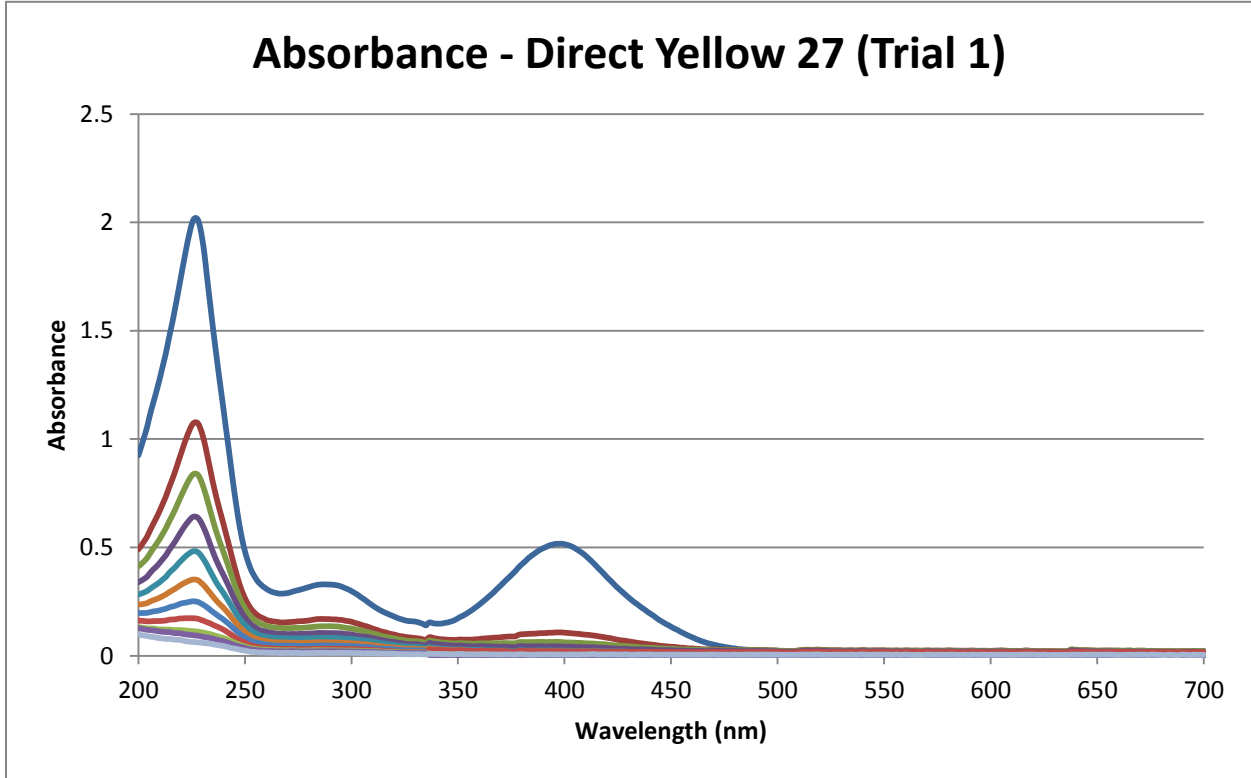
Sample	S1	S2	S3	S4	S5	S6	S7	S8	S9	S10	S11	S12
Time	0	15	30	45	60	75	90	105	120	135	150	165
Peak (at $\lambda_{max}$ )	1.163	0.678	0.414	0.265	0.166	0.099	0.066	0.041	0.030	0.019	0.018	0.011
Concentration	25.12	14.71	9.04	5.85	3.72	2.28	1.57	1.03	0.80	0.57	0.53	0.38
$\ln(C_0/C)$	0.000	0.535	1.022	1.457	1.909	2.398	2.772	3.190	3.443	3.784	3.858	4.186



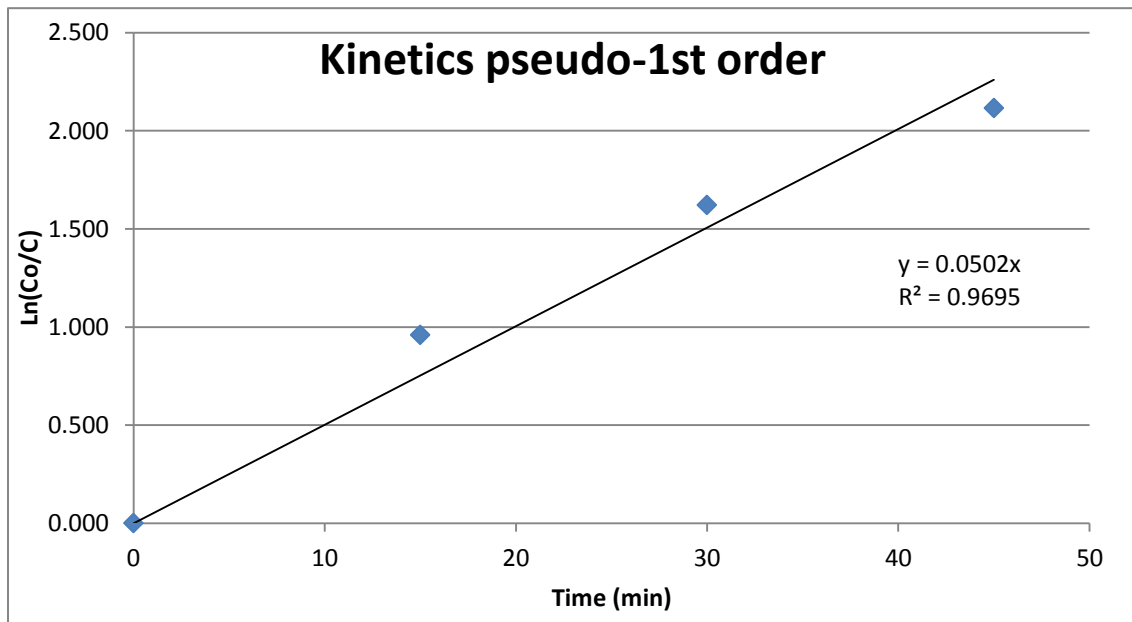
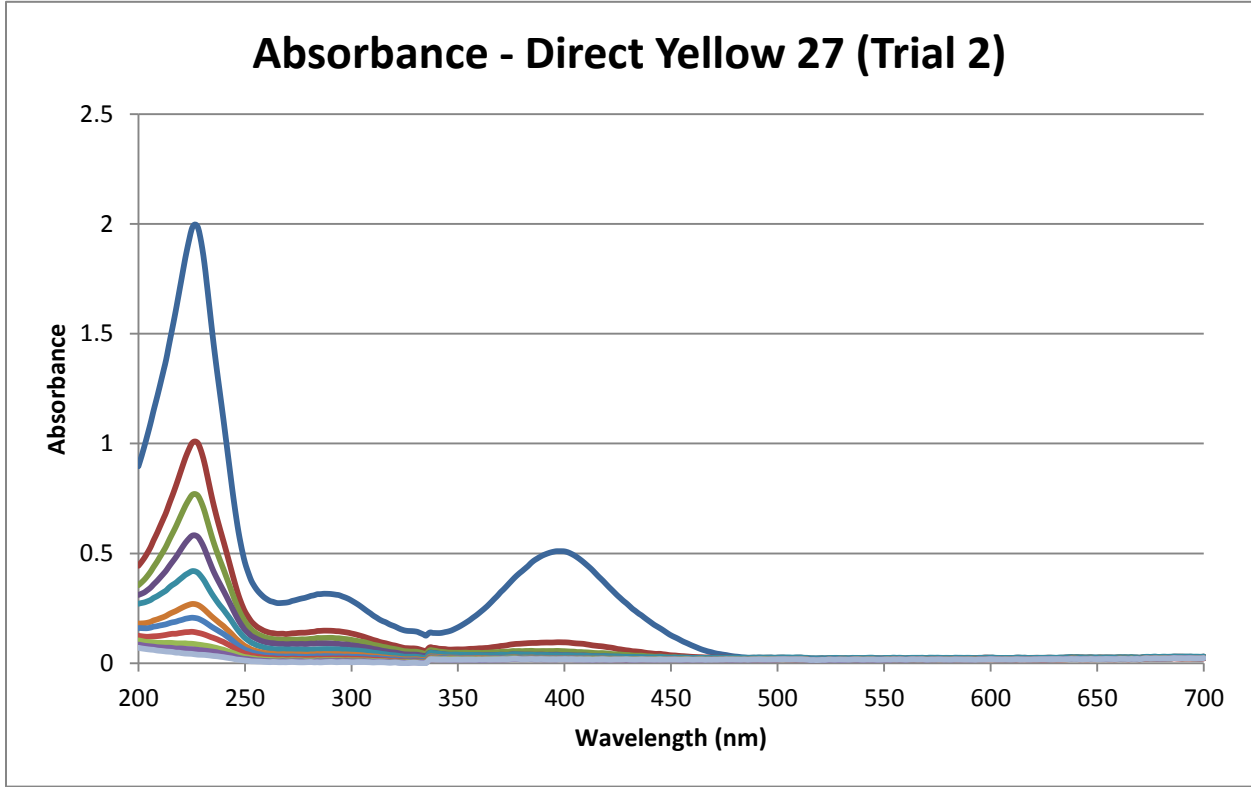
Sample	S1	S2	S3	S4	S5	S6	S7	S8	S9	S10	S11	S12
Time	0	15	30	60	75	105	120	135	150	165	0	15
Peak (at $\lambda_{max}$ )	1.198	0.696	0.466	0.238	0.120	0.100	0.086	0.079	0.075	0.053	1.198	0.696
Concentration	25.86	15.08	10.16	5.26	2.73	2.30	1.99	1.84	1.77	1.30	25.86	15.08
$\ln(C_0/C)$	0.000	0.539	0.934	1.593	2.247	2.420	2.563	2.641	2.684	2.993	0.000	0.539



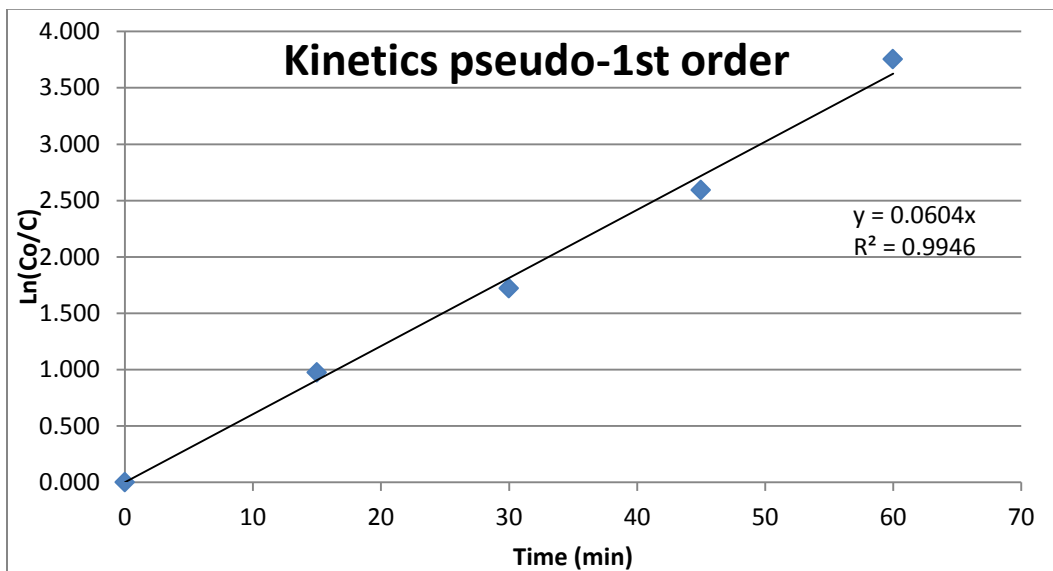
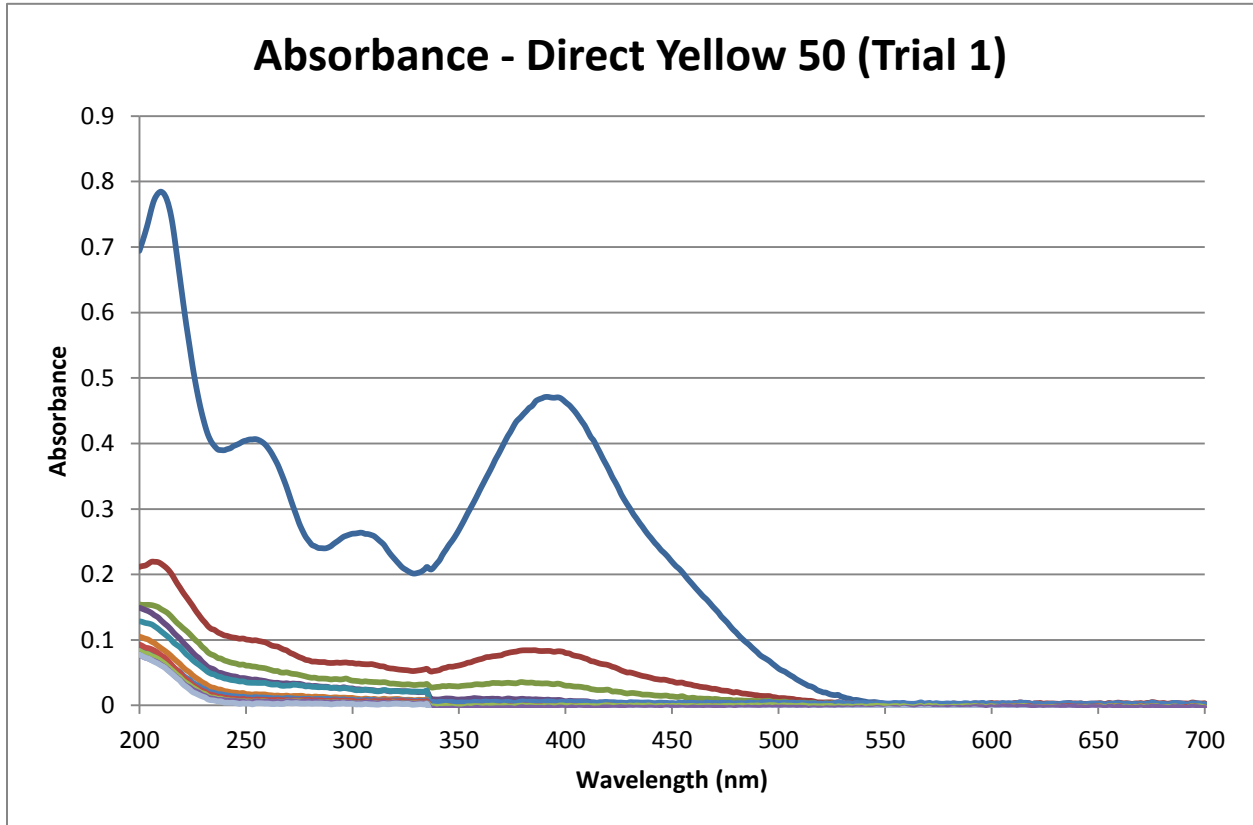
Sample	S1	S2	S3	S4	S5	S6	S7	S8	S9	S10	S11	S12
Time	0	15	30	45	60	75	90	105	120	135	150	165
Peak (at $\lambda_{max}$ )	0.517	0.209	0.108	0.064	0.043	0.024	0.020	0.013	0.021	0.004	0.000	0.006
Concentration	26.04	10.71	5.69	3.49	2.46	1.53	1.31	0.98	1.34	0.53	0.29	0.62
$\ln(C_0/C)$	0.000	0.889	1.521	2.009	2.361	2.836	2.991	3.285	2.965	3.890	4.486	3.735



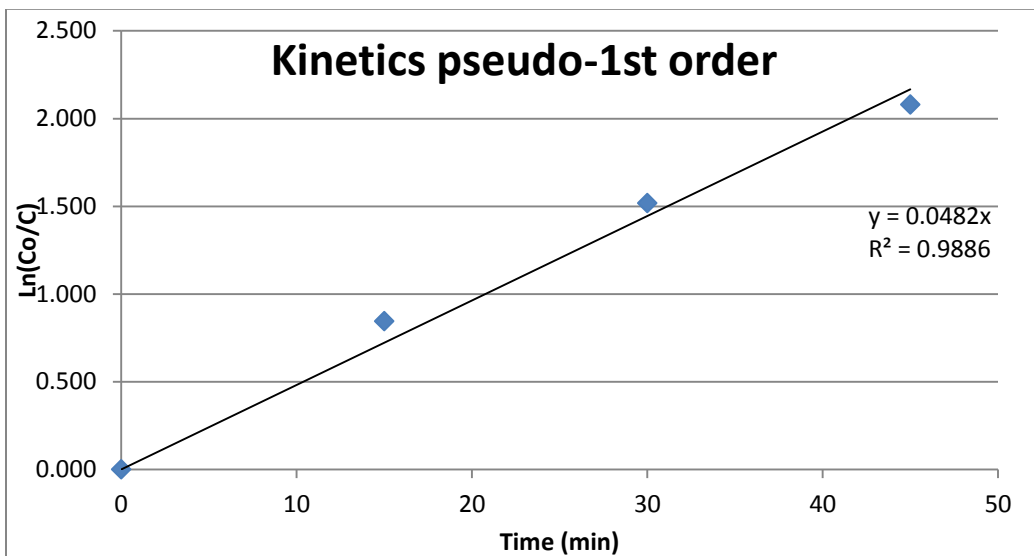
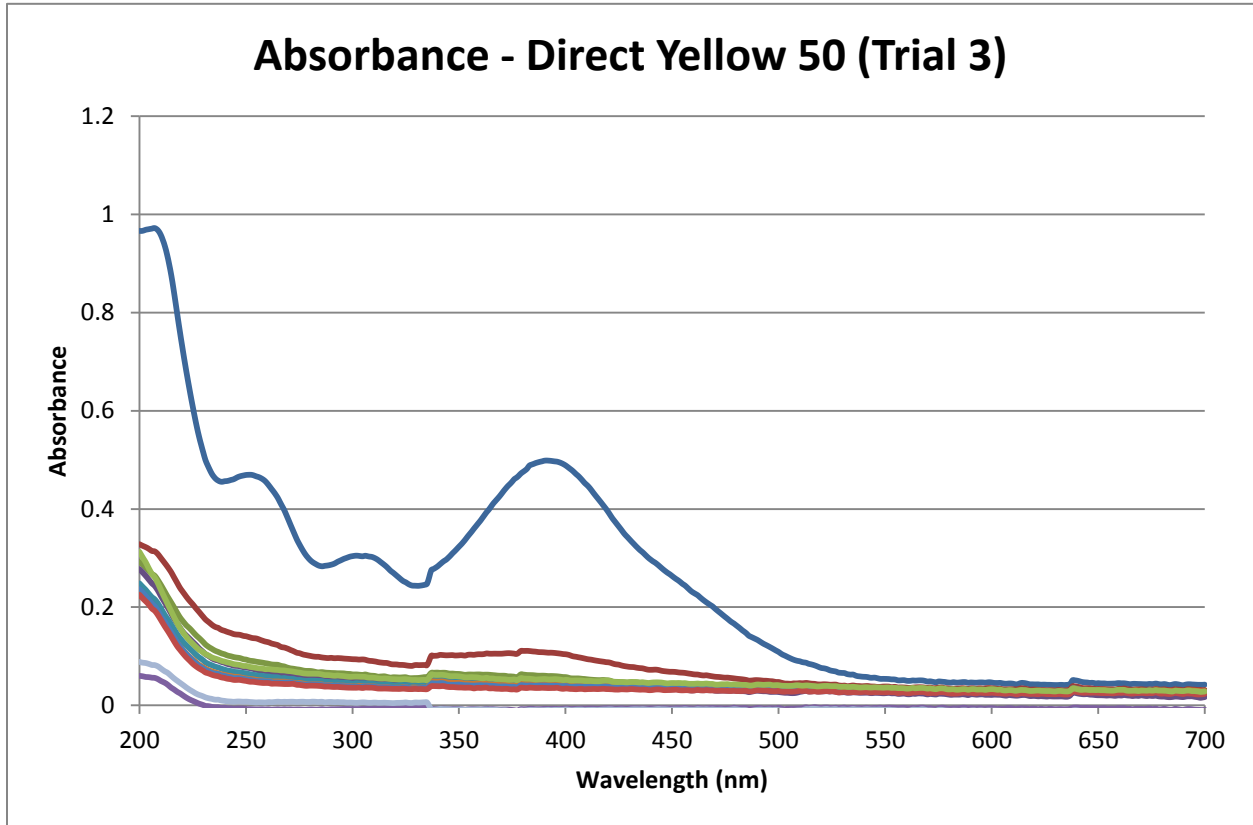
Sample	S1	S2	S3	S4	S5	S6	S7	S8	S9	S10	S11	S12
Time	0	15	30	45	60	75	90	105	120	135	150	165
Peak (at $\lambda_{max}$ )	0.510	0.191	0.096	0.056	0.038	0.036	0.024	0.023	0.020	0.020	0.019	0.019
Concentration	25.70	9.85	5.08	3.10	2.20	2.13	1.54	1.45	1.34	1.34	1.24	1.25
$\ln(C_0/C)$	0.000	0.960	1.621	2.115	2.459	2.491	2.817	2.873	2.955	2.955	3.028	3.024



Sample	S1	S2	S3	S4	S5	S6	S7	S8	S9	S10	S11	S12
Time	0	15	30	45	60	75	90	105	120	135	150	165
Peak (at $\lambda_{max}$ )	0.470	0.176	0.082	0.032	0.008	-0.011	-0.002	0.005	-0.002	-0.001	-0.004	-0.010
Concentration	23.18	8.75	4.16	1.74	0.54	-0.39	0.06	0.39	0.06	0.08	-0.07	-0.35
$\ln(C_0/C)$	0.000	0.974	1.718	2.592	3.752	--	5.896	4.079	5.896	5.628	--	--



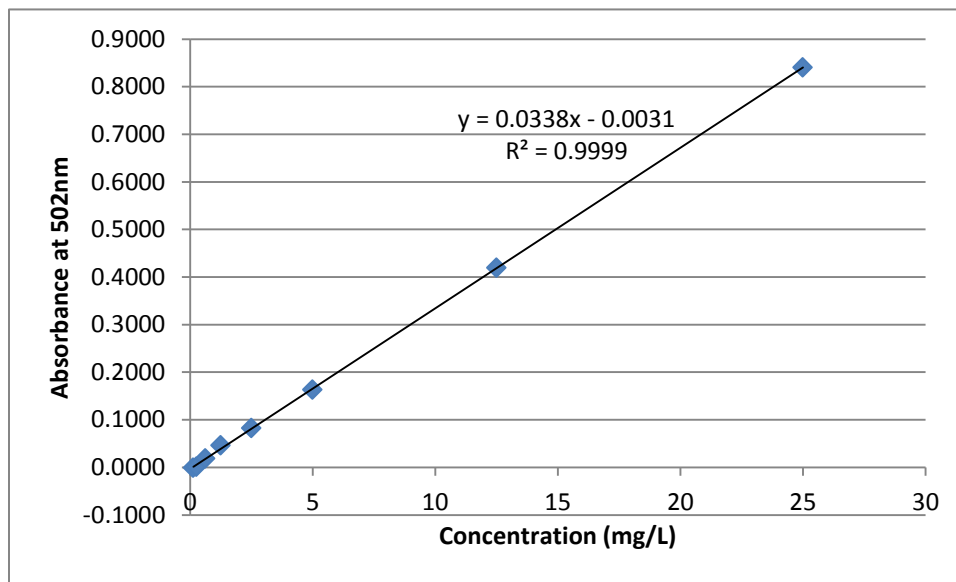
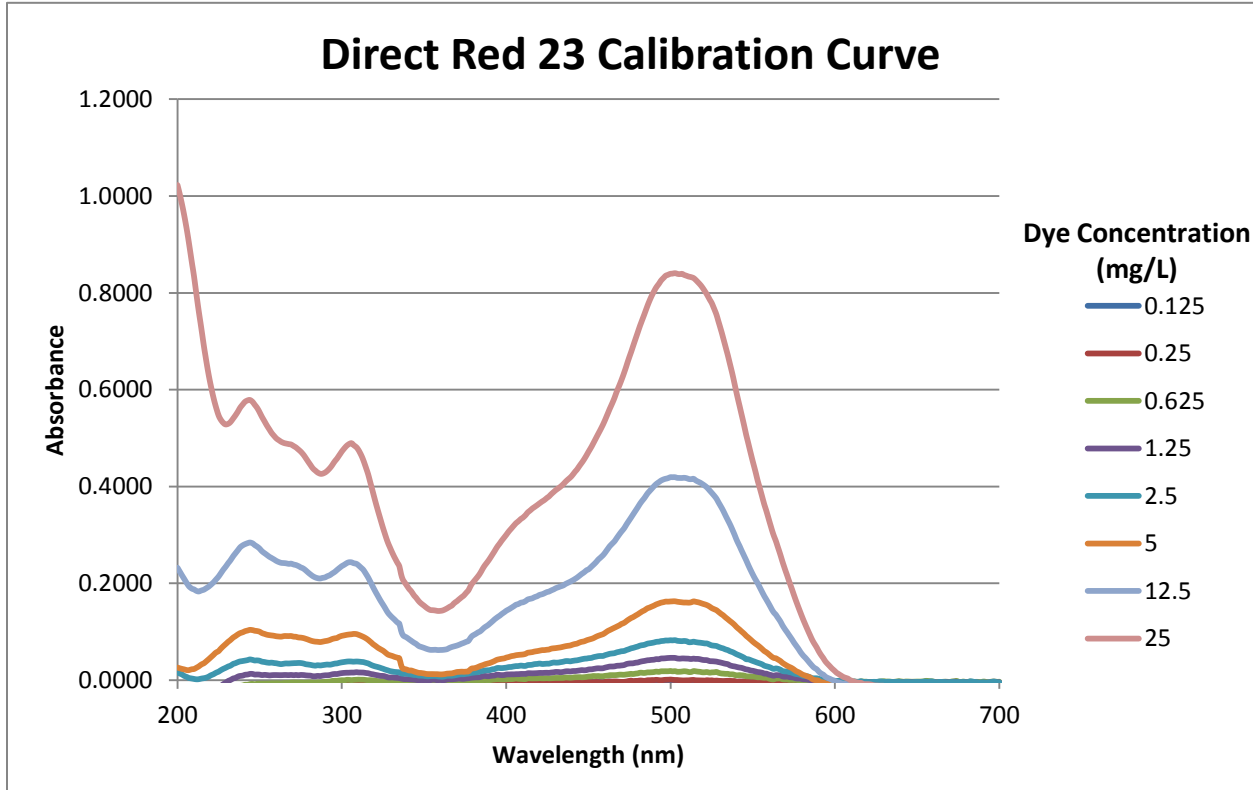
Sample	S1	S2	S3	S4	S5	S6	S7	S8	S9	S10	S11	S12
Time	0	15	30	45	60	75	90	105	120	135	150	165
Peak (at $\lambda_{max}$ )	0.497	0.212	0.107	0.060	0.041	0.045	0.043	0.040	0.035	0.054	-0.007	-0.009
Concentration	24.50	10.54	5.38	3.06	2.15	2.37	2.25	2.11	1.88	2.77	-0.19	-0.30
$\ln(C_0/C)$	0.000	0.843	1.516	2.079	2.434	2.335	2.390	2.453	2.566	2.180	--	--





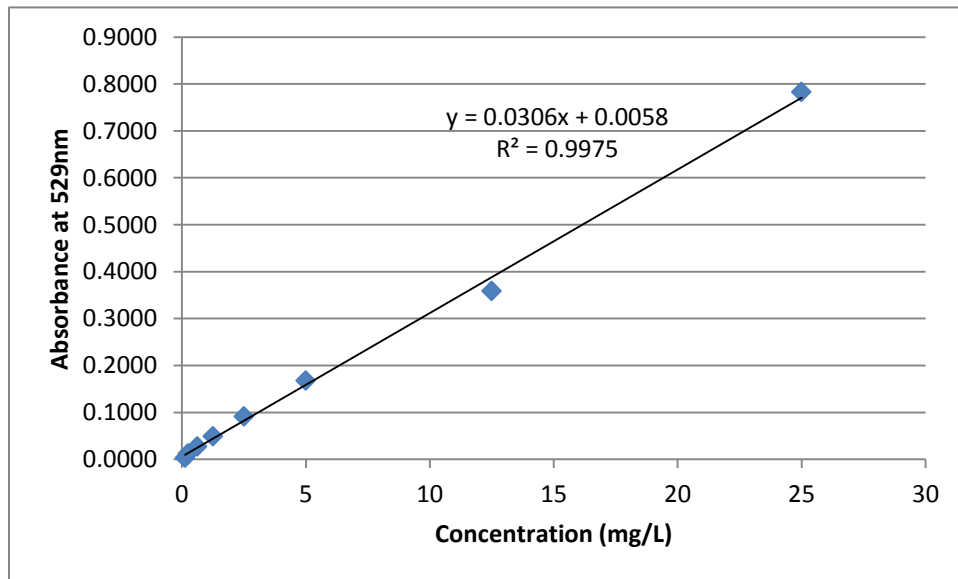
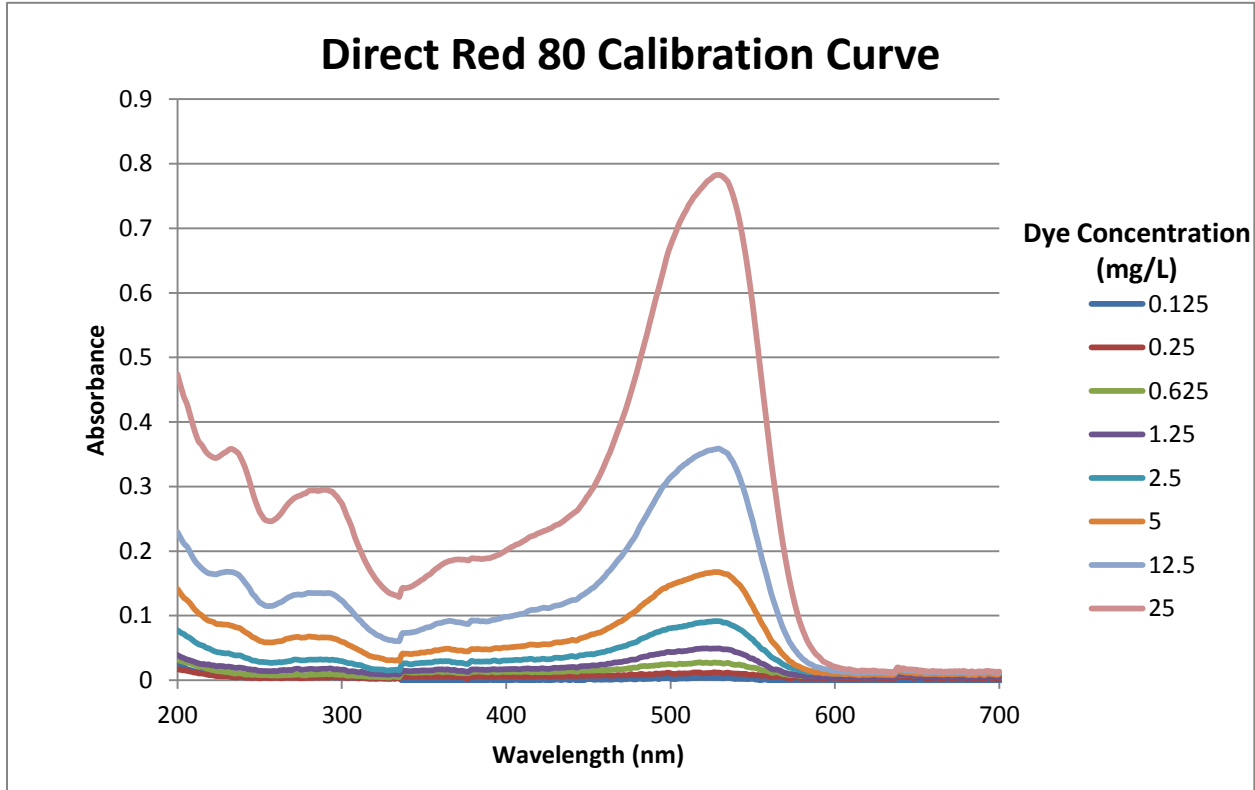
DR23\_C

Concentration (mg/L)	0.125	0.25	0.625	1.25	2.5	5	12.5	25
Peak (at $\lambda_{max}$ )	-0.0012	0.0007	0.0186	0.0462	0.0826	0.1631	0.4194	0.8404



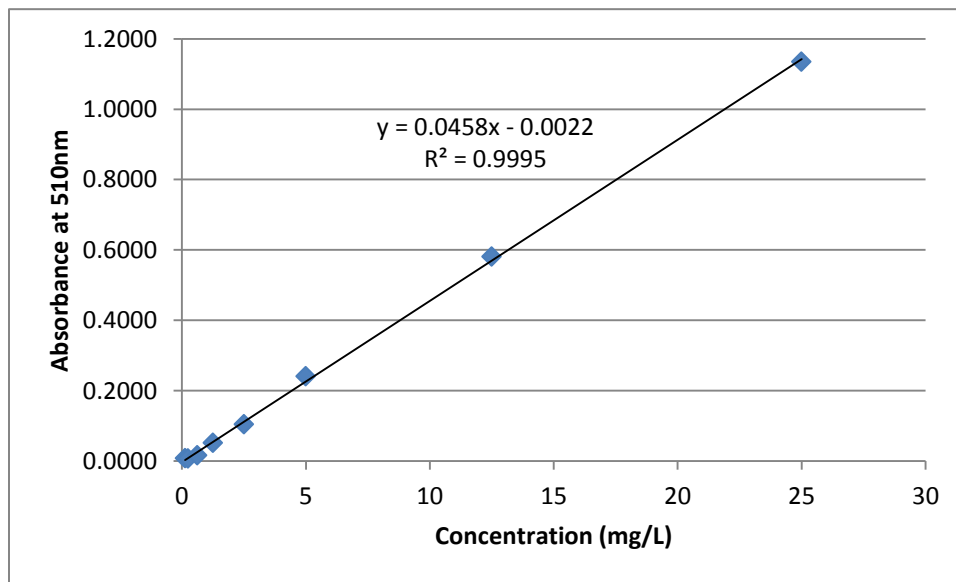
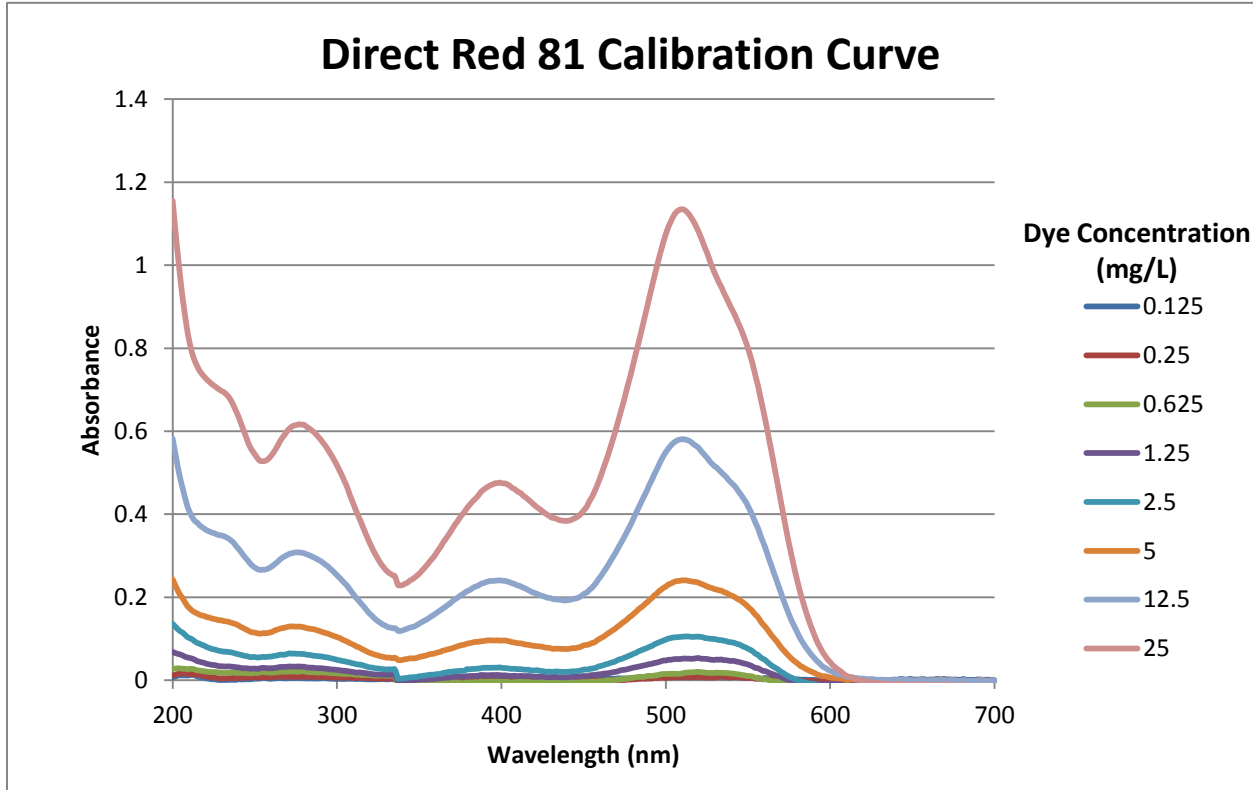
DR80\_C

Concentration (mg/L)	0.125	0.25	0.625	1.25	2.5	5	12.5	25
Peak (at $\lambda_{max}$ )	0.0036	0.0119	0.0271	0.0493	0.0915	0.1675	0.3589	0.7828



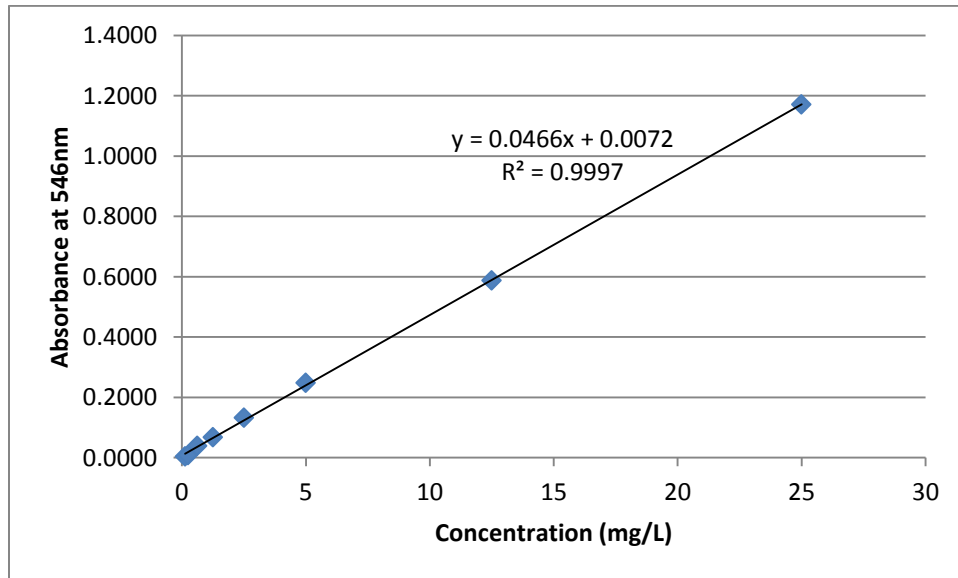
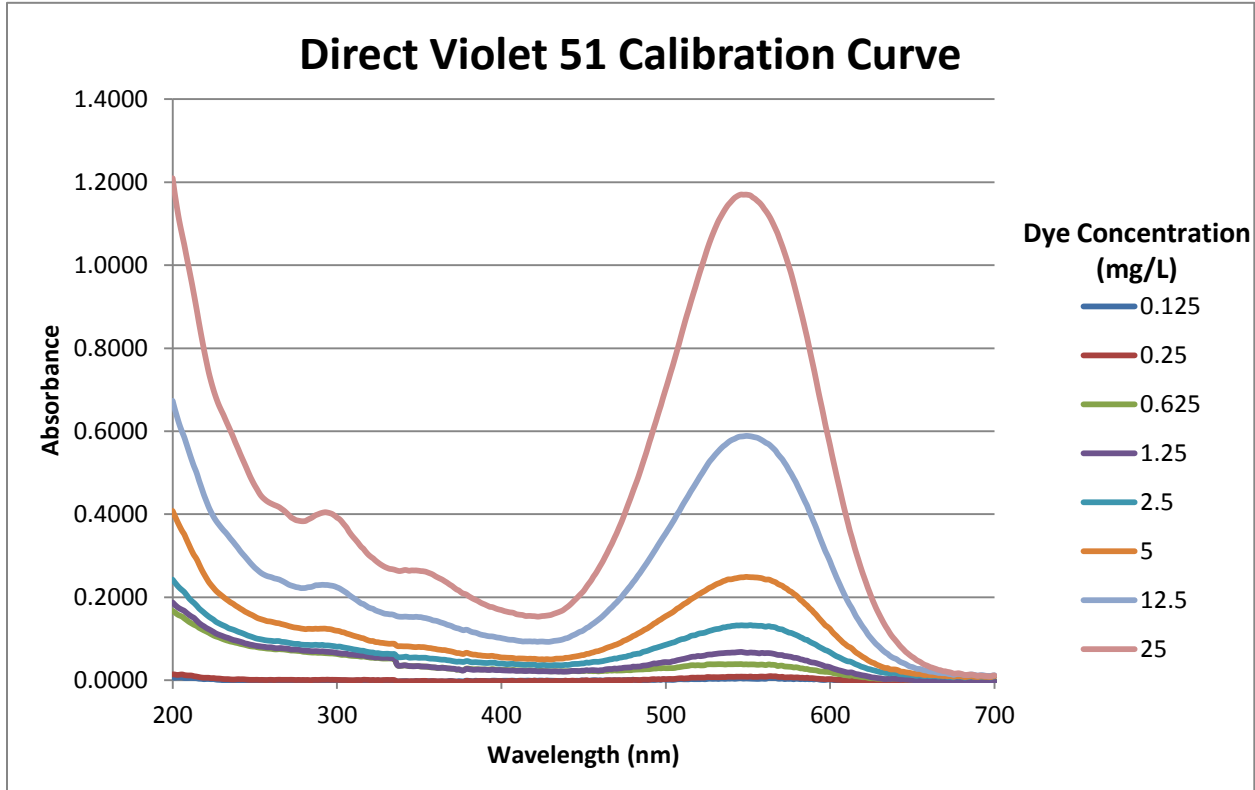
DR81\_C

Concentration (mg/L)	0.125	0.25	0.625	1.25	2.5	5	12.5	25
Peak (at $\lambda_{max}$ )	0.0036	0.0119	0.0271	0.0493	0.0915	0.1675	0.3589	0.7828



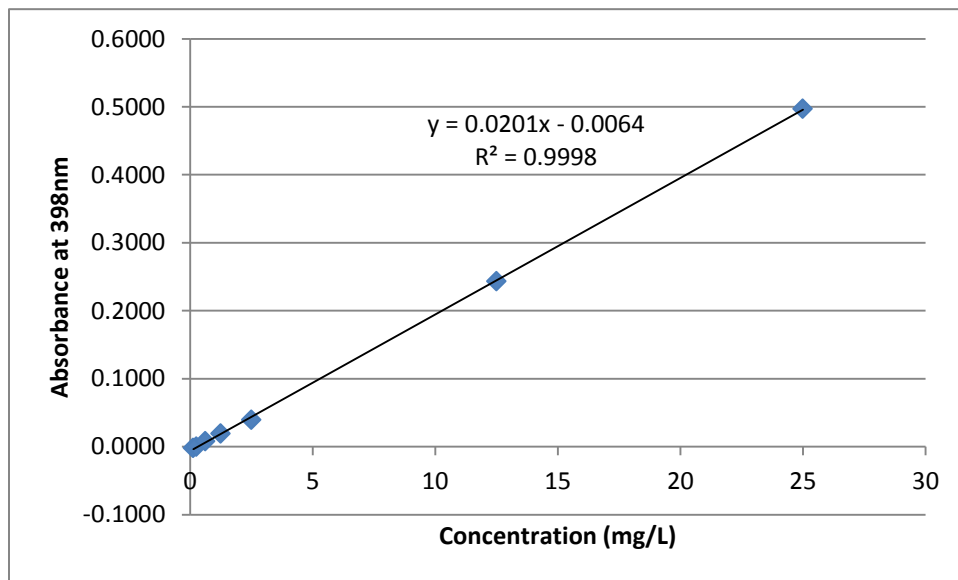
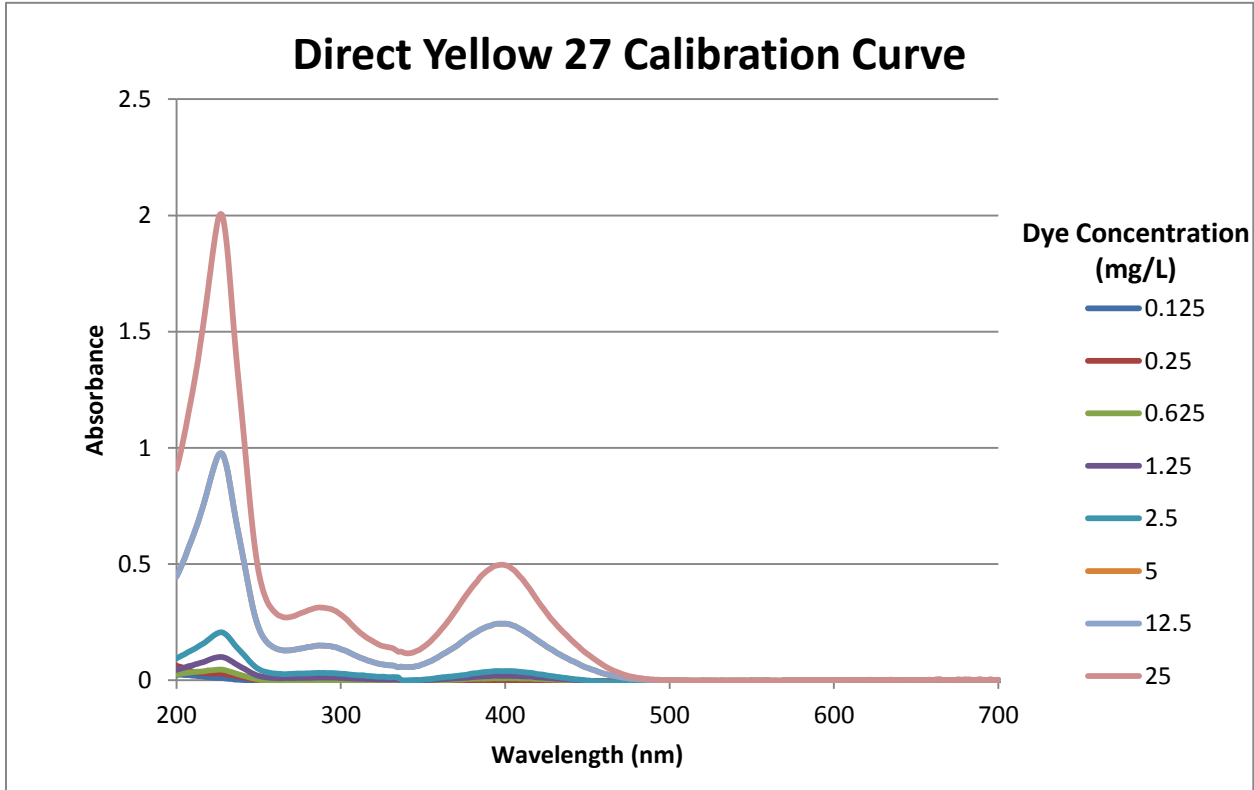
DV51\_C

Concentration (mg/L)	0.125	0.25	0.625	1.25	2.5	5	12.5	25
Peak (at $\lambda_{max}$ )	0.0047	0.0087	0.0389	0.0682	0.1324	0.2480	0.5873	1.1704



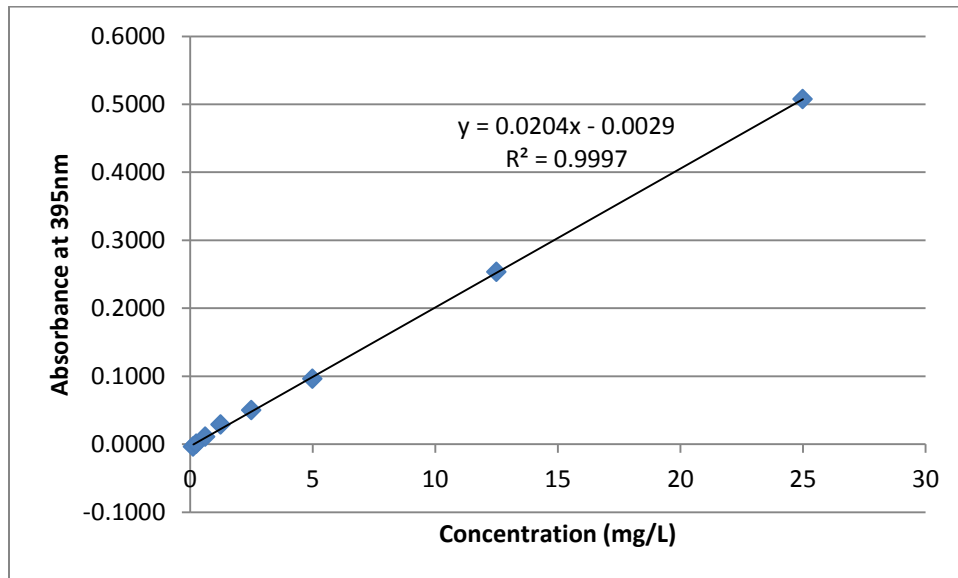
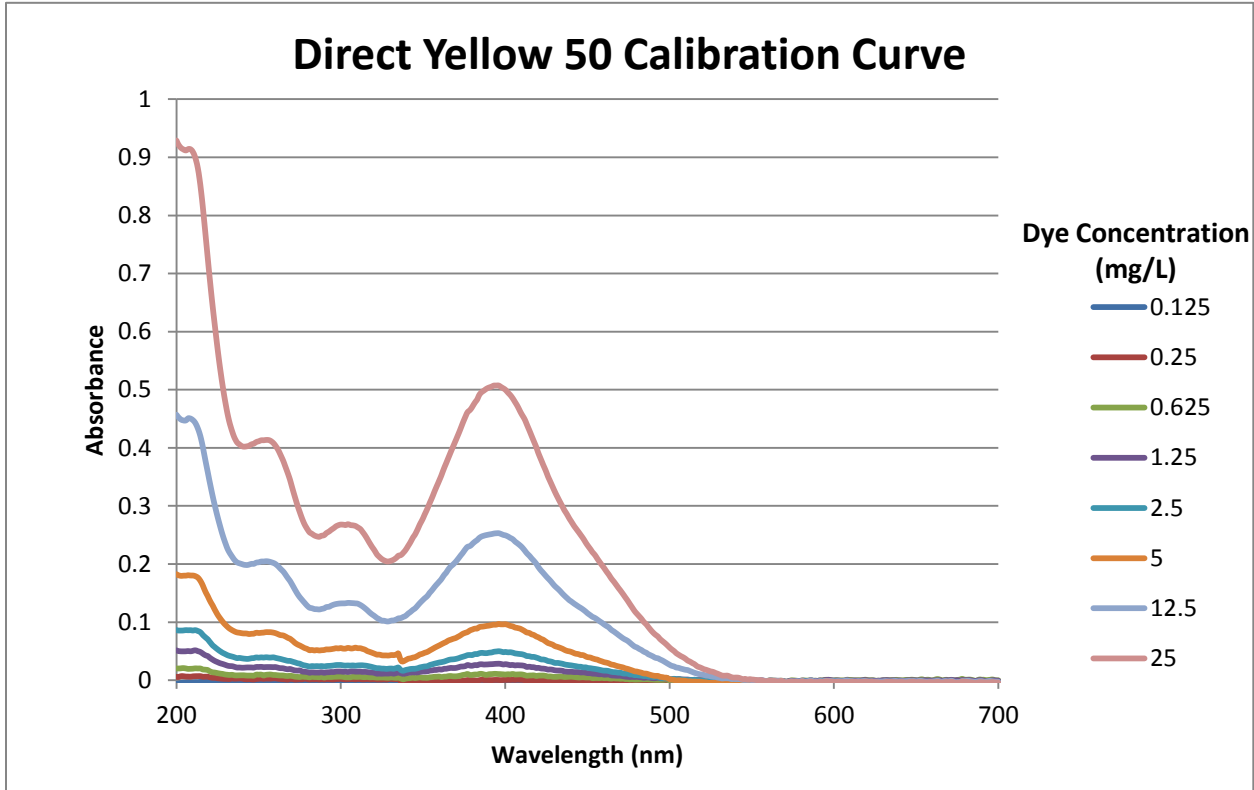
DY27\_C

Concentration (mg/L)	0.125	0.25	0.625	1.25	2.5	5	12.5	25
Peak (at $\lambda_{max}$ )	-0.0023	0.0000	0.0080	0.0189	0.0392	--	0.2432	0.4970



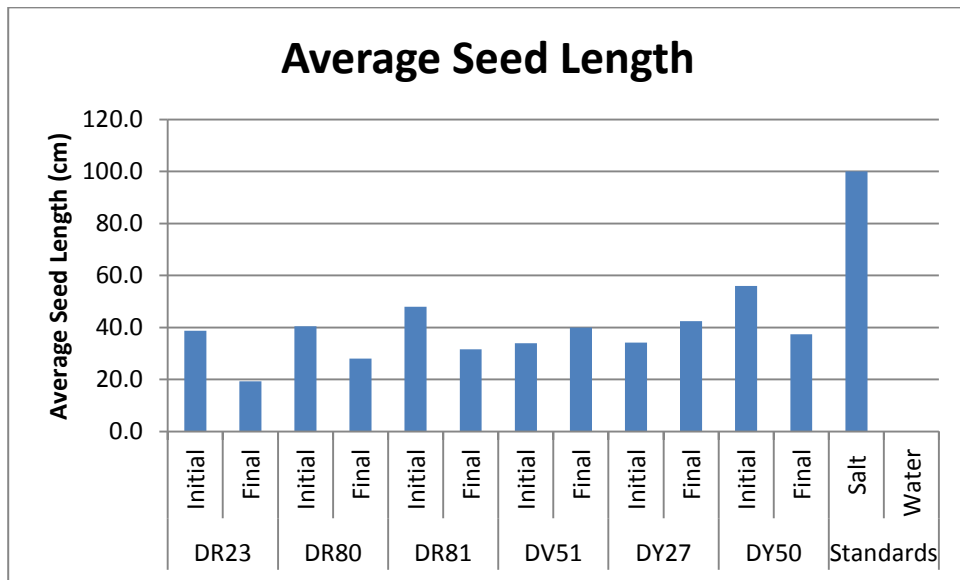
DY50\_C

Concentration (mg/L)	0.125	0.25	0.625	1.25	2.5	5	12.5	25
Peak (at $\lambda_{max}$ )	-0.0040	0.0005	0.0108	0.0283	0.0496	0.0960	0.2530	0.5073



## Appendix B: Lettuce Test

Sample ↓		Seed Length (cm)								Average Seed Length	Relative Toxicity	% Change	Relative Change
		1	2	3	4	5	6	7	8				
DR23	Initial	1.2	2.5	3.3	3.7	4	3	3.5	3.3	3.063	38.8	50%	
	Final						4	4	4.1	4.033	19.3		-19.4
DR80	Initial					1.6	3.1	3.6	3.6	2.975	40.5	69%	
	Final					3.1	3.6	3.7	4	3.600	28.0		-12.5
DR81	Initial			0.1	1	2.9	3.4	4	4.2	2.600	48.0	66%	
	Final				2.2	3.4	3.4	3.9	4.2	3.420	31.6		-16.4
DV51	Initial					3.2	3.2	3.3	3.5	3.300	34.0	118%	
	Final					2.2	3	3.3	3.5	3.000	40.0		6.0
DY27	Initial	3.2	3.3	3	2.7	3	3.5	3.6	4	3.288	34.3	124%	
	Final				0.9	3.4	3.2	3.6	3.3	2.880	42.4		8.2
DY50	Initial					1.2	1.7	1.9	4	2.200	56.0	67%	
	Final			0.8	2	3.1	4.1	4.2	4.6	3.133	37.3		-18.7
Standards	Salt								2.8	0.000	100.0	N/A	
	Water				1.4	3.6	3.6	4	4.4	5.000	0.0		



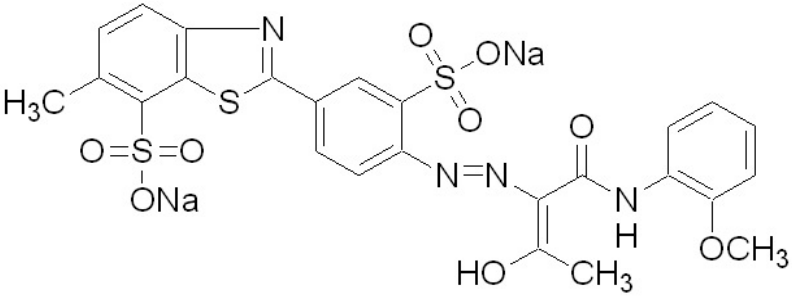
## Appendix C: Dye Information

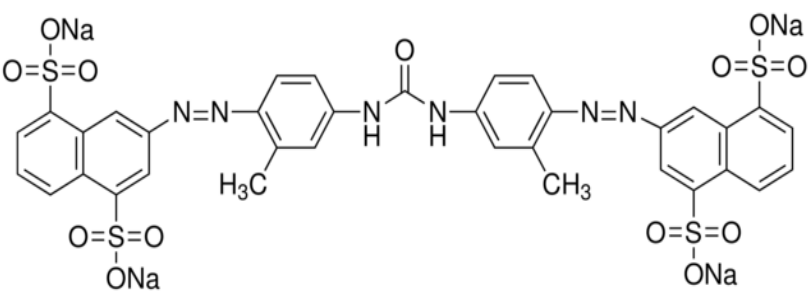
	Name: <b>Direct Red 81</b>
	Formula: <b>C<sub>29</sub>H<sub>19</sub>N<sub>5</sub>Na<sub>2</sub>O<sub>8</sub>S<sub>2</sub></b>
	Weight: <b>675.60 g/mol</b>
	$\lambda_{\max}$ : <b>510nm</b>
	Sulfate Groups: <b>2</b>
	Azo Groups: <b>2</b>
Rings: <b>5</b>	

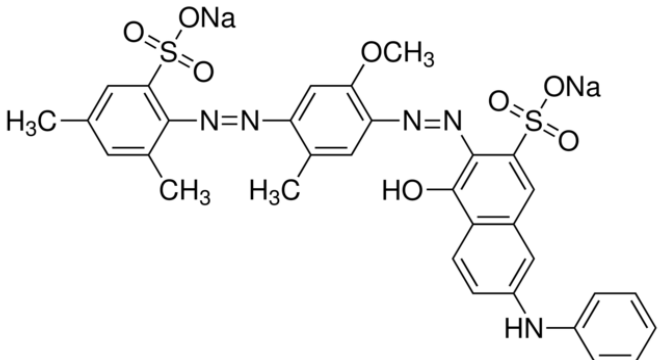
	Name: <b>Direct Red 80</b>
	Formula: <b>C<sub>45</sub>H<sub>26</sub>N<sub>10</sub>Na<sub>6</sub>O<sub>21</sub>S<sub>6</sub></b>
	Weight: <b>1371.07 g/mol</b>
	$\lambda_{\max}$ : <b>529nm</b>
	Sulfate Groups: <b>6</b>
	Azo Groups: <b>4</b>
Rings: <b>8</b>	

	Name: <b>Direct Red 23</b>
	Formula: <b>C<sub>35</sub>H<sub>25</sub>N<sub>7</sub>Na<sub>2</sub>O<sub>10</sub>S<sub>2</sub></b>
	Weight: <b>813.71 g/mol</b>
	$\lambda_{\max}$ : <b>502nm</b>
	Sulfate Groups: <b>2</b>
	Azo Groups: <b>2</b>
Rings: <b>6</b>	



 <p style="text-align: center;">sc-214913</p>	Name: <b>Direct Yellow 27</b>
	Formula: <b>C<sub>25</sub>H<sub>20</sub>N<sub>4</sub>Na<sub>2</sub>O<sub>9</sub>S<sub>3</sub></b>
	Weight: <b>662.62 g/mol</b>
	$\lambda_{\max}$ : <b>398nm</b>
	Sulfate Groups: 2
	Azo Groups: 1
Rings: 4	

	Name: <b>Direct Yellow 50</b>
	Formula: <b>C<sub>35</sub>H<sub>24</sub>N<sub>6</sub>Na<sub>4</sub>O<sub>13</sub>S<sub>4</sub></b>
	Weight: <b>956.82 g/mol</b>
	$\lambda_{\max}$ : <b>395nm</b>
	Sulfate Groups: 4
	Azo Groups: 2
Rings: 6	

	Name: <b>Direct Violet 51</b>
	Formula: <b>C<sub>32</sub>H<sub>27</sub>N<sub>5</sub>Na<sub>2</sub>O<sub>8</sub>S<sub>2</sub></b>
	Weight: <b>719.1 g/mol</b>
	$\lambda_{\max}$ : <b>546nm</b>
	Sulfate Groups: 2
	Azo Groups: 2
Rings: 5	

## Appendix D: Sample Calculations

### Sample calculation for ammonia and nitrate

$$\text{Direct Red 23} = \frac{25 \frac{\text{mg}}{\text{L}}}{813.71 \frac{\text{g}}{\text{mol}}} = 31 \frac{\mu\text{mol}}{\text{L}}$$

Direct Red 23 has three nitrogen atoms not in azo-bonds so the highest concentration of ammonia and nitrate ions is three times the molar concentration of the dye.

$$31 \frac{\mu\text{mol}}{\text{L}} \times 3 = 93 \frac{\mu\text{mol}}{\text{L}}$$

The measured amount of ammonia was 0.57 mg/L.

$$\frac{0.57 \frac{\text{mg}}{\text{L}}}{17.031 \frac{\text{g}}{\text{mol}}} = 33 \frac{\mu\text{mol}}{\text{L}}$$

The measured amount of nitrates was X mg/L.

$$\frac{X \frac{\text{mg}}{\text{L}}}{62.005 \frac{\text{g}}{\text{mol}}} = X \frac{\mu\text{mol}}{\text{L}}$$

The total number of moles and the percent difference from the expected was solved following the below method.

$$33 \frac{\mu\text{mol}}{\text{L}} + X \frac{\mu\text{mol}}{\text{L}} = Y \frac{\mu\text{mol}}{\text{L}}$$
$$\frac{93 \frac{\mu\text{mol}}{\text{L}} - Y \frac{\mu\text{mol}}{\text{L}}}{93 \frac{\mu\text{mol}}{\text{L}}} \times 100 = Z\%$$